DANMARKS OG GRØNLANDS GEOLOGISKE UNDERSØGELSE RAPPORT 2018/41

Source and occurrence of radionuclides in geothermal water

With focus on the Margretheholm geothermal plant

Mette Olivarius, Troels Laier, Christian Knudsen, Sebastian N. Malkki,
Tonny B. Thomsen, Simon H. Serre, Lars Kristensen,
Mads E. Willumsen & Lars Henrik Nielsen

GEOLOGICAL SURVEY OF DENMARK AND GREENLAND
DANISH MINISTRY OF ENERGY, UTILITIES AND CLIMATE

DANMARKS OG GRØNLANDS GEOLOGISKE UNDERSØGELSE RAPPORT 2018/41

Source and occurrence of radionuclides in geothermal water

With focus on the Margretheholm geothermal plant

Mette Olivarius, Troels Laier, Christian Knudsen, Sebastian N. Malkki,
Tonny B. Thomsen, Simon H. Serre, Lars Kristensen,
Mads E. Willumsen & Lars Henrik Nielsen

GEOLOGICAL SURVEY OF DENMARK AND GREENLAND
DANISH MINISTRY OF ENERGY, UTILITIES AND CLIMATE

GEUS

Dansk resume

Det geotermiske demonstrationsanlæg på Margretheholm producerer vand fra sandsten fra Bunter Sandsten Formation fra ca. 2,6 km dybde. I Københavnsområdet findes desuden et andet potentielt geotermisk reservoir bestående af sandsten fra Gassum Formation, der befinder sig på ca. 1,8–2,0 km dybde ved Margretheholm. Bunter og Gassum sandstenene har uens sammensætning, fordi de er dannet under forskelige geologiske og klimatiske forhold. Dette betyder bl.a. at den kemiske sammensætning af det vand de indeholder forventes at være forskellig.

Formålet med dette studie er at undersøge vand og sandsten fra Bunter og Gassum formationerne for at forstå den geologiske baggrund for blyproblemerne på Margretheholmværket, og at vurdere om problemerne kan forventes at fortsætte eller afhjælpes, hvis værket omstilles til produktion fra Gassum Formation. Endvidere er formålet at vurdere om blyproblemer kan undgås, hvis der opføres geotermiske anlæg i København med indvinding fra Gassum Formation.

Referencemateriale fra de geotermiske anlæg i Thisted og Sønderborg er inddraget i studiet, idet der her produceres vand fra Gassum Formation, således at vandkemien kan sammenlignes direkte med sandstenskemien i modsætning til Margretheholm, hvor boringerne kun giver information om sandstenene via prøver af borespåner, hvorimod vandprøver ikke for indeværende kan fremskaffes fra Gassum Formation. Baseret på analysematerialet er det vurderet i hvor høj grad Gassum Formation i Københavnsområdet forventes at være sammenlignelig med Gassum Formation i Thisted og Sønderborg, og der er gjort rede for hvor meget sammensætningen af vand og sandsten fra Bunter Formation adskiller sig fra Gassum Formation.

Den geologisk-tekniske rapport er struktureret således, at der begyndes med en introduktion der belyser baggrunden for studiets iværksættelse og derpå følger en geologisk beskrivelse af Bunter og Gassum formationerne. Dernæst redegøres der for hvilke prøver, der er udtaget og hvilke analysemetoder, de er undersøgt med. De nye data beskrives i resultatafsnittet og perspektiveres i diskussionsafsnittet. Efter konklusionerne følger seks appendikser, der giver en oversigt over historikken af injektionsproblemerne på Margretheholm, oprindelsen af bly i formationsvand, bly-koncentrationer i formationsvand fra danske boringer, henfaldsserien der leder til dannelse af bly-210 og mineralogien af reservoirerne. Denne del, som er ud over det egentlige studie, er medtaget som service for at fastholde og systematisere de mange erfaringer, der er opsamlet på værket.

Galvanisk korrosion forårsager ophobning af (metallisk) bly i rør og filtre i anlægget på Margretheholm, og affaldet betegnes som NORM (naturligt forekommende radioaktivt materiale), idet blyet indeholder radioaktivt bly (bly-210). Problemet med NORM affald opstår først når bly akkumuleres, idet radioaktiviteten af vandet i de tre geotermiske anlæg ligger langt under NORM grænsen. Bly er over tid akkumuleret i flowline og injektionsboring på Margretheholm, mens det markant lavere blyindhold i vandet i Thisted og Sønderborg anlæggene kun har forårsaget ubetydelig ophobning af bly.

Den totale mængde bly i Bunter vandet er ca. 20 gange højere i Margretheholm end i Gassum vandet fra Thisted og Sønderbog. Samme tendens ses for koncentrationen af radioaktivt bly-210, som er ca. 30 til 60 gange højere i vandet fra Margretheholm end i de to andre anlæg. På baggrund heraf forventes indholdet af total bly og radioaktivt bly i Gassum vand i Københavnsområdet at være markant lavere end i Bunter vand. Denne antagelse er baseret på, at de geologiske forhold på dannelsestidspunktet for Gassum sandet sandsynligvis var nogenlunde de samme i København som i Sønderborg, Thisted og landet i øvrigt.

Forholdene på de tre undersøgte Gassum Formation lokaliteter (Thisted, Sønderborg, Stenlille) er nogenlunde ens når det gælder saltholdighed (klorid 100 g/L), temperatur (ca. 50°C) og sandsynligvis også sulfidindhold. Blyindholdet i formationsvandet i Gassum Formation i København er formentlig lidt højere end de andre lokaliteter som følge af den forventede lidt højere saltholdighed og højere temperatur (ca. 54°C ifølge prognose) på grund af den lidt større dybde i København. Lavt sulfidindhold, høj saltholdighed og høj temperatur fremmer betingelserne for høj koncentration af bly, hvilket afspejles i den væsentligt højere temperatur (73°C) og højere saltholdighed (klorid 137 g/L) af Bunter vandet i København.

Det markant lavere blyindhold der sandsynligvis findes i Gassum vand end i Bunter vand i Københavnsområdet mindsker risikoen for betydelige blyudfældninger og de dermed forbundene gener som fx clogging af injektionsboringen med bly. Blyudfældninger på "udsatte steder" såsom på offer-anode monteret over posefiltre kan ikke udelukkes, som erfaringerne fra anlægget i Sønderborg viser. Radioaktivitetsmålingerne på filtrene i Sønderborg viste, at disse lå tæt under den grænse SIS opererer med for at kunne afgøre om genstanden skal karakteriseres som NORM affald. Det kan derfor ikke udelukkes, at man ved kommende anlæg i København er nødt til tage højde herfor i design af anlæg og drift for at undgå at skulle håndtere NORM affald. De materialer der anvendes ved opførelse af geotermiske anlæg skal vælges omhyggeligt for at modvirke scaling. En omlægning af Margretheholmanlægget fra produktion af vand fra Bunter Formation til Gassum Formation vil ikke nødvendigvis eliminere blyproblemerne helt, da de også afhænger af tilgængeligheden af korroder-bart materiale i anlægget.

Bly-210 er en kortlivet isotop med en halveringstid på 22,2 år, der stammer fra henfald af uran, så derfor er de mest sandsynlige kilder til uran blevet undersøgt. Bly-210 og andre radioaktive isotoper i vandet må stamme fra formationen hvorfra vandet produceres og ikke fra omgivende formationer, som tilstedeværelsen af den kortlivede radium-224 isotop med halveringstid på 3,6 dage viser. Resultaterne viser, at zirkonkorn udgør den mest sandsynlige primære kilde til radioaktiviteten. Mineralet har et generelt højt uranindhold, og zirkoner der har ekstra højt uranindhold bliver ødelagt af radioaktiviteten i dem. Dermed er det lettere for de radioaktive datterprodukter, heriblandt bly-210, at trænge ud af mineralet til formationsvæsken.

Andelen af zirkoner der har ekstra højt uranindhold er højere i Bunter Formation end i Gassum Formation. Dette er i overensstemmelse med, at sandet i Bunter Formation er blevet transporteret væsentligt kortere fra kildeområde til aflejring, da formationen blev dannet, end det er tilfældet for Gassum Formation. Det er derfor sandsynligt at et højere antal af de skrøbelige zirkoner med ekstra højt uranindhold har overlevet transporten og derfor akkumuleret i Bunter Formation.

Gas-isotop analyser viser at der ikke er sket tilførsel fra en dybere og moden organisk kilde, såsom alunskiferen der er kendetegnet ved et meget højt indhold af uran. De geokemiske analyser af sandsten og lersten viser at uran ikke forekommer fortrinsvis i ler-rige dele af Bunter og Gassum formationerne, hvorimod uranindholdet har korrelation med indholdet af zirkonium og titan hvilket indikerer at tungmineraler såsom zirkon er den primære kilde til uran. Diagenetiske processer kan dog også spille en væsentlig rolle i forhold til koncentrationen af radioaktive isotoper i vand ved at binde uran i cement og frigive det ved opløsning, og arealet af kontaktfladen mellem matrix og porevand kan også være en vigtig parameter.

Content

Appendixes **56**

1. Introduction

This report contains the results of the study “Kilder til radionuklider i geotermisk vand” (Sources of radionuclides in geothermal water) conducted in 2018 by GEUS for HOFOR A/S.

Related to a major cleanup of the injection well (MAH1A) in 2015 at the geothermal demonstration plant at Margretheholm, a number of analyses were obtained in the period 2015–2017 to identify causes of the increasing injection pressure occurring in MAH1A since its commissioning in 2005. A detailed description of the injectivity history is given in Appendix 1.

The analyses suggest that radionuclides (designated as NORM; naturally occurring radioactive material) accumulate, essentially ^{210}Pb, which precipitates as metallic lead in the geothermal surface facilities and in the wells due to a galvanic process. The presence of ^{210}Pb requires a source of this short-lived isotope (22.2 years half-life), as shown in Appendix 2. Clogging of the injection well as well as precipitation of NORM creates technical and safety challenges in ensuring stable operation and thus ensuring sufficient demonstration value from the plant within an operationally reasonable financial framework.

As part of the licensing program, Hovedstadsområdets Geotermiske Samarbejde (HGS) has conducted an analysis of the economy in an expansion with small geothermal plants (EUDP Pilot Hole 1b, WP4). This study is based on the Gassum Formation as the primary geothermal reservoir, as opposed to existing wells at the Margretheholm plant, which utilize the Bunter Formation.

The primary purpose of the present project is therefore to evaluate the risk of whether geothermal production from the Gassum Formation reservoir in the Copenhagen area may include similar challenges with NORM as the Bunter Formation does.

Hence, the project is designed to:

1) Investigate the origin and extent of radionuclides in geothermal water from the Bunter Formation reservoir in Margretheholm by comparing water chemistry with an assessment of possible radionuclide sources in the reservoir rock.
2) Assess the risk that similar radionuclide problems may occur for Gassum Formation by comparing the chemistry of geothermal water from Gassum Formation with the occurrence and amount of possible sources of radionuclides in the sandstone reservoir based on relevant locations (Margretheholm, Thisted and Sønderborg).

The project consists of the following sub-tasks:

- Compile and evaluate the reliability of data regarding the lead-content in formation water from previous analyses.
- Analyse geothermal water from the geothermal plants in order to relate the composition to the reservoir geology (Gassum vs. Bunter Formation).
    - Radionuclide concentrations in water samples from Margretheholm, Thisted and Sønderborg to assess whether the content is related to the reservoir type.
    - Isotopic analyses of dissolved nitrogen and methane in the formation water in Margretheholm to determine the source of the high content.
- Analyze rock samples for the presence and frequency of possible sources of radionuclides (primarily zircon and monazite grains as well as clasts of organic-rich shales to the extent that they are present).
    - Bulk analyses of washed and sorted cuttings samples (core samples could provide better precision, but there are only core materials available from few intervals). The analysis program is based on the relatively simple and cheap HH-XRF method, supported by a small number of more advanced calibration analyses.
        - Bunter Formation from Margretheholm: to identify the source of the present problem.
        - Gassum Formation from Margretheholm: for input to risk assessment using a new reservoir.
        - Gassum Formation from other geothermal plants: for assessing the risk of corresponding problems using Gassum Formation as reservoir in the Copenhagen area.
    - Mineralogical scanning of selected samples and chemical scanning of Gassum Formation core in order to obtain greater understanding of the distribution of radionuclide sources.
    - Chemical and mineralogical analysis of heavy minerals from samples from Margretheholm to identify the source of the existing problem.
- Evaluate if corresponding radionuclide problems may be expected to occur in future geothermal installations with Gassum Formation sandstone as target in the Copenhagen area, by comparing the results of the water chemistry with insights to the source of the radionuclides obtained through analyses of reservoir rocks.

2. Geological background

The Copenhagen area is located in the easternmost part of the Norwegian-Danish Basin, which was formed by crustal stretching followed by late Carboniferous–early Permian rifting and Mesozoic–Cenozoic thermal-dominated subsidence (Figure 1) (Vejbæk 1997). Thereby a km-thick succession of sandstones, siltstones, mudstone, carbonates and evaporites accumulated in the basin. Of these, the Triassic–Jurassic succession includes several potential geothermal reservoir sandstones such as the Gassum Formation and the Bunter Sandstone Formation (Figure 2), which are named Gassum Fm and Bunter Fm, respectively, in the remaining part of this report.

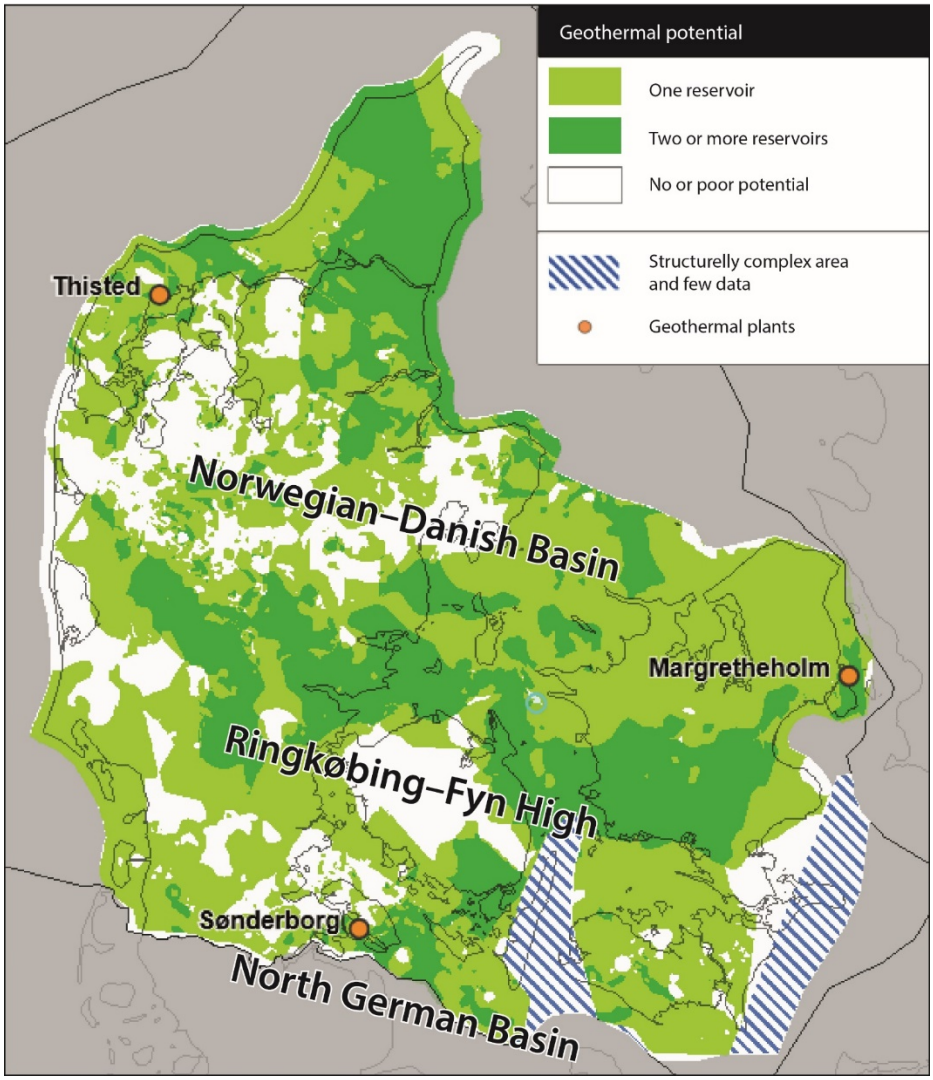

Figure 1: Map from the 'Geotermi WebGIS-portal' (DybGeotermi.geus.dk) showing the geothermal potential in the Danish area and the location of the three geothermal plants (Vosgerau et al. 2016).

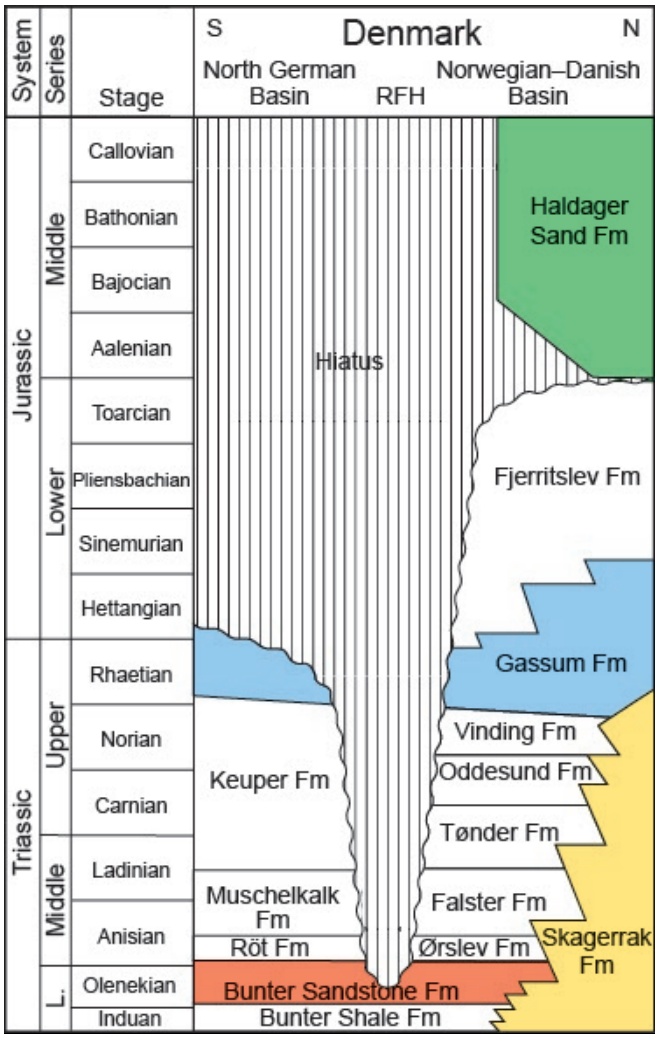

Figure 2: Stratigraphic scheme of the Danish Lower Triassic – Middle Jurassic succession where the highlighted formations contain potential geothermal reservoir sandstones (simplified after Michelsen & Clausen 2002).

The Lower Triassic Bunter Fm is widespread in the North German Basin and in the southern part of the Norwegian–Danish Basin, where it is synchronous with the oldest part of the Lower–Upper Triassic Skagerrak Fm that accumulated in the northern part of the basin (Michelsen & Clausen 2002). The arid to semi-arid climate resulted in deposition of aeolian and ephemeral fluvial sand interbedded with silt- and mudstones formed in shallow lakes with occasional evaporite deposition (Clemmensen 1985). In general, the sandstones are considered to be widespread with relatively good lateral continuity in areas unaffected by faults or salt structures.

The Upper Triassic–Lower Jurassic Gassum Fm is present in most of the Norwegian–Danish Basin, except where major salt structures occur and on the basement blocks of the Ringkøbing–Fyn High (Michelsen et al. 2003, Nielsen 2003). The formation was deposited in a humid climate and consists of marine and fluvial sandstones interbedded with marine and lagoonal mudstones, minor siltstones and thin coal beds formed during a periods with recurrent sea-level changes. In general, the sandstones are considered to be widespread with relatively good lateral continuity in areas unaffected by faults or salt structures.

3. Samples and methods

New samples included in this study:

- Water sample from the Margretheholm plant (producing from Bunter Fm)
- Water sample from the Sønderborg plant (producing from Gassum Fm)
- Water sample from the Thisted plant (producing from Gassum Fm)
- Gas samples from the Margretheholm plant (producing from Bunter Fm)
- Cuttings samples from the Bunter Fm in the Margretheholm-1 well
- Cuttings samples from the Gassum Fm in the Margretheholm-1 well
- Cuttings samples from the Gassum Fm in the Sønderborg-1 well
- Core samples from the Gassum Fm in the Thisted-3 well

The samples of formation water and reservoir sandstone from the Gassum Fm were included in the study in order to compare their composition with those of the Bunter Fm, since high radionuclide concentrations have only been encountered in the geothermal plant that produces from the Bunter Fm and not in those where the Gassum Fm constitutes the reservoir.

3.1 Radionuclides in water

Water samples for analysis of radionuclides were collected from the geothermal plants at Sønderborg, Thisted and Margretheholm during March – April 2018. Warm water, 46-70°C, from the production wells were filtered directly through a 0.45 µm membrane filter into screw cap glass bottles, 1-5 liters. The samples were then brought to DTU Nutech at Roskilde within 5 hours after sampling. At Thisted, water was collected from the new Thisted-5 well located 1.5 km from the old Thisted-2 production well. The well had been in operation for almost 3 months producing over 100 m^3 per hour.

Lead isotopes (^{212}Pb and ^{210}Pb) were analyzed as follows. Upon delivery of samples, 5-10 liter of each sample were acidified and stable lead (about 50 mg) was added. The samples were made alkaline with ammonia to precipitate hydroxides. The precipitates were collected by centrifugation, dissolved and re-precipitated using $PbSO_4$. The precipitate was dissolved in NH3 and EDTA and transferred to a 50 ml container for gamma measurement. The whole procedure was done in about 8 hours in order to minimize the decay and ingrowth of the ^{212}Pb. The samples were counted on a characterized BEGe-detector repeatedly during a three-day period to follow ^{212}Pb ingrowth/decay. Recovery of lead was determined by ICP-OES on a known aliquot of each sample.

Due to difficulties analyzing ^{210}Pb using gamma spectrometry, an additional technique was applied. About 600 ml of water from each well was precipitated using $Fe(OH)_3$ and stable lead as yield monitor. The precipitate was dissolved in 2M HCl and added to a Triskem Sr-spec column, which strongly adsorb lead but few other elements. 2M HCl and 6M HNO_3 were used to elute ^{210}Bi and ^{210}Po, respectively. Lead was eluted using 6M HCl and a known fraction of the eluate was removed for analysis of lead recovery (ICP-OES), while the rest

was evaporated and transferred to a liquid scintillation vial and counted for ^{210}Pb and ^{210}Bi ingrowth rate on a Quantulus (Wallac/Perkin Elmer) ultra low-level liquid scintillator.

Radium-isotopes (^{226}Ra, ^{228}Ra and ^{224}Ra) were analyzed as follows. About 300 ml of water from each well was acidified using HCl and gamma counted on characterized high-purity germanium (BEGe, Mirion) detectors for 3-4 days. The 968 and 911 keV peaks from ^{228}Ac (6 h half-life and in equilibrium with ^{228}Ra) were used to quantify ^{228}Ra. For ^{226}Ra (186 keV) and ^{224}Ra (241 keV), indicative values were obtained.

Following the $Fe(OH)_3$ precipitate for lead, the remaining supernate was subject to a MnO_2 precipitate to co-precipitate radium. Suitable amount of dissolved $MnCl_2$ and $KMnO_4$ was added to the alkaline sample to create a MnO_2 precipitate which was collected and dissolved in weak HCl-H_2O_2, transferred to a 50 ml container and gamma counted repeatedly for about 2 weeks to obtain changes in ^{224}Ra activity. Due to slow precipitation of insoluble sulphates in the container, the sample was reworked and the precipitate dissolved in EDTA.

3.2 Gas isotope geochemistry

Gas samples for stable isotope analysis of carbon and nitrogen were collected on April 9 at Margretheholm and sent to BGR in Hannover. Gas tapped from the de-gassing valve mounted on the lid of the filter housing was collected in 120 mL serum bottles kept under water until the crimp cap had been placed to isolate the gas.

The stable carbon isotopic compositions of C_1 – C_3 hydrocarbons were analyzed with gas chromatography isotope ratio mass spectrometry (GC-IRMS), using an Agilent GC 6890 coupled to a Thermo MAT253. Samples were injected via a split-splitless injector either directly on column or via a sample loop. C_1 – C_3 hydrocarbons were separated on a Poraplot Q column (ID 0.32 mm, 25 m). The GC-program was: -20°C (held for 2 min), 8°C/min heating and 14 min at a final temperature 180°C. C_1 – C_3 were oxidized on a CuO/Ni/Pt combustion furnace operated at 960°C. The carrier gas was He. The carbon isotope ratios are expressed in a per mil deviation from the Vienna Belemnite (VPDB) standard in the usual delta-notation: $\delta^{13}C$ $[(R_{sample}/R_{standard})-1] \times 1000$, where R is the $^{13}C/^{12}C$ ratio and $R_{standard}$ = 0.0112372. GC-C-IRMS precision was checked daily using a laboratory standard with known isotopic composition. Standard deviations for replicate injections were less than ±0.5‰.

The stable isotopic ratio of nitrogen $^{15}N/^{14}N$ was analyzed with gas chromatography isotope ratio mass spectrometry (GC-IRMS) according to the procedure described by Sohns et al. (1994). The GC component of the system (Packard 430) has a column length of 3 m and a diameter of ⅛ in. and is packed with 5Å molecular sieve as adsorbent. The GC is set to a constant temperature of 75°C with a head pressure of the He carrier gas of about 270 kPa. The nitrogen isotope ratio is expressed in a per mil deviation from atmospheric nitrogen in the usual delta-notation: $\delta^{15}N$ $[(R_{sample}/R_{standard})-1] \times 1000$, where R is the $^{15}N/^{14}N$ ratio.

3.3 HH-XRF geochemistry

X-ray fluorescence (XRF) by a portable handheld (HH) instrument was used to analyze 150 samples, which comprise 30 from Bunter Fm in Margretheholm-1, 68 from Gassum Fm in Margretheholm-1, 14 from Karlebo Mb of Fjerritslev Fm in Margretheholm-1, 13 from Gassum Fm in Sønderborg-1 and 25 from Gassum Fm in Thisted-3. Handpicking with tweezers was used to sort the individual fragments from the washed cuttings samples into sandstone and claystone when relevant, since each cuttings sample represents an interval of the well that may comprise both lithologies, which were then analyzed separately. By this technique, all the recognizable cavings could be excluded from the samples.

Samples of 7.5 g were crushed to < 250 µm in a tungsten carbide mortar and analysed by a Niton XL3t (Thermo-Fisher Scientific, software version 8.4F) XRF device at GEUS. The crushed samples were put in sample cups with a thin polypropylene film at the bottom and then placed on top of the mounted instrument that faced upwards. Measurements of standard samples within the data series were conducted to ensure the data quality. Each sample was analyzed twice and the average value was calculated.

3.4 ICPMS geochemistry

Inorganic geochemistry was measured on 30 samples, which comprise 8 from Bunter Fm in Margretheholm-1, 10 from Gassum Fm in Margretheholm-1, 4 from Gassum Fm in Sønderborg-1 and 8 from Gassum Fm in Thisted-3. Both sandstone and claystone samples were included. Sorting of the washed cuttings fragments into these lithologies was done similarly as with the samples for HH-XRF.

Quantitative geochemistry analysis with focus on trace element concentrations was performed on a PerkinElmer Elan 6100DRC quadrupole inductively coupled plasma mass spectrometer (ICP-MS) at GEUS. For each analysis, at least 5 g of material was crushed to < 100 µm in a tungsten carbide mortar prior to digestion. The analyses include 41 elements measured twice for each sample after subjecting it to different digestion techniques. One sample was dissolved directly in hydrofluoric acid, whereas the other sample first included borate melting in order to dissolve the most difficult minerals like zircon that is relevant for this study because of its high U content. To ensure the data quality, reference standard samples were measured concurrently during the acquisition of the data series.

3.5 XRF core scanning

Core scanning by XRF spectroscopy was used to determine the elemental composition of a total of 21 m core from the Gassum Fm in the Thisted-3 well, comprising core 3 from 1210.5–1222.1 m and core 4 from 1222.1–1236.2 m. A stationary Itrax Core Scanner at the Natural History Museum of Denmark at University of Copenhagen was applied with 2 minutes analysis time of every 0.5 cm of core by scanning up to 11 cm of the core diameter. A high-resolution color photo and an x-ray photo were made at the beginning of each scan. Some gaps exist in data since the core lacks some thin intervals and because the scanner could not measure the surface of the most porous layers.

Peak areas (photon counts) were determined by making a curve fit of the spectra, where the elements included in the fitting were chosen during the data processing. The peak area depends on the sensitivity of the instrument to the given element, and it is for example not very sensitive to Si so the peak area will be relatively small even when the concentrations are large. Optimal fitting cannot be obtained for all elements at the same time, so the parameters were chosen to fit best with the most important elements. However, the concentrations of e.g. U and Pb were close to the detection limit so the estimated contents of these elements are highly uncertain. The validity value shows if the detector was close to the sample, and the mean square error shows how good the fit is. Semi-quantitative values were calculated by calibration of the dataset.

3.6 SEM mineral scanning

Five samples were selected for automated mineral scanning comprising two from the Bunter Fm in Margretheholm-1 and three from the Gassum Fm distributed as one from each of the Margretheholm-1, Sønderborg-1 and Thisted-3 wells. Samples were embedded in epoxy and prepared as polished thin sections that were coated with carbon. The thin sections were analyzed at GEUS by a Zeiss Sigma 300VP field emission scanning electron microscope (SEM) coupled with two Bruker XFlash 6|30 129 eV energy dispersive X-ray spectrometers (EDS) to rapidly image and chemically map the samples using a step size of 10 µm. The level of backscatter electron (BSE) brightness is used to distinguish the rock from the epoxy. An X-ray spectrum was acquired for each measurement such that the chemical composition of each individual mineral phase is known.

The Zeiss Mineralogic software platform was applied to determine the mineralogical composition of each analysis based on a mineral library adjusted to the current samples. The analyses were grouped into mineral phases for which the grain-size parameters were calculated. The method cannot distinguish between detrital and authigenic phases. Rock fragments are not identified but split into separate minerals, and some minerals are grouped due to similar chemical composition. Additional scans with smaller step size were performed on selected areas such as pyrite cement, where also element maps were produced.

3.7 Heavy mineral analyses by CCSEM

Five samples from approximately the same depths as the samples used for mineral scanning were selected for heavy mineral analysis. The samples were crushed and heavy mineral concentrates were produced by heavy liquid separation of the 45–500 µm grain size fraction with a density of >2.8 g/cm3. The heavy mineral concentrates were mounted in epoxy. Computer-controlled scanning electron microscopy (CCSEM) by a Zeiss Sigma 300VP field emission SEM at GEUS was used to analyze the modal abundances of about 2000 grains per sample (Keulen et al. 2008, 2012). The element composition of each grain was determined by combining EDS with contrasted BSE micrographs.

The Zeiss Mineralogic software platform was used to determine the mineralogy of each heavy mineral grain based on a mineral library adjusted to the current samples, and the grain-size parameters were calculated. The minerals that are not relevant for this study are excluded from the results, such as mica minerals and authigenic minerals.

3.8 U-Th-Pb analyses by LA-ICPMS

Five samples from approximately the same depths as the samples used for mineral scanning and heavy mineral composition were chosen for analysis of selected minerals comprising zircon and rutile. This was done to measure the contents of U, Th and Pb in each grain and to obtain their radiometric ages. The analyses were performed on hand-picked grains that were mounted in epoxy after being collected from crushed samples sorted on a water-shaking Wilfley table. Grains with all available types of shapes and sizes were included.

The laser ablation inductively coupled plasma mass spectrometry (LA-ICPMS) was performed at GEUS using an Element2 magnetic sector-field mass spectrometer from ThermoFisher Scientific that is coupled to a NWR-213 laser ablation system from Elemental Lasers Inc. Analysis procedures basically followed as described in Frei & Gerdes (2009). Data were acquired from single spot analysis of 25 µm in diameter using an impulsed laser beam with a nominal laser fluence of 10 J/cm2 and a pulse rate of 10 Hz. Total acquisition time for single analysis was max. 1.5 min., including 30 sec. gas blank measurement followed by laser ablation for 30 sec. and washout for 30 sec. in an air-tight chamber. About 200–300 nanograms of material was liberated and transported by helium gas through inert Tygon tubing to the mass spectrometer for isotopic determination. To minimize instrumental drift, a standard-sample-standard analysis protocol was followed, bracketing eight analyses by three measurements of the standard zircon GJ-1 (Jackson et al. 2004). For quality control of the standard analyses, the Harvard 91500 (Wiedenbeck et al. 1995, 2004) and Plesovice (Slama et al. 2008) standard reference zircons were measured regularly during the analysis sequences, yielding a typical average age accuracy and precision of < 3%. U, Th and Pb concentrations was calculated based on the content of these elements in the GJ-1 zircon standard.

The data reduction was carried out through the software Iolite v. 2.5 (Paton et al. 2011; Petrus & Kamber 2012). Reported analytical uncertainties for the ages are 2σ. Common Pb correction was applied when required for the age dating. The combined histogram and probability density plots (PDP) were produced through the jAgeDisplay software by Thomsen et al. (2016). In the PDP, $^{206}Pb/^{238}U$ ages are used for zircons younger than 1100 million years (Ma) and $^{207}Pb/^{206}Pb$ ages for older zircon grains, because $^{206}Pb/^{238}U$ ages are more accurate for the younger age interval. In the PDP, the concordant ages (i.e. with a discordance of <10%) are shown as dark grey areas, whereas discordant zircons (i.e. >10% discordance) are marked with a light grey color on the same axis (i.e. not cumulative). The probability ages displayed on the PDP are calculated from the concordant ages only. Sufficiently zircon crystals for analysis appeared in all samples, while rutile occurred more scarce, especially in the Bunter Fm where only a single usable grain was found. All samples were screened also for other heavy minerals with high U-content such as monazite, apatite and titanite, but none of these occurred in any significant amount and thus were not analysed.

4. Results

4.1 Dissolved gas in Margretheholm formation water

Formation water from Bunter sandstone at Margretheholm has a fairly high content of dissolved gas; 0.15 vol/vol ratio at ambient pressure and temperature. Samples of exsolved gas were analyzed with respect to chemical and isotopic composition in order to be able to determine the origin of nitrogen and hydrocarbons.

No apparent organic-rich rock exists between the crystalline bedrock and the Bunter sandstone, which could explain the presence of light hydrocarbons observed in the formation water (Table 1). Data on nitrogen-rich gases existing in pre-Zechstein reservoirs compiled during the NW European gas atlas project pointed to maturity source for the nitrogen-rich gas. The maturity of the source rock was inferred partly from the carbon stable isotopic ratios of methane and ethane (Gerling et al. 1999), whereas the stable isotopic ratio of nitrogen helped determine the organic matter type; marine versus terrestrial.

The isotopic data for methane and ethane presented in Table 2 were plotted in the diagram of Gerling et al. (1999) (Figure 3). The Margretheholm data plots far from the gases of high maturity source rocks, possibly due to mixing with a little microbial gas. The isotopic ratio of carbon dioxide of -14.3 ‰ indicates an organic origin. Part of the carbon dioxide may have been converted to methane by bacteria.

Table 1: Composition of gas in Bunter sandstone water from Margretheholm.

Constituent	Vol%	Constituent	ppm
Hydrogen	0.06	Ethane	465.8
Helium	2.26	Ethene	0
Nitrogen	91.53	Propane	63
Oxygen/Argon	0.66	Propene	0
CO	0	I-Butane	3
CO2	0.24	N-Butane	3
Methane	5.2		

Table 2: Isotopic ratio of hydrocarbons, carbon dioxide and nitrogen in Bunter sandstone water from Margretheholm.

Constituent	isotope ratio	standard
δ13-CH4	-41	[‰ VPDB]
δ2H-CH4	-104.3	[‰ SMOW]
δ13-C2H6	-29.2	[‰ VPDB]
δ13-C3H8	-28.5	[‰ VPDB]
δ13_CO2	-14.3	[‰ VPDB]
δ15_N2	-7.65	[‰ Atm]

The isotopic ratio of nitrogen of -7,65 ‰ points to a terrestial organic matter source of fairly low thermal maturity. Thus, it is concluded, that neither hydrocarbons nor the nitrogen are derived from a highly mature source such as the Alum shale in the region.

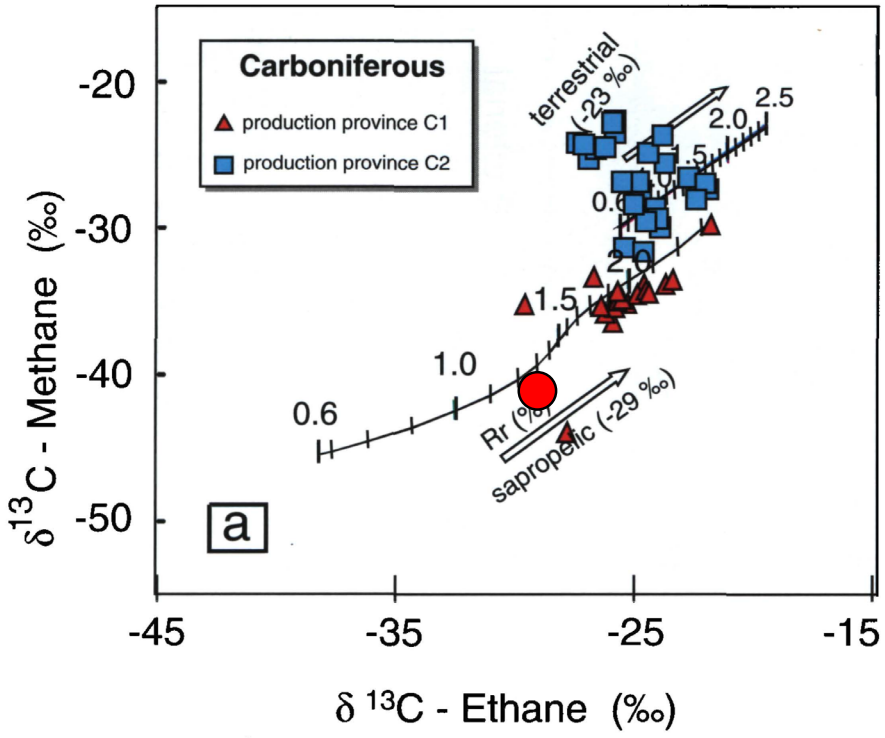

Figure 3: Margretheholm gas plotted as a red dot on an isotope diagram showing nitrogen-rich gases of high thermal maturity (~1.5–2.0% Rr) in NW Europe. C1 gases are from marine organic matter whereas those from C2 were generated from terrestrial source materials (modified from Gerling et al. 1999).

4.2 Natural radioactivity of formation water

The origin of lead in formation water and the lead concentration in Gassum formation water are described in Appendixes 3–4, and all the available data of lead content in formation water measured during well tests of Danish onshore wells are summarized in Appendix 5.

Formation water from the geothermal plants at Thisted, Sønderborg and Margretheholm were filtered on-site in order to exclude suspended particles and brought to the laboratory within five hours. It was considered important to keep storage time as short as possible to be able determine the activities of the short-lived radionuclides which may help determine the migration path from its source.

The activity of Ra-226, the radionuclide most often reported for deep formation waters, varies from 6 to 13.5 Bq/kg for the three Danish sites, with Margretheholm showing the highest value (Table 3). Ra-228 activity varies from 5.8 to 35.1 Bq/kg.

Table 3: Specific activity of radionuclides in formation water.

Locality/Well	Sampling date	Ra-226 [Bq/kg]	±	Pb-210 [Bq/kg]	±	Ra-228 [Bq/kg]	±	Th-228 [Bq/kg]	±	Ra-224 [Bq/kg]	±
Sønderborg/SG-2	20-03-2018	6.0	0.5	0.042	0.01	5.8	0.5	0.66	0.05	11	1.7
Thisted/Thi-5	03-04-2018	10.7	1	0.072	0.02	12.1	1	1.2	0.1	9	1.4
Margretheholm/MAH-2	09-04-2018	13.5	1.5	2.46	0.74	35.1	2	2.4	0.2	49	7.4

Ra-226 and Ra-228 are intermediates formed during decay of U-238 and Th-232 in the Earth's crust. The end products of the decay reactions are Pb-206 [1] and Pb-208 [2], respectively. Most intermediates of the decay chain shown in Appendix 2 have extremely low solubility and will not enter the formation water, but radium is an exception, see [3] and [4]. Lead may also be water soluble depending on the concentration of hydrogen sulfide in the formation water (Kharaka et al. 1987) and has therefore been included in reactions [3] and [4]. The half-lives of the radionuclides are also indicated in reactions [3] and [4].

$^{238}U \rightarrow {}^{206}Pb + 8\ {}^{4}He$ [1]

$^{232}Th \rightarrow {}^{208}Pb + 6\ {}^{4}He$ [2]

$^{238}U\ (4.5x10^{9}\ y) \rightarrow \rightarrow {}^{226}Ra\ (1600\ y) \rightarrow {}^{222}Rn\ (3.8\ d) \rightarrow \rightarrow {}^{210}Pb\ (22.2\ y)$ [3]

$^{232}Th\ (14x10^{9}\ y) \rightarrow {}^{228}Ra\ (5.75\ y) \rightarrow \rightarrow {}^{228}Th\ (1.9\ y) \rightarrow {}^{224}Ra\ (3.6\ d) \rightarrow \rightarrow {}^{212}Pb\ (10.6\ h)$ [4]

Assuming secular equilibrium for reaction [3], then approximately the same activity concentration for Ra-226 and Pb-210 should be expected, which is apparently not the case since the Pb-210 activity concentration is less than 1% of that of Ra-226 for Sønderborg and Thisted formation waters (Table 3). For Margretheholm, the Pb-210 activity concentration is approximately 20% of that of Ra-226. For comparison it should be mentioned that formation waters from the Bunter sandstone and Rotliegend reservoirs in the North German Basin show roughly the same activity concentration for both Pb-210 and Ra-226, whereas formation waters from Late Triassic reservoirs formed under more humid climate conditions have much lower Pb-210 activity concentrations, usually below detection limit (Degering & Köhler 2016). Produced waters from ten different Norwegian oil fields are also very low with respect to Pb-210 activity concentration, mostly below 0.02 Bq/kg (Norsk olje og gass 2012). Due to degassing during sampling, quantitative measurements of radon (Rn-222), reaction [3], could not be performed.

Regarding migration of radionuclides, the source of radionuclides in the formation water must exist in the reservoir itself and probably quite close to the well bore, since the very short-lived Ra-224 (half-life 3.2 days) is also present in the water. This is in accordance with results of other investigations such as Hammond et al. (1988) and Degering et al. (2015); the latter found the source to be located less than 8 m from the well bore. A large number of data on natural radionuclides in formation waters from oil fields and geothermal operations was presented by Fisher (1998) (Figure 4), who also discussed water rock reaction controlling the concentrations of radionuclides in formation water.

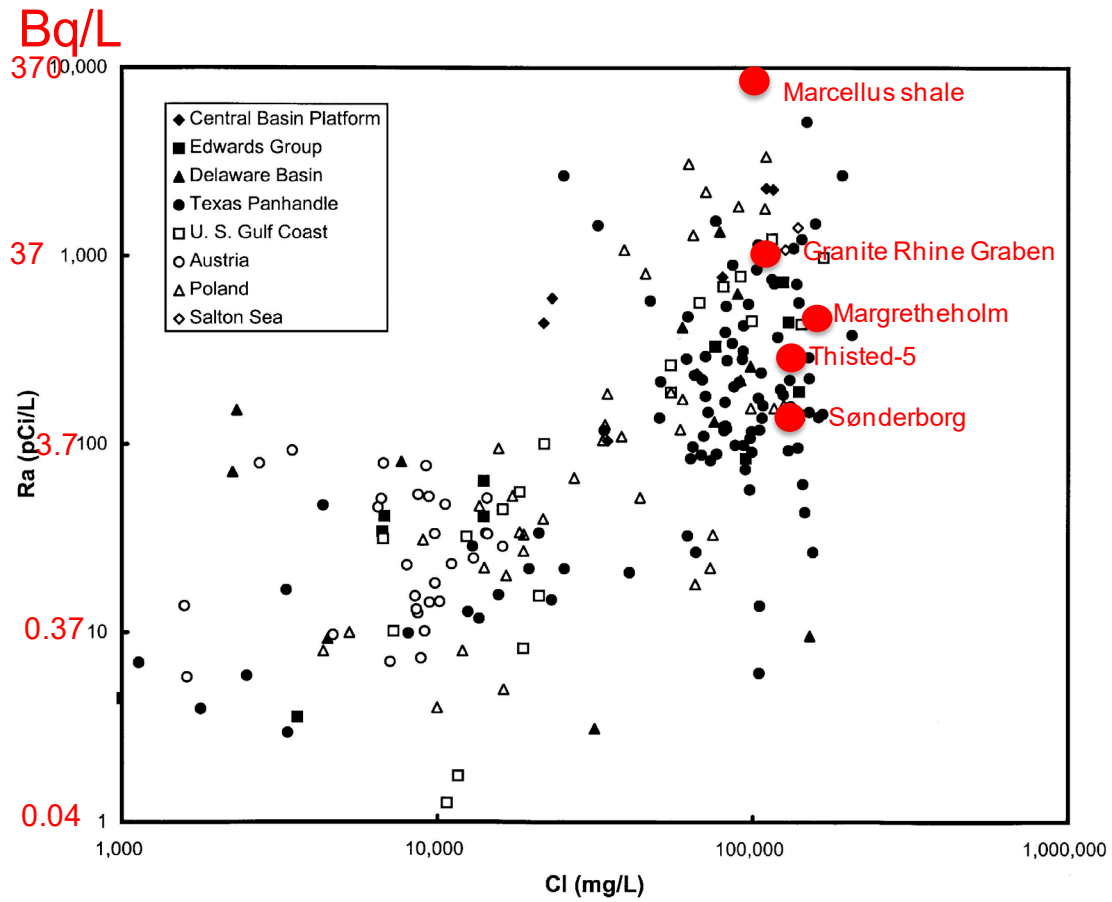

Figure 4: Plot of Ra activity concentration versus Cl concentration (modified from Fisher 1998).

The generally low Ra activity concentration in less saline waters is partly due to adsorption of radium to mineral grains. At higher salinity (above 20,000 mg/L), radium in formation water is mainly controlled by the U and Th content in the rock. Bunter and Rotliegend formation waters of the North German Basin plot between Margretheholm and granite, whereas those in Late Triassic (Rhaet) sandstone plot between Sønderborg and Thisted (Figure 4).

4.3 Characterization of radioactive waste - NORM rules

Operations involving radioactive material require approval by the Danish Health Authority, Radiation Protection (SIS). This includes Naturally Occurring Radioactive Material (NORM) as well. Any material containing one or more radionuclide exceeding the limits listed in BEK 85/2018 (Table 4) should be considered NORM.

Table 4: Exemption limits for natural radionuclide.

Radionuclide	Concentration Bq/g
Pb-210	5
Ra-226	1
Ra-228	2
Th-228	1

For mixtures of radionuclides, the summation rule applies: $\sum_k \frac{C_k}{C_{U,k}} \leq 1$, where C*k* denote the activity concentration of radionuclide *k* and C*U*,*k* denote its exemption limit. By applying the summation rule for the radionuclides in the analyzed formation water, values from 0.009 to 0.032 are obtained, which is far below 1 that is the limit for NORM material (Table 5).

Table 5: Sum of radionuclides in formation water relative to NORM limit including relative ^{210}Pb content.

Locality / Well	Sampling date	$\sum_k \frac{C_k}{C_{U.k}}$	^{210}Pb [Bq]/ sum [Bq] %	Pb (mg/L)	^{210}Pb/Pb (ppb)	^{228}Th/ ^{228}Ra
Sønderborg / SG-2	20-03-2018	0.009	0.3	0.02	0.74	0.11
Thisted / Thi-5	03-04-2018	0.017	0.3	0.004	6.37	0.10
Margretheholm / MAH-2	09-04-2018	0.032	4.6	0.40	2.18	0.07

Furthermore, the radioactivity of lead-210 only makes up 0.3–4.6% of the total radioactivity in the water. Using the half-live of lead-210, the concentration of lead-210 can be calculated from its activity concentration (Table 3), which appears to constitute only 0.74–6.37 ppb of the total lead content (mg/L) in the water (Table 5).

Radionuclide analyses were previously performed on various solid wastes from the three plants, mainly from Margretheholm (Table 6). Using the summation rule, all wastes should be considered TNORM (T for technical), except the bag-filter from Sønderborg. The minor fine more metallic fraction isolated from the filter material (from another filter of the same batch) for a start showed a higher lead content compared to the rest and gave a value of 7. Knowing both the lead concentration in the fine fraction and its activity concentration (GEUS 2016), the lead-210 relative to total lead was calculated showing an extremely low content of 0.58 ppb (Table 6) comparable to the formation water of 0.74 ppb (Table 5).

Radionuclide analysis on total filter was performed on the ash residue after ignition, thereby reducing its weight to about one fifth. The bag-filter itself was made up of a plastic polymer.

Lead-210 accounted for only 11% of the total radioactivity of all of the filter content, but reached almost 89% in the fine more metallic fraction (Table 6).

Table 6: Sum of radionuclides in various solid wastes relative to NORM limit including relative ^{210}Pb content.

Sample type	Locality/Well	Date	$\sum_k \frac{C_k}{C_{U.k}}$	^{210}Pb [Bq]/ sum [Bq] %	Pb %	^{210}Pb/Pb (ppb)	^{228}Th/ ^{228}Ra
Bottom hole solids	MAH-2	11-10-2015	167	95.9	~80	0.32	0.20
Bag-filter, workover	Margretheholm	04-11-2015	95	72.0			0.73
Cartridge filter, workov.	Margretheholm	24-11-2015	29	82.7			0.72
Bag-filter, start-up	Margretheholm	06-02-2017	99	89.1			0.46
Bag-filter, 78 days run	Margretheholm	05-05-2017	110	67.6			0.28
Coating heat exchanger	Margretheholm	09-08-2016	952	<0.01			0.50
Bag-filter, 6 months run	Sønderborg	04-12-2015	3*)	11.2			0.77
Bag-filter, fine fraction	Sønderborg	14-07-2015	7	88.6	1.3	0.58	1.22
Bag-filter, fine fraction	Thisted/Thi-2	29-01-2018	2	54.6			

*) Value for ash residue. Correcting for weight loss on ignition, a value of 0.5 obtained.

The higher lead-210 activity of the fine fraction is due to its higher lead content of 1.3% compared to the lead content in the total filter <0.2%. The higher lead content is related to the higher iron/corrosion product content in the metallic fraction. Lead is being deposited on iron due to galvanic corrosion according to reaction [5] (TNO 2014).

$Pb^{2+} + Fe \rightarrow Pb_{metallic} + Fe^{2+}$ [5]

The reason why the radioactivity exceeds the NORM limit for most solid wastes from Margretheholm is the relatively high lead content, caused by deposition of lead (from formation water) due to galvanic corrosion (GEUS 2017a). An exception is the grey coating on the heat exchanger plates, which consisted of a mixture of barium and strontium sulfate. Radium share chemical characteristics with strontium and barium that belong to the same group in the periodic table, which forms low-soluble sulfates. Heat exchanger plates in the Margretheholm plant are made of titanium, which do not undergo galvanic corrosion with lead.

The percentage of lead in each of the Margretheholm solid samples analyzed for their specific radioactivity was not determined, so lead-210 relative to total lead could not be estimated. However, the bottom-hole sample from the MAH-2 production well appeared to be pure lead, and assuming a percentage of 80, a value of 0.32 ppb is obtained (Table 6), which is less than that for formation water of 2.18 ppb, but still of the same order of magnitude.

The age of the solids may be determined from the thorium-228/radium-228 ratio by exploiting their different half-lives of 1.9 and 5.75 y respectively, reaction [4] (Zielinski et al. 2001). When comparing the thorium-228/radium-228 ratio of the various solids from Margretheholm with the change in this ratio with age (Table 7), most solids appear to be only a few years old. When comparing bag-filters containing material from workover and start-up, they appear to be older than a bag-filter used during normal steady operation for 78 days (Table 6).

Table 7: Change in relative thorium-228/radium-228 ratio with age.

t (y)	0.5	1	2	3	4	5	6	7	8	9	10	15
228Th /228Ra	0.17	0.32	0.58	0.78	0.93	1.05	1.15	1.22	1.28	1.33	1.36	1.46

4.4 Geochemistry of rock samples

The distribution of U and Th in the Bunter and Gassum Fm is investigated, because minerals or organic material within the reservoirs are likely to have sourced the radionuclides that causes the NORM problems, so the contents of relevant elements in the rocks can be compared to the radionuclide concentrations in the produced water. From Margretheholm-1, the sampling included all cuttings samples from Gassum Fm and all cuttings samples from the injection interval in Bunter Fm. Similarly from Sønderborg-1, where all cuttings samples from the injection interval were sampled. From Thisted-3, sampling was primarily done in the cored section of the injection interval, besides a few cuttings samples.

The correlation between data obtained from XRF and ICP-MS analyses is fairly good, with R^2 values e.g. of 0.89 for Al, 0.85 for Ti, 0.97 for Zr, 0.77 for Pb and 0.60 for Th. Thus, the element concentrations measured by the fast and cheap HH-XRF method are adequate for a screening of samples. However, it cannot be used to give reliable results of elements present in very low concentrations such as U that for most of the samples occurs in amounts below the XRF detection limit.

The handpicking of cuttings fragments with division of the samples into sandstone and claystone fragments has been successful, as evident by the significantly higher Al-content observed in far most of the claystone samples as compared to the sandstone samples from the Margretheholm-1 and Sønderborg-1 wells (Figures 5–8). When comparing these results of the cuttings samples with those of the core samples from Thisted-3 (Figure 9), there appear to be more variation in Al-content among the sandstones from the core samples, which presumably reflects that a larger lithological variation exists than what can be revealed by sorting of cuttings fragments from a meter-thick depth interval.

The sandstones of the Bunter and Gassum Fm are comparable with regards to their chemical composition, except for some of the mobile elements such as Ca and Mg, and also the claystones from the formations are quite alike (Table 8). U occurs in low amounts of 1–4 ppm in all analyzed samples, Th is present in amounts of 2–21 ppm and Pb amounts to 5–25 ppm. The two samples with highest U-content are from Thisted-3 and they are enriched in other trace elements too including Cr and Zr, which shows that the samples have high contents of heavy minerals.

The correlation between U and Al concentrations is poor in the analyzed samples, reflecting that U does not preferentially reside in the fine-grained sediments (Figure 10). The correlation between U and both Ti and Zr is better, indicating that much of the U may be present in heavy minerals such as Ti-minerals and zircon. Zr and hence zircon is more abundant in the sandstones than in claystones in both formations, whereas Ti is most abundant in the claystones, indicating that Ti apart from heavy minerals also is residing in clay minerals (Table 8, Figure

11). There is no clear correlation between Pb and Fe, which shows that Pb must be residing in other minerals additional to pyrite (Figure 12). The total amount of Pb in the sandstones is slightly higher in the Bunter Fm than in the Gassum Fm (Table 8).

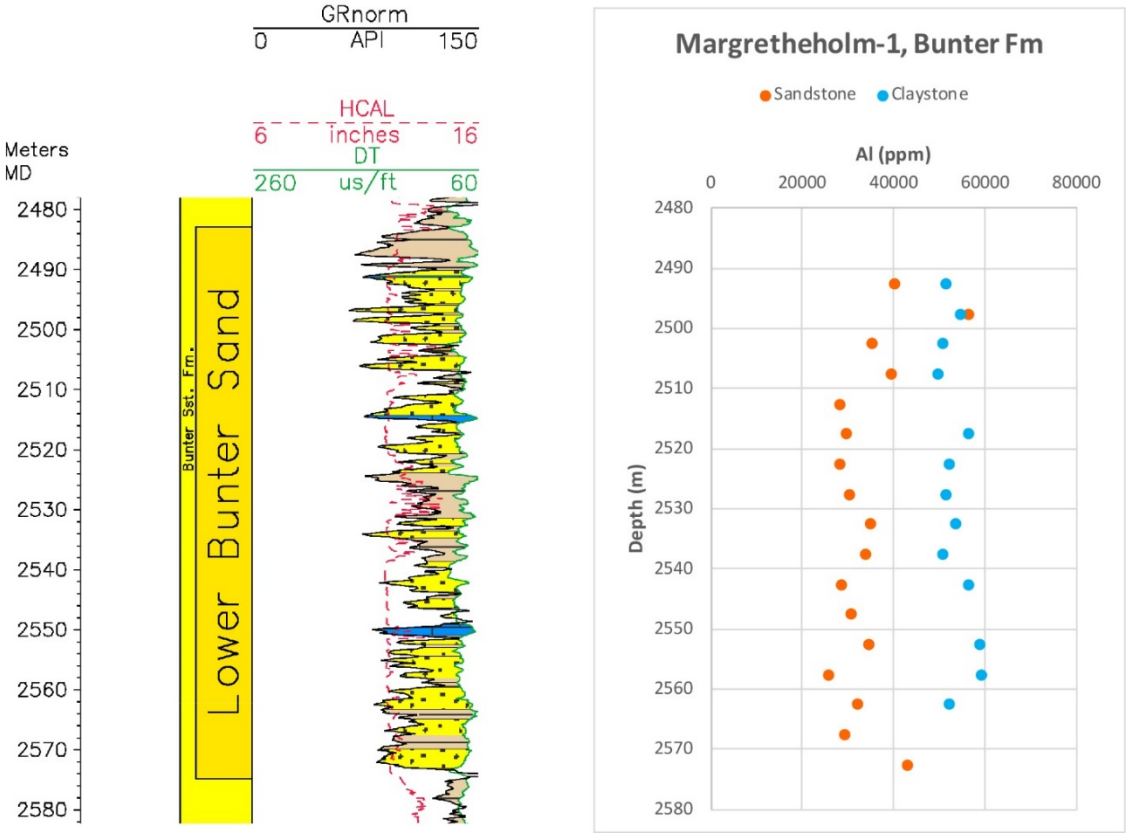

Figure 5: Well logs and Al content based on XRF of cuttings samples from the Margretheholm-1 well.

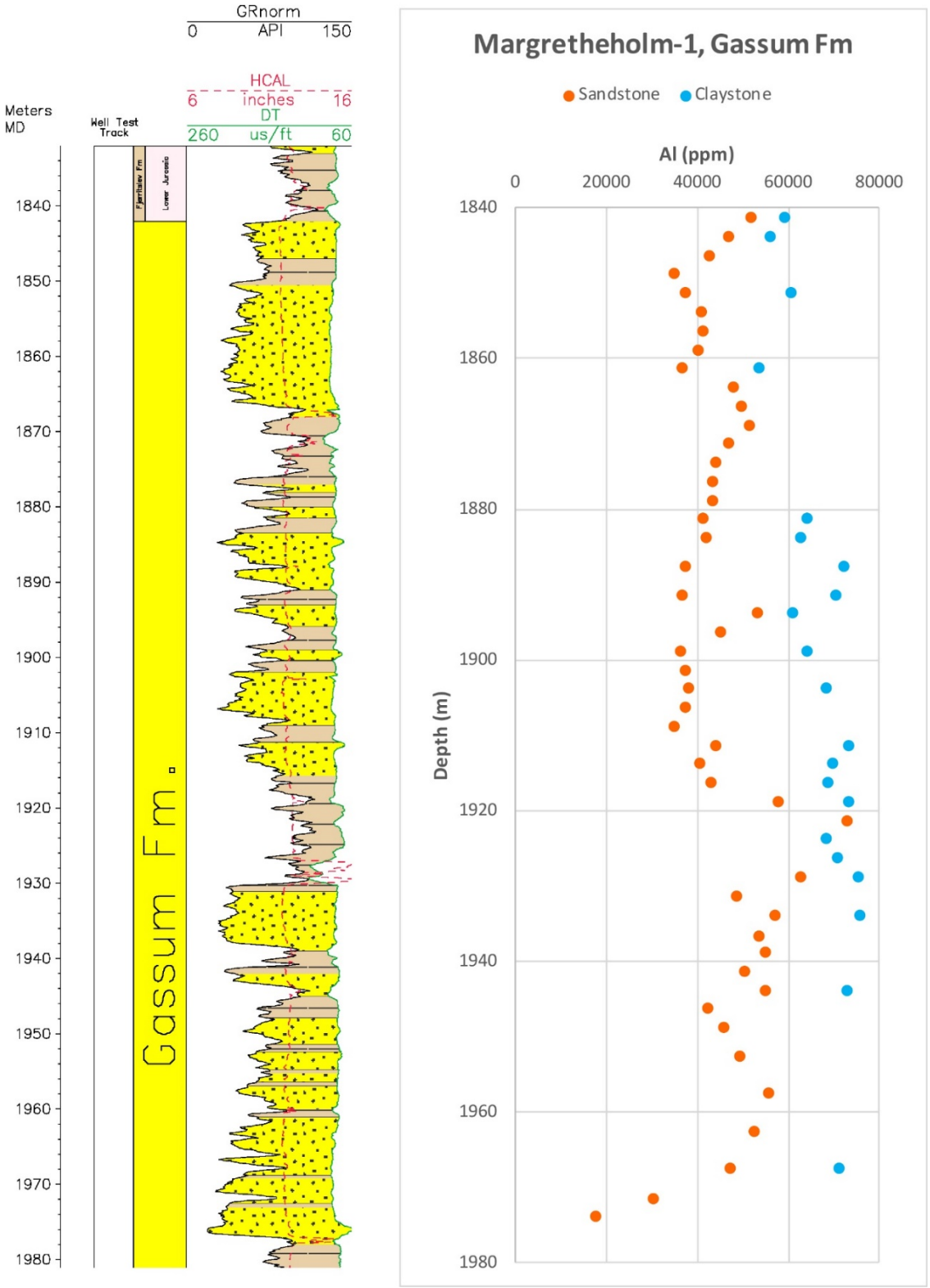

Figure 6: Well logs and Al content based on XRF of cuttings samples from the Margretheholm-1 well.

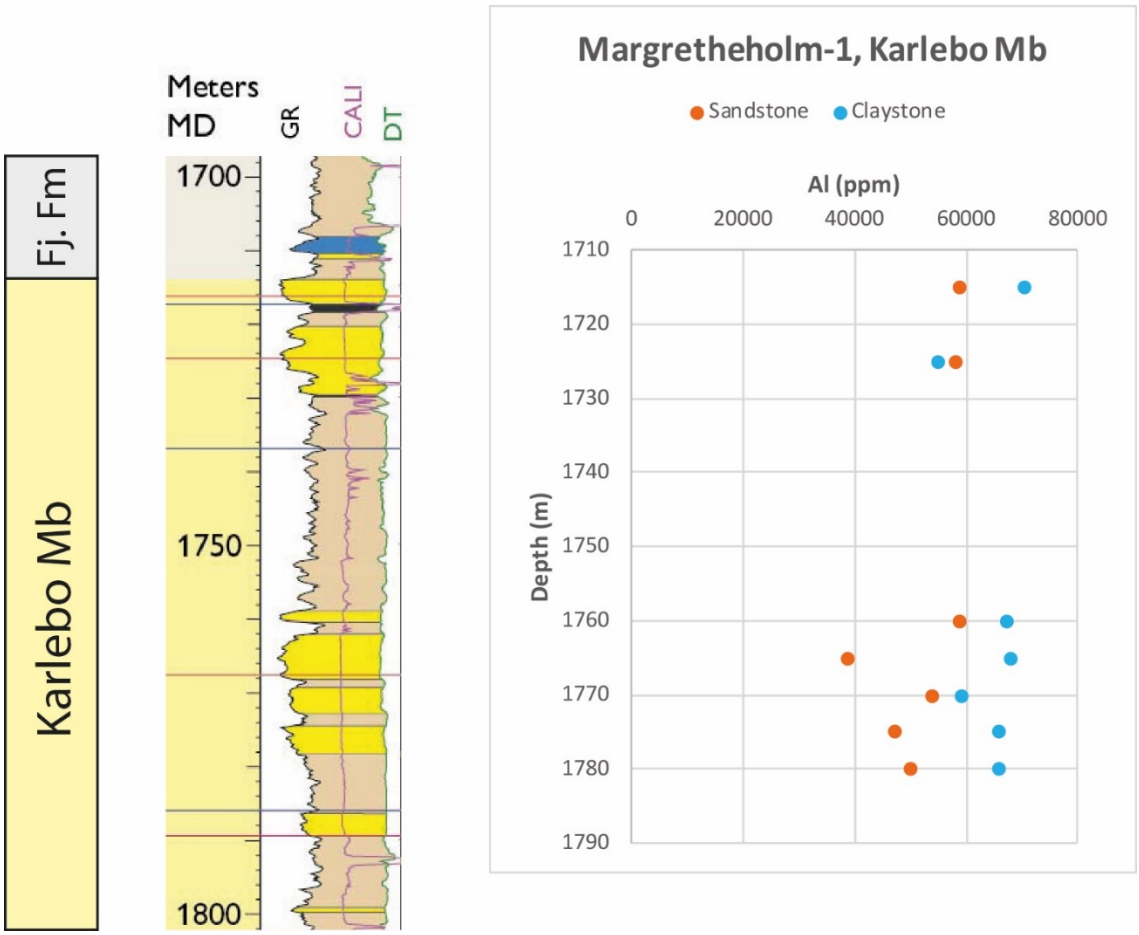

Figure 7: Well logs and Al content based on XRF of cuttings samples from the Margretheholm-1 well.

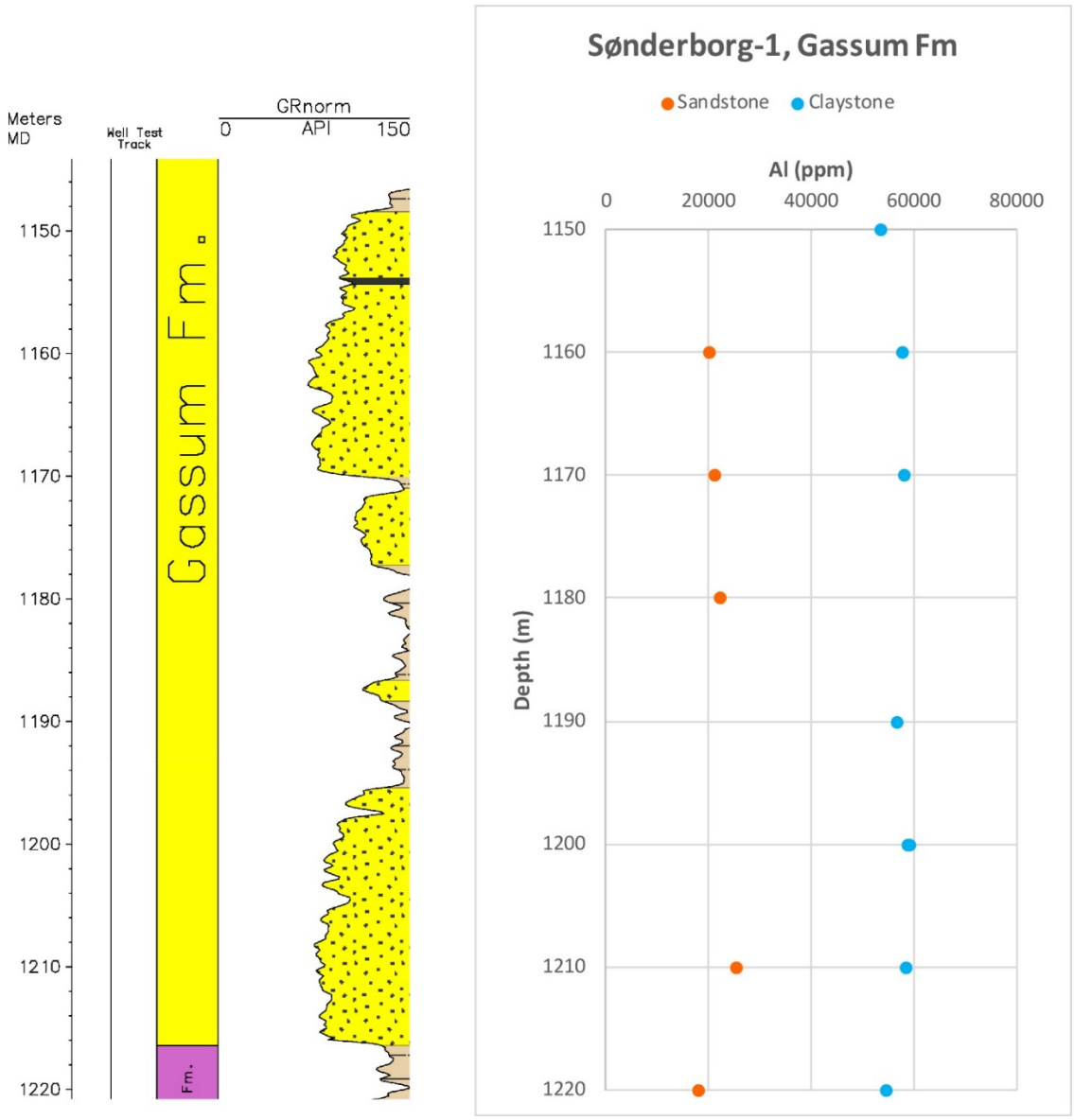

Figure 8: Well logs and Al content based on XRF of cuttings samples from the Sønderborg-1 well.

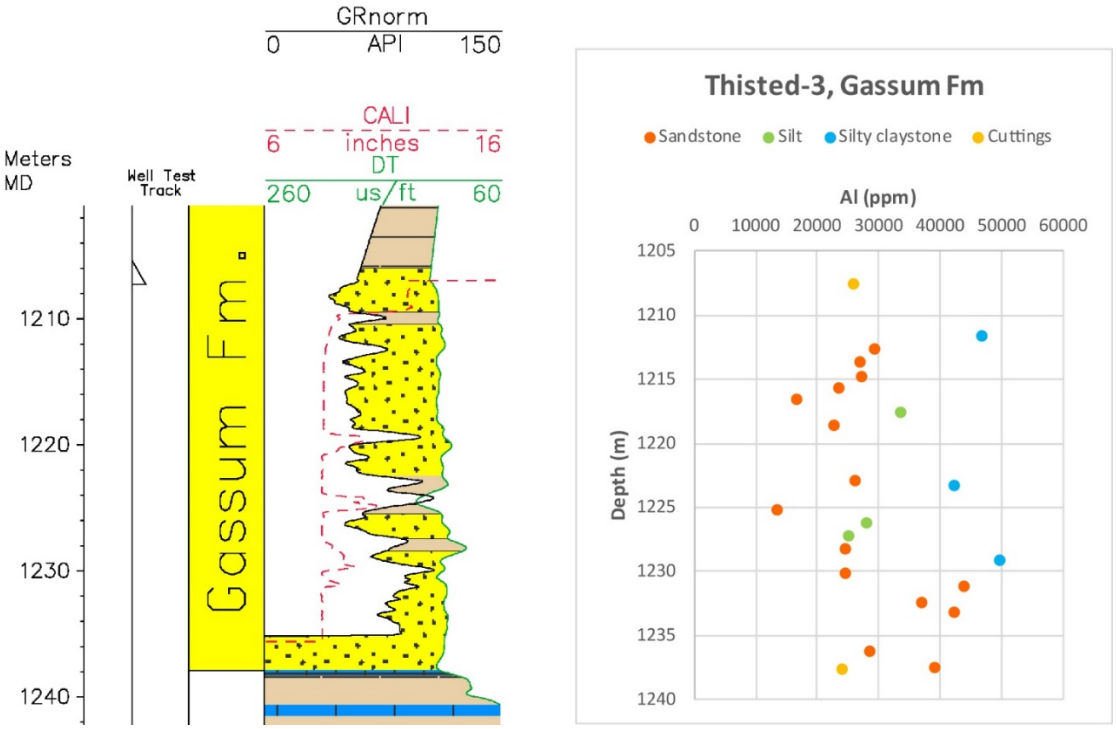

Figure 9: Well logs and Al content based on XRF of core samples from the Thisted-3 well.

Table 8: Selected results of ICP-MS analysis of samples from Gassum and Bunter Fm.

Stratigraphy	Well	Depth	Lithology	Al (%)	Ti (%)	Zr (ppm)	Pb (ppm)	Th (ppm)	U (ppm)
Gassum Fm	Thisted-3	1214.67	Sandstone	2.88	0.12	119.88	12.92	2.61	0.99
		1218.58	Sandstone	2.85	0.24	251.22	14.55	3.22	1.26
		1222.80	Sandstone	3.64	0.55	960.03	9.33	20.69	4.21
		1227.10	Sandstone	2.35	0.35	406.87	11.78	7.46	2.48
		1229.10	Claystone	6.57	0.53	327.68	18.39	13.04	4.12
		1232.30	Sandstone	4.38	0.36	444.98	12.18	7.73	2.39
		1236.20	Sandstone	3.46	0.32	201.93	16.08	5.73	1.08
Gassum Fm	Sønderborg-1	1160.00	Claystone	11.10	0.62	210.56	18.66	12.05	3.01
		1160.00	Sandstone	2.11	0.20	124.76	5.38	2.36	0.64
		1200.00	Claystone	10.73	0.63	248.74	15.13	11.27	2.86
		1200.00	Sandstone	10.52	0.77	342.79	10.55	11.57	3.16
Gassum Fm	Margretheholm-1	1841.25	Sandstone	6.55	0.53	361.93	13.09	11.58	2.99
		1856.25	Sandstone	4.88	0.47	417.74	9.40	9.33	2.67
		1883.75	Claystone	9.23	0.66	263.99	15.60	14.19	3.00
		1883.75	Sandstone	5.65	0.43	300.64	10.07	9.09	1.92
		1896.25	Sandstone	5.88	0.46	379.18	13.08	9.46	2.29
		1913.75	Sandstone	5.32	0.50	471.51	15.08	10.11	2.89
		1933.75	Sandstone	11.74	0.60	215.00	15.99	12.01	2.92
		1948.75	Sandstone	6.44	0.48	359.79	13.05	7.24	2.19
		1967.50	Claystone	12.14	0.65	220.59	25.02	11.72	2.60
		1967.50	Sandstone	7.02	0.53	368.55	12.81	8.37	2.22
Bunter Fm	Margretheholm-1	2492.50	Sandstone	5.32	0.46	536.25	14.90	10.15	2.87
		2507.50	Claystone	7.54	0.55	225.20	16.09	12.28	2.82
		2507.50	Sandstone	5.34	0.43	341.19	17.01	11.05	2.40
		2532.50	Claystone	7.65	0.50	175.69	15.98	11.85	2.79
		2532.50	Sandstone	4.99	0.38	200.53	13.97	8.59	2.19
		2552.50	Claystone	8.00	0.57	202.02	15.18	11.98	2.70
		2552.50	Sandstone	4.64	0.35	244.97	15.42	8.24	1.45
		2572.50	Sandstone	6.11	0.43	294.32	21.36	11.54	2.45
Gassum Fm, sandstones (average values)				5.35	0.43	357.93	12.21	8.66	2.27
Gassum Fm, claystones (average values)				9.95	0.62	254.31	18.56	12.45	3.12
Bunter Fm, sandstones (average values)				5.28	0.41	323.45	16.53	9.91	2.27
Bunter Fm, claystones (average values)				7.73	0.54	200.97	15.75	12.04	2.77

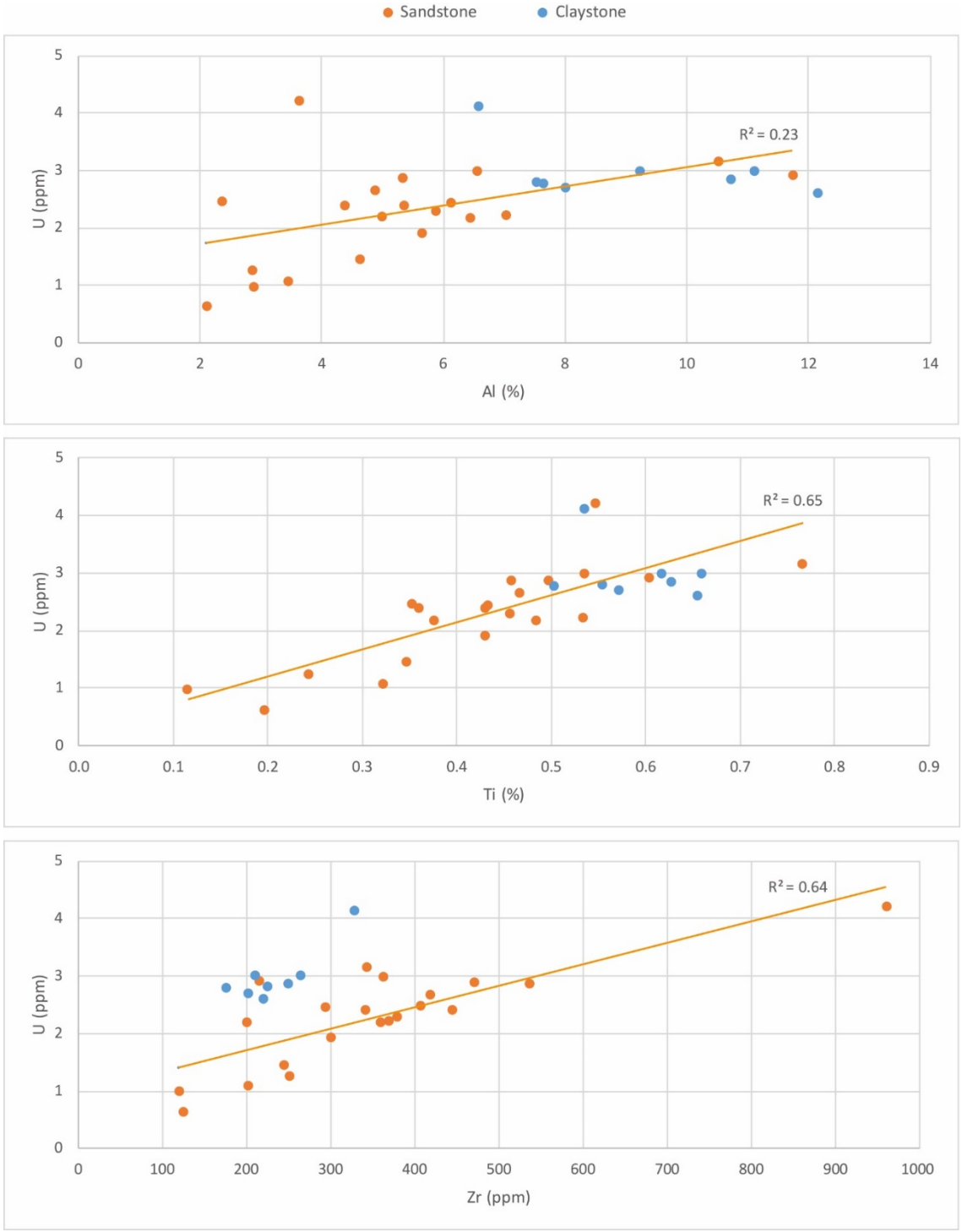

Figure 10: Element concentrations based on ICP-MS analyses of Bunter and Gassum Fm (see Table 8). The trendlines are calculated from the sandstone samples.

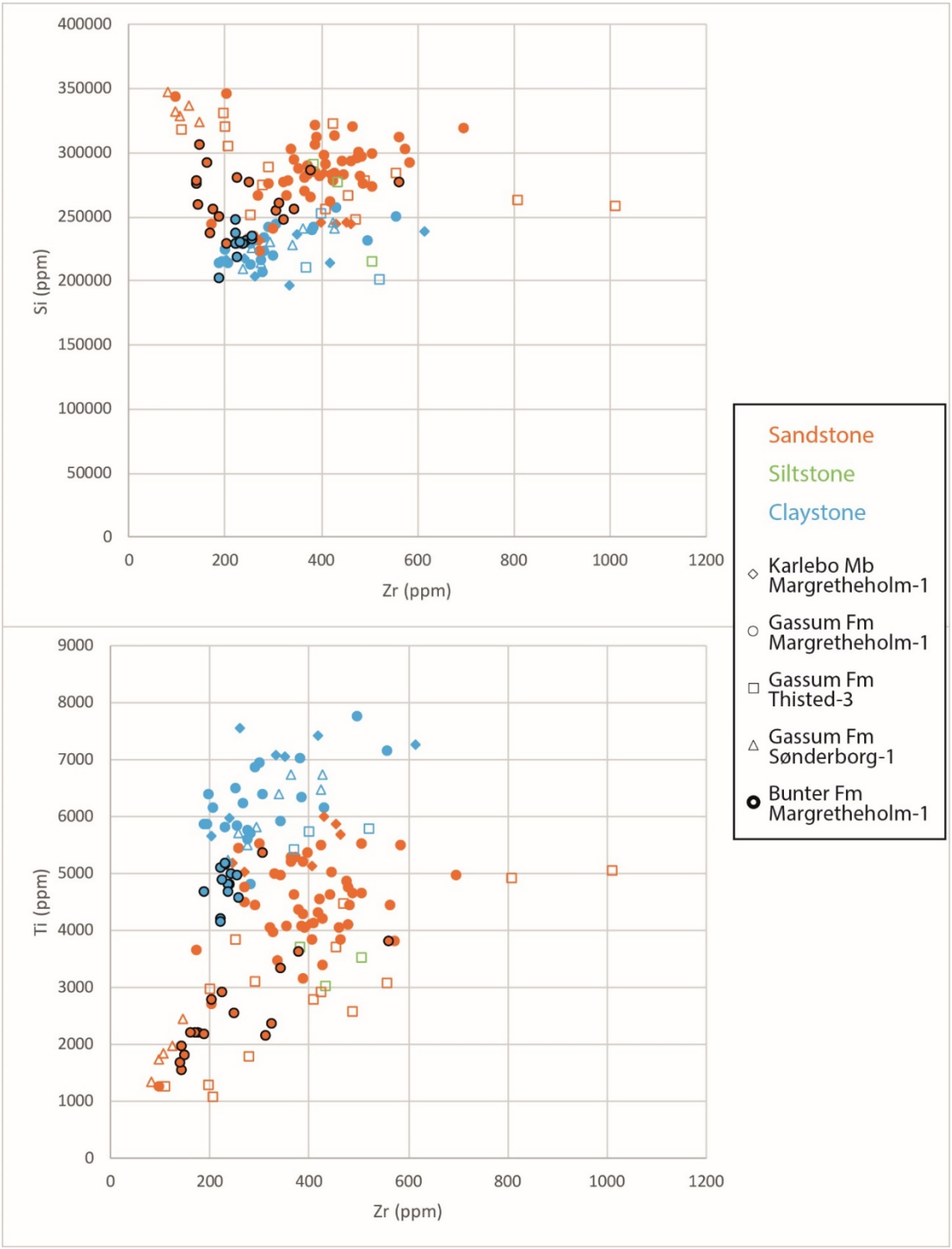

Figure 11: Element concentrations based on HH-XRF analyses.

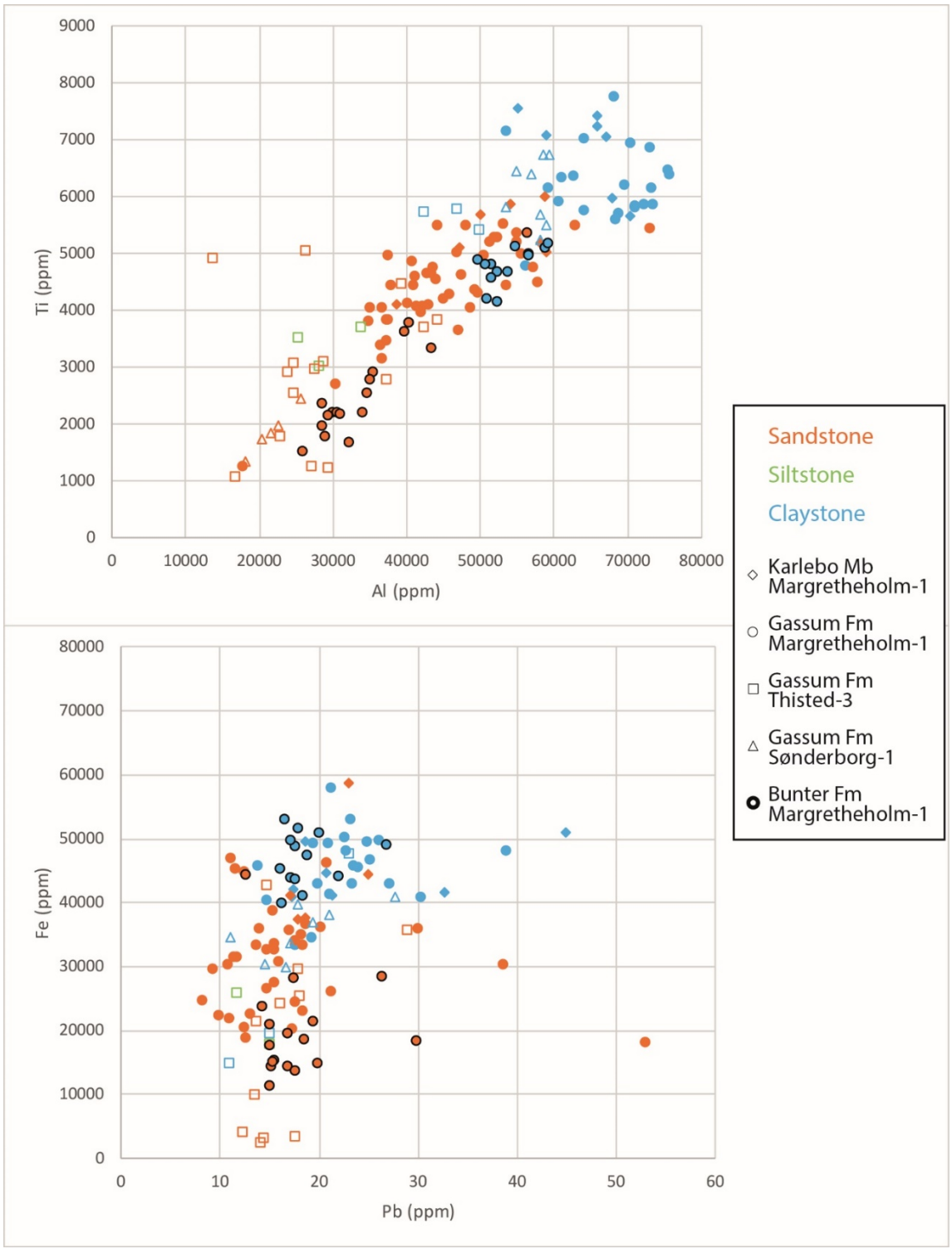

Figure 12: Element concentrations based on HH-XRF analyses.

4.5 Geochemical core scanning

The aim of the scanning was to evaluate the distribution of radioactive elements in the drill-core. The purpose of this is to try to understand in which geological units and minerals the radioactive elements are located in the subsurface. Two cores from Thisted-3 were scanned (Figure 13) since they are from Gassum Fm that is used for geothermal production in Thisted, whereas cores do not exist from the Bunter or Gassum Fm in Copenhagen.

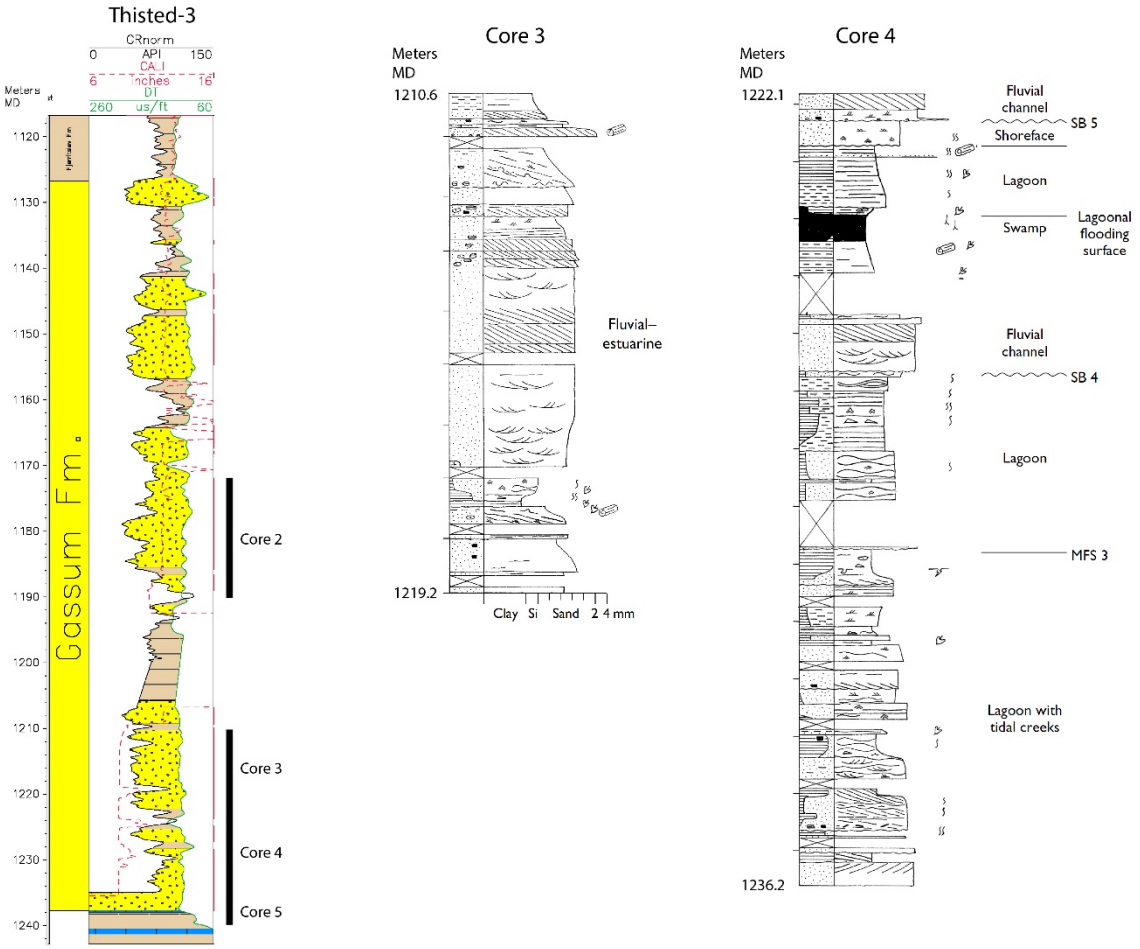

Figure 13: Position of core 3 and 4 from the Thisted-3 well shown on well logs. The lithological logs of the cores are from Nielsen (2003).

In core 3, the uppermost part of the scanned section is very rich in Ca, which is an expression of the calcareous (marly) nature of the sediment here (Figure 14). Below this marly layer there is a c. 1.5 m thick sequence characterized by elevated contents of Zr (c. 500–1000 ppm Zr) and Ti (c. 0.3–0.7% TiO_2) with three peaks with >3000 ppm Zr and >1.5% TiO_2. These peaks are likely to represent heavy mineral rich laminae enriched in zircon (Zr) and ilmenite and rutile (Ti). Presumably, the contents of Zr and Ti in this 1.5 m thick sequence are primarily caused by their presence in mica and clay. The sandy sequence at c. 1212.5–1217.0 m shows an upwards increase in Al and decrease in Si indicating an upwards-fining sequence. Near the base of this sandy interval at c. 1216.9 m, a few Zr and Ti peaks suggest the presence of heavy mineral enriched layers. The lower part of core 3 seems to be rich in clay and mica minerals with high contents of Al and Fe, and the contents of Zr and Ti contained in the clay and mica are elevated.

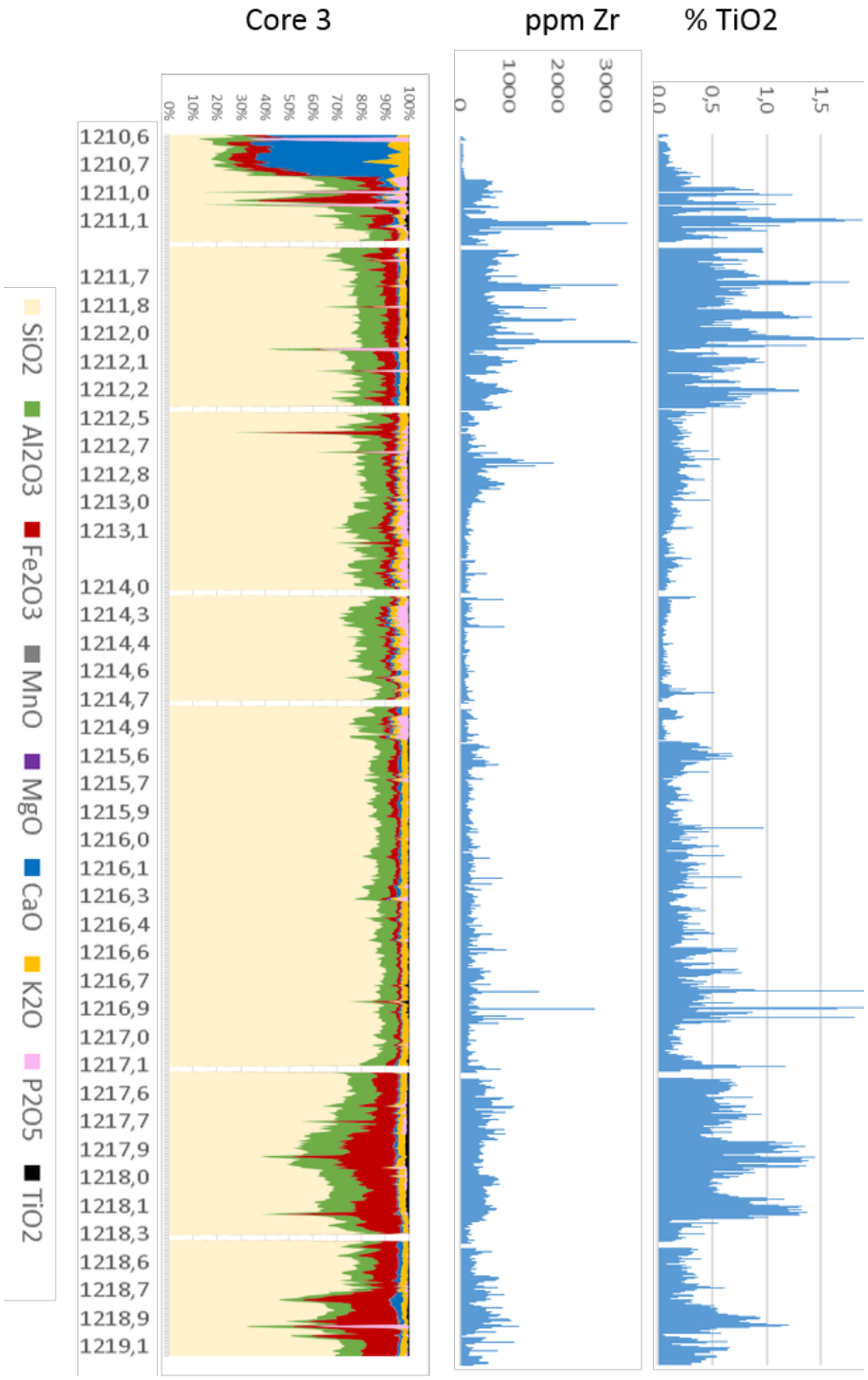

Figure 14: XRF scanning results from Thisted-3, core 3. Major elements are adjusted to 100%.

Core 4 consists of alternating Si-rich (sandy) and Al/Fe-rich (clayey) intervals. In the top of the section, there is a sandy unit with a remarkable feature where a narrow peak in U, TiO_2 and Zr contents coincides at 1222.35 m (Figure 15). This peak is interpreted as caused by high contents of heavy minerals with U and Zr located in the mineral zircon and Ti in ilmenite and rutile. The content of Zr is elevated in the interval at c. 1222.5–1223.2 m. This is probably tied to elevated contents of zircon, but it can be noted that U is relatively low here compared to the thin heavy mineral layer just above. The lignite layer at c. 1225.2–1226.2 m has elevated U content. At the base of this layer at c. 1225.9 m, the U and Zr contents are coupled suggesting that both U and Zr are contained in zircon. The high SiO_2 content in this lignite interval is an artefact since the total is adjusted to 100%. At 1231.7 and 1231.8 m, there are two narrow peaks in the U, TiO_2 and Zr contents. This feature is presumably caused by high contents of heavy minerals with U and Zr located in zircon and Ti in ilmenite and rutile, similarly to the peak in the top of the core.

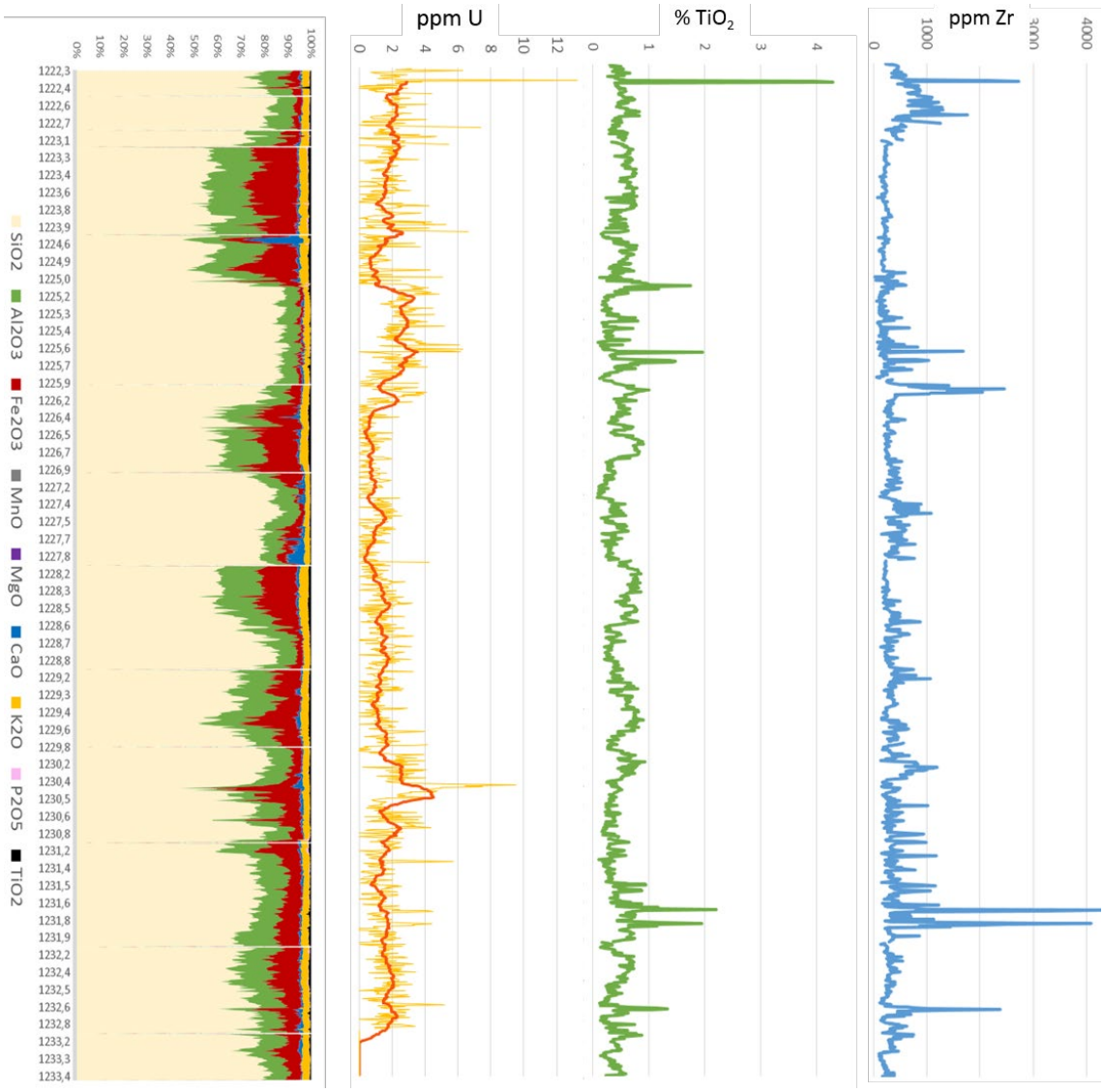

Figure 15: XRF scanning results from Thisted-3, core 4. Major elements are adjusted to 100%. Red line in U is floating average (over 20 measurements).

4.6 Mineral and element mapping

Mineralscan and element mapping of selected samples was conducted to investigate if Pb may have precipitated in cementing minerals in the reservoir and to understand the mineralogical maturity of the sediment which may give input to the interpretation of possible U-sources.

Mineralscan performed by SEM on thin sections gave especially good results on the core sample from Gassum Fm in Thisted-3 and on the cuttings sample from Gassum Fm in Margretheholm-1 for which the cuttings are particularly well preserved (Figure 16). The cuttings samples from Bunter Fm in Margretheholm-1 were largely separated into single grains during drilling so the mineralscans of these samples cannot give a porosity estimation or indications of the texture, but still provide usable information about grain-size parameters and mineralogical composition of the sandstones (Figure 17). The mineral maps of the scanned areas are shown in full in Appendix 6 along with tables summarizing their composition. Nuggets of drilling mud with enclosed sandstone fragments in the sample from Bunter Fm in Margretheholm-1 at 2502.50 m makes the data unrepresentative of the sandstone composition, seen for example as an overrepresentation of biotite in the results. Similarly, the results from Gassum Fm in Sønderborg-1 are not representative for the reservoir sandstone since mudstone fragments have been preferentially preserved in the cuttings fragments.

The mineralscans from Gassum Fm in Margretheholm-1 and Thisted-3 show that the sandstones are quite similar in terms of texture and porosity distribution (Figure 16). However, the proportion between quartz and feldspar grains is different with the most quartz-rich sandstone present in Margretheholm-1 whereas albite and K-feldspar are common constituents in the sandstone from Thisted-3. K-feldspar is also common in Bunter Fm in Margretheholm-1, but the grain size parameters are very different from the Gassum Fm since the Bunter Fm samples consist of grains that are larger and more angular (Figure 17) indicating a more local provenance.

Element mapping of pyrite cement was performed to investigate if the mineral binds Pb during its growth (Figure 18). EDS analysis showed a normalized stoichiometric concentration of 0.3% Pb centrally in pyrite cement in a sample from Gassum Fm in Margretheholm-1, and larger amounts were found along the rims of the cement so pyrite may keep on building in Pb even after its growth phase has ceased. Only small amounts of pyrite have formed in Bunter Fm due to its arid depositional conditions, so less Pb is likely to have been bound in authigenic minerals in Bunter Fm as compared with Gassum Fm.

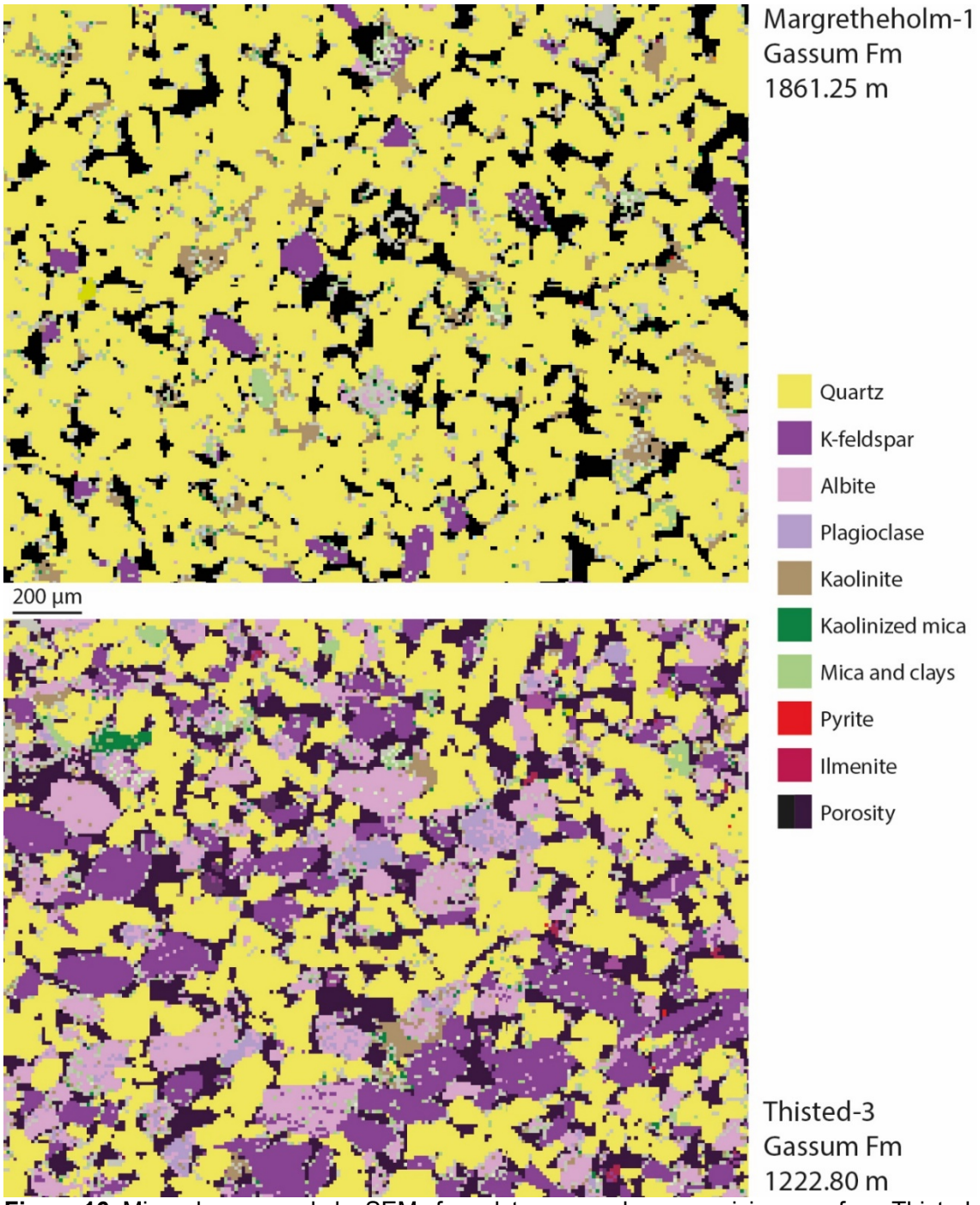

Figure 16: Mineralscans made by SEM of sandstone samples, comprising core from Thisted-3 and well-preserved cuttings from Margretheholm-1.

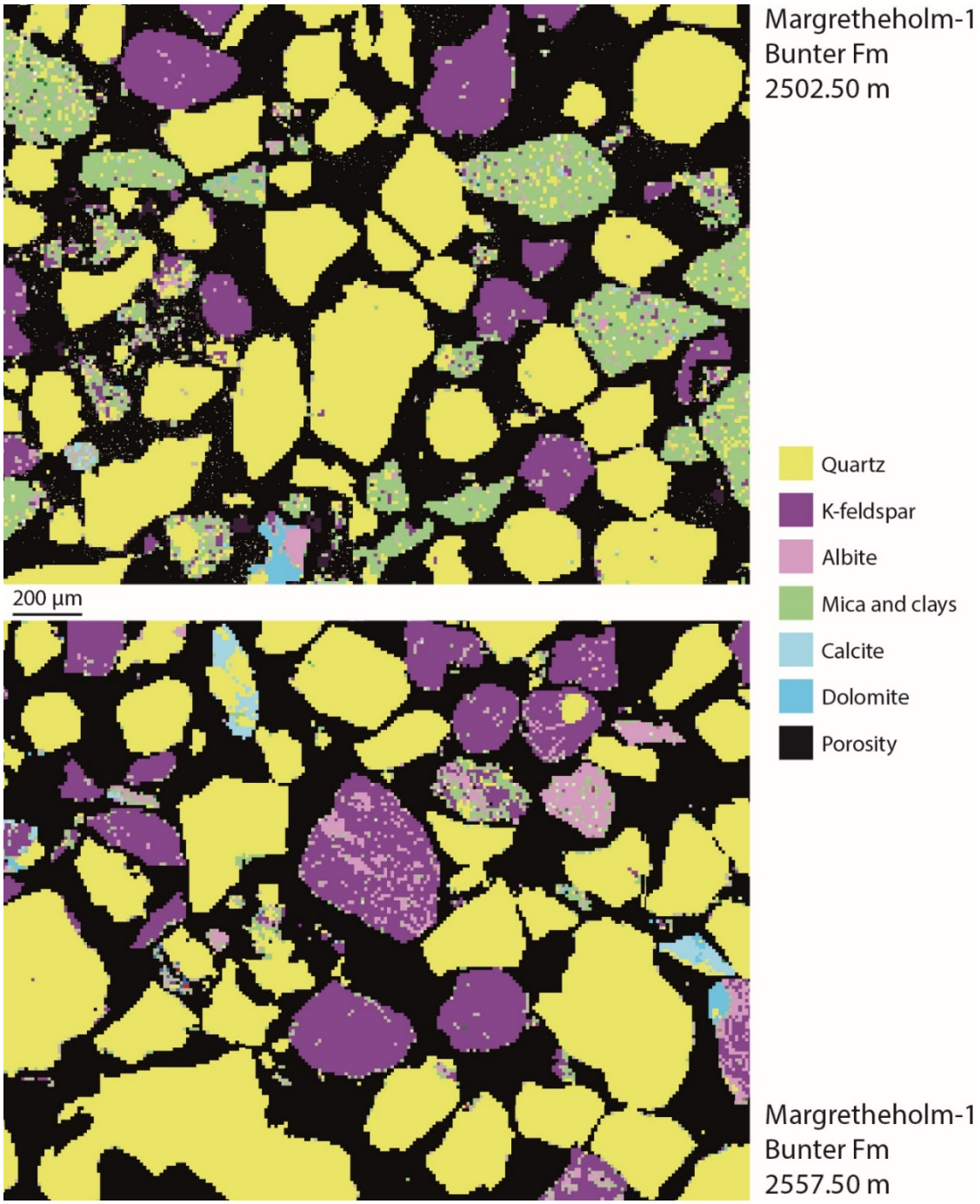

Figure 17: Mineralscans made by SEM of cuttings fragments of sandstone.

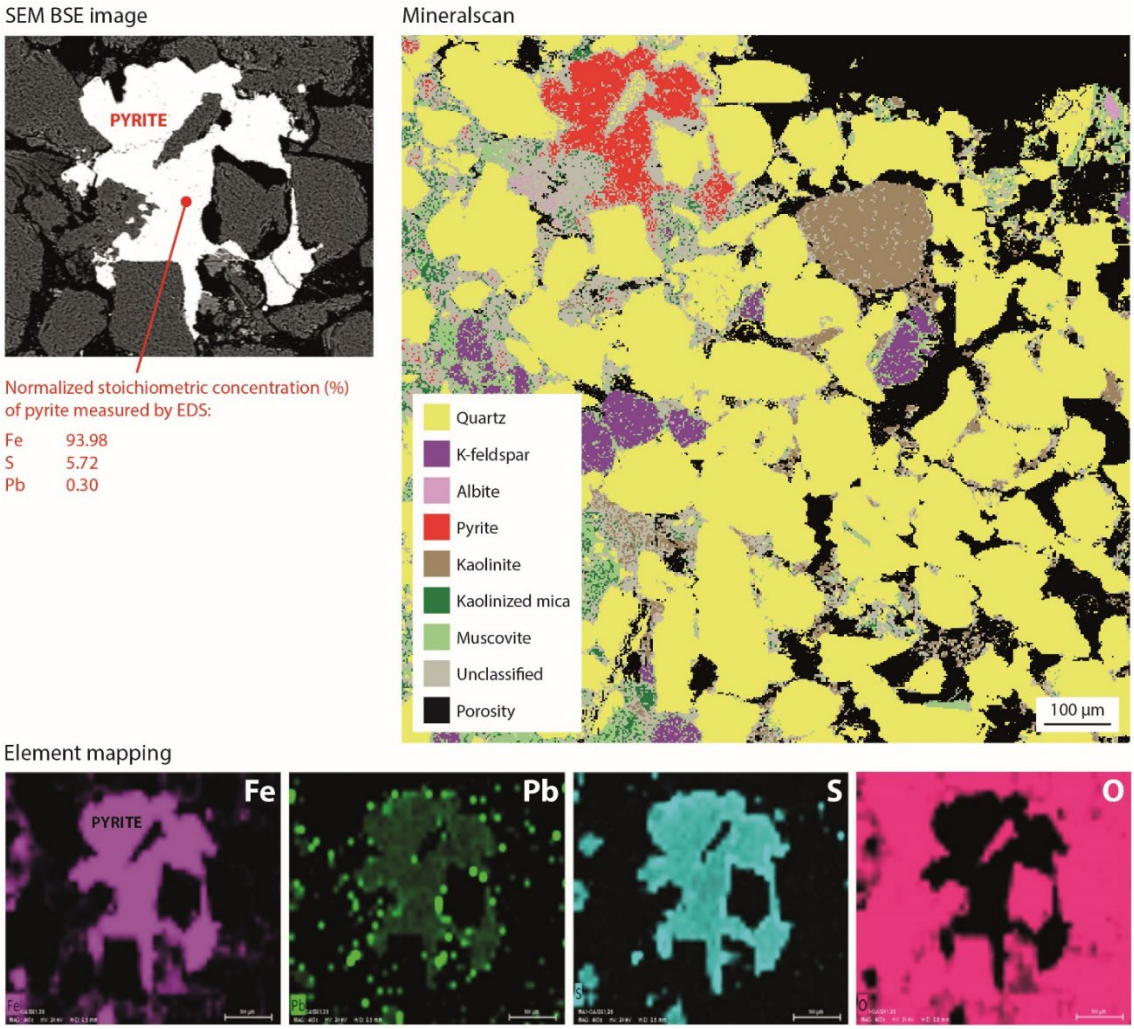

Figure 18: Mineral and element mapping made by SEM of pyrite cement from Gassum Fm sandstone from the Margretheholm-1 well at 1861.25 m.

4.7 Heavy mineral assemblage

Mapping of heavy mineral concentrates with measurement of their composition was done to identify possible sources of radionuclides and the possible differences between Bunter and Gassum Fm.

Analysis of the heavy mineral assemblage by CCSEM turned out to be difficult in some of the cuttings samples. This was probably because the material was unintentionally weight separated prior to sampling of the cuttings at the drilling rig, whereby most heavy mineral grains have been excluded from the samples. Therefore, two of the samples are not included in the results because of their too low contents of relevant grains, and instead have three core samples from Stenlille wells been included to give a reliable estimate of the heavy mineral composition of Bunter versus Gassum Fm (Figure 19).

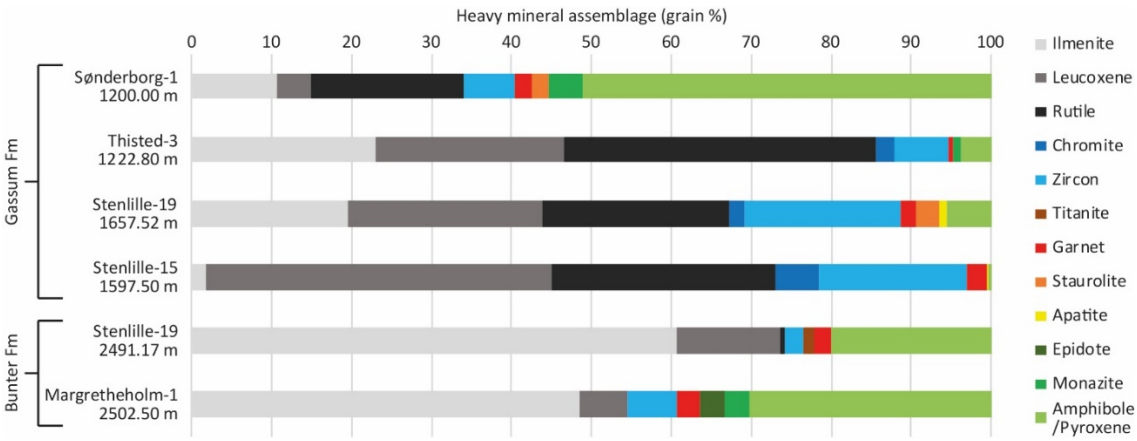

Figure 19: Heavy mineral assemblages analyzed by CCSEM.

The heavy mineral assemblages of Bunter Fm in Margretheholm and Stenlille have large ilmenite content, whereas the Gassum Fm in Stenlille, Sønderborg and Tønder have larger contents of the altered Ti-minerals; leucoxene and rutile. The largest amounts of zircon are found in Gassum Fm in Stenlille, whereas the content in Sønderborg is diluted by a large amount of amphibole/pyroxene, which indicates a local source for some of the sediment. All sediment in Bunter Fm could be derived from a single source, whereas the imbalance between mature and immature components in Gassum Fm in Sønderborg indicates a mixture between several sediment supplies. The marked dominance of mature components in Gassum Fm in Stenlille and Thisted show that the sediment has been reworked or transported a long distance prior to deposition.

4.8 U-content in heavy minerals

Analysis of the U content and radiometric age of a large number of heavy mineral grains from both Bunter and Gassum Fm were carried out in order to investigate if specific sources of radionuclides could be identified, and to estimate the sediment maturity by determining the provenance of the sediment.

The LA-ICPMS analyses of zircon show that some of the grains from both the Bunter and Gassum Fm have high contents of U, Th and Pb (Figure 20). However, the highest values are found in zircons from Bunter Fm, which also have the highest average amounts of all three elements (Table 9). On the other hand, the CCSEM analyses show that zircon may in general constitute a smaller proportion of the heavy mineral assemblage in Bunter Fm than in Gassum Fm (Figure 19), and the geochemical results show that the total amount of Zr and hence zircon is comparable between the formations (Table 8).

In general, the total amount of U, Th and Pb present in zircon grains may thus be approximately equal in the two formations. A screening of in-house zircon data from Bunter/Skagerrak Fm in other areas of Denmark show a similar pattern as the new zircon data from Bunter Fm in Margretheholm including some grains with particularly high amounts of U, Th and Pb. This indicates that metamict zircons occur in this formation and, although not abundant, that the metamict zircon grains might constitute a potential significant source for the supply of radionuclides into the formation water.

Rutile was the only other U-rich mineral that occurred in amounts large enough for analysis, however, only a single rutile grain was located in the Bunter Fm, whereas more grains were present in Gassum Fm (Figure 21). The contents of U, Th and Pb are much smaller in rutile than in zircon (Table 9). Thus, combined with the very low fraction of rutile in Bunter Fm in Margretheholm, rutile can be excluded as a possible source of radionuclides to the formation water.

When applying the LA-ICPMS results for calculation of radiometric ages, it is clear that the sediment in Bunter Fm in Margretheholm was supplied from a local source area as evident by the narrow age distribution (Figure 22). The zircon ages show the age of the basement in which the mineral formed. During erosion, the zircon grains were transferred into the sedimentary system where they may have experienced several episodes of reworking and sedimentation. Comparison of the zircon age distributions of the Gassum and Bunter Fm demonstrates that the Gassum Fm contains a wider spectrum of ages signifying sediment supply from several provenance areas. Especially the age distributions from Margretheholm-1 and Sønderborg-1 are diverse and yet they are remarkably alike. This indicates that they have a similar sedimentary genesis.

Figure 20: U, Th and Pb concentrations in zircon grains measured by LA-ICP-MS.

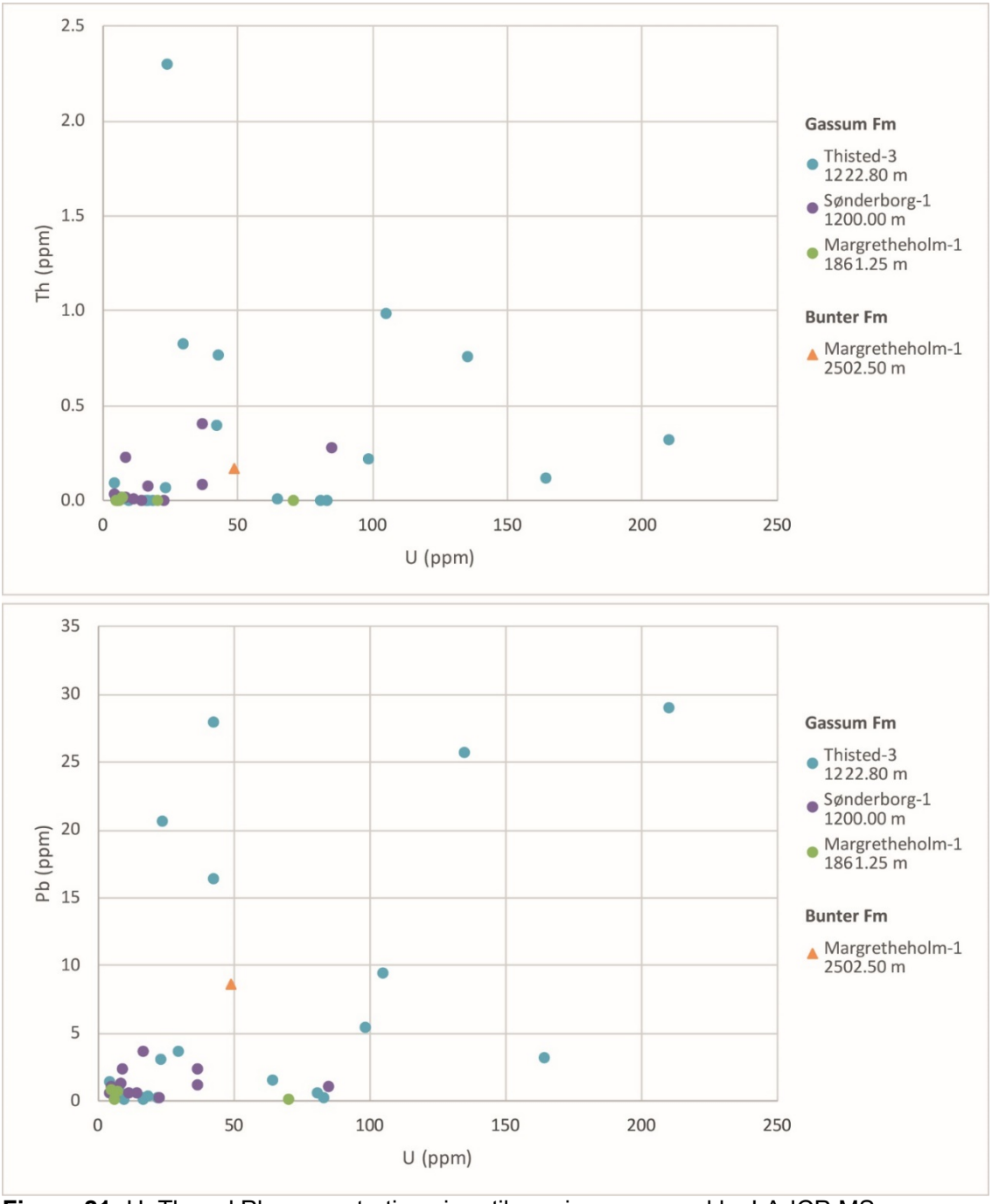

Figure 21: U, Th and Pb concentrations in rutile grains measured by LA-ICP-MS.

Table 9: U, Th and Pb concentrations in zircon and rutile grains calculated as averages of all analyzed grains.

Mineral type	U [ppm]	Th [ppm]	Pb [ppm]	Number of grains	Formation
Zircon grains	443.7	190.5	805.7	155	Bunter Fm
Zircon grains	360.4	108.4	409.2	310	Gassum Fm
Rutile grains	48.8	0.2	8.6	1	Bunter Fm
Rutile grains	40.4	0.2	4.3	39	Gassum Fm

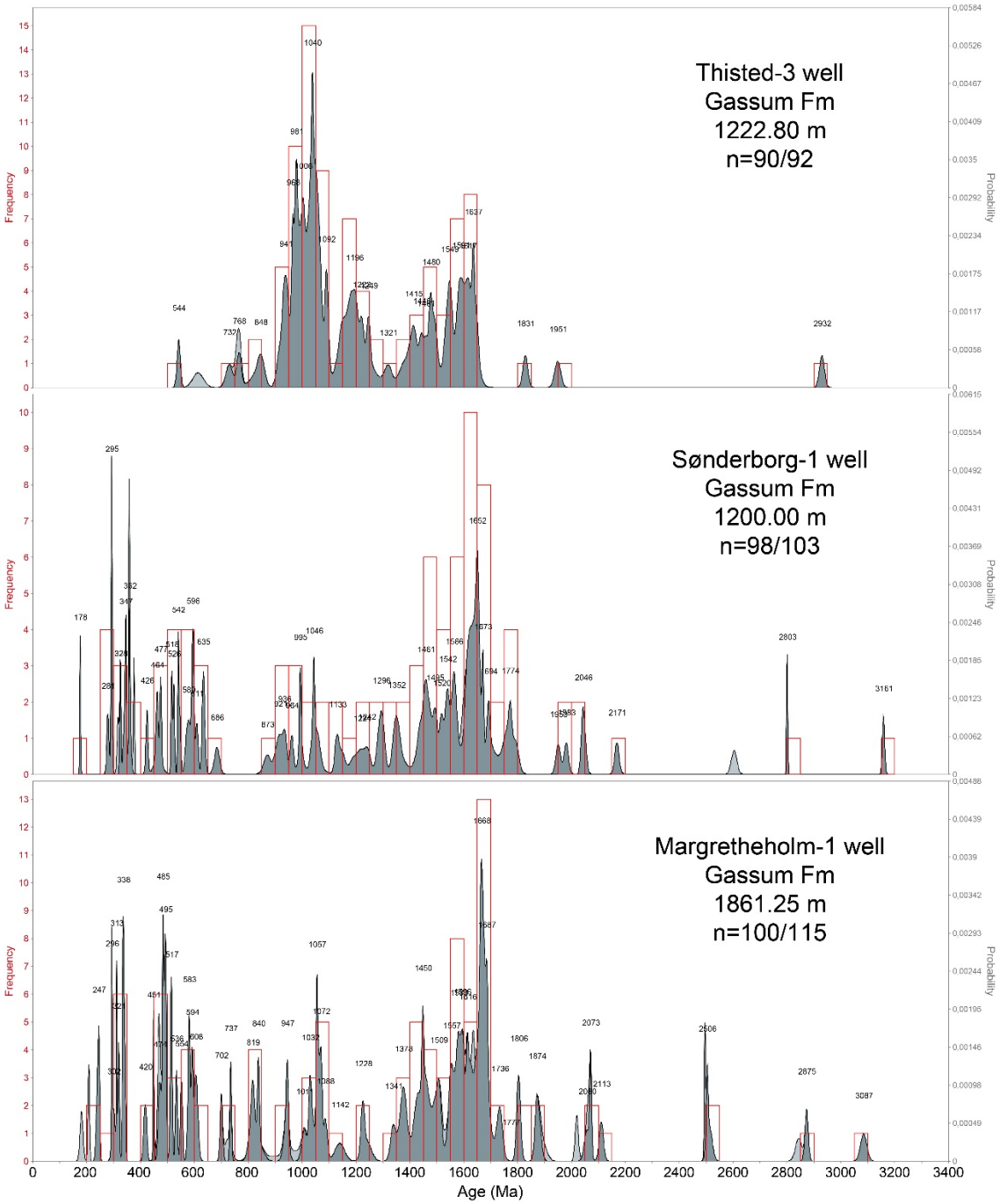

(figure continues on next page)

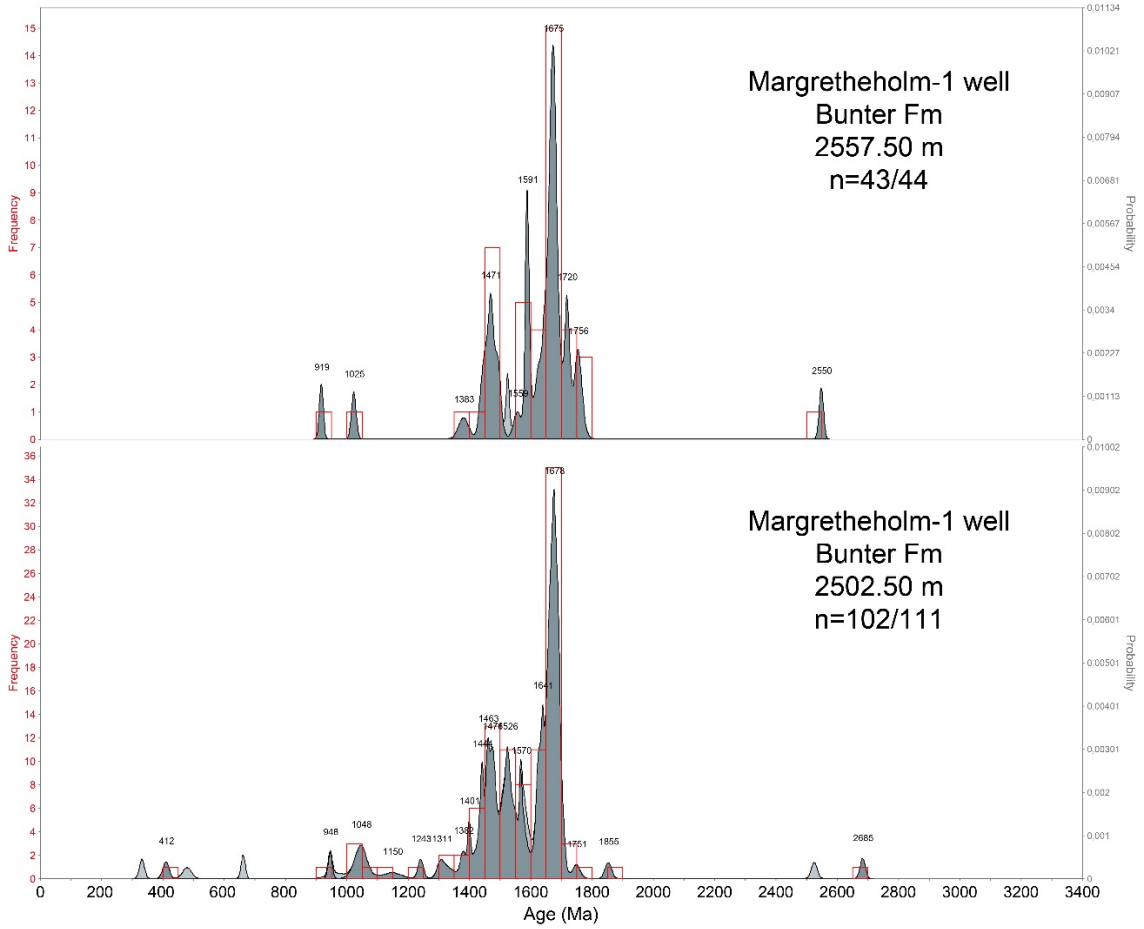

Figure 22: Zircon U–Pb age distributions of samples from Bunter and Gassum Fm. The ages of the probability peaks are denoted in million years (Ma). The probabilities of ages with <10% discordance are plotted in dark grey, while the discordant ages are shown in light grey, which is signified by n (the number of accepted analyses out of the total number of analyses). The histograms have 50 Ma bin size and include only concordant ages.

5. Discussion

5.1 Source of radioactive isotopes

^{210}Pb results from decay of U and must originate from the formation from which water is produced since there is only short time available to bring the radioactive isotopes to the surface after the decay in the U-containing minerals. Thus, most likely the radioactive isotopes originate from minerals in the reservoir itself and not from adjacent formations. The reservoir sandstones contain a number of U-rich heavy minerals that has the potential to constitute the primary sources of radioactivity (Figure 19). For example, zircons with a high U-content are often being completely or partly destroyed by the radioactivity that they carry (i.e. the process of metamictization). This process liberates or loosens radioactive daughter products so they can reach e.g. the formation fluid. Therefore, the present state of the occurring U-rich minerals was studied in detail.

The frequency of zircons with high U-content is higher in Bunter/Skagerrak Fm than in Gassum Fm (Table 9, Figure 20). Sandstones from Bunter/Skagerrak Fm are more mineralogically immature than sandstones from Gassum Fm, which indicate that a smaller degree of chemical and mechanical degradation from source area to deposition has happened for the Bunter/Skagerrak Fm (Figures 16 & 17). This can explain that relatively fragile, metamict zircons with higher U-content may have survived the sedimentary processes.

The mineralogical immaturity of the Bunter/Skagerrak Fm is a result of the arid climate during deposition, but also the short sediment transport distance to Copenhagen from the provenance in Sweden that is shown by the radiometric ages of zircon (Figure 22). Hence, metamict zircons may have had the best odds of surviving the transport and deposition in this area, whereas the Gassum Fm in Copenhagen is mineralogically mature as seen by its high quartz content (Figure 16) and is reflected in the radiometric ages revealing that several source areas including reworking of older sediments have supplied the sediment.

The geochemical analyses of rock samples and core scanning show that U does not preferentially occur in claystones so organic-rich lithologies can be excluded as a primary source of the radioactive isotopes (Table 8, Figures 13 & 15). Instead, the U-concentration has correlation with Ti and Zr, which indicates that U is mostly present in heavy minerals such as Ti-minerals and zircon. Such minerals are present in the sandstones, but the heavy mineral assemblage is immature in the Bunter Fm so the relative proportions of ilmenite, rutile and zircon are small (Figure 19). However, rutile and Ti-rich alteration products were excluded as likely sources of radioactive isotopes since their U-content is low.

5.2 Pb-content in formation water

The content of ^{210}Pb is about 30–60 times larger in the Bunter Fm in Copenhagen compared to the Gassum Fm in Thisted and Sønderborg. The formation water from the Gassum Fm in Thisted, Sønderborg and Stenlille shows a twenty times lower Pb-content (0.02 mg/L) compared to the water from Bunter Fm in Margretheholm (0.4 mg/L). The ratios of these three Gassum Fm sites are similar in terms of salinity (chloride 100 g/L) and temperature (about 50°C) and probably also sulphide content to which organic content is of importance. Gassum Fm below Aars and Farsø in Himmerland lies deeper (about 3 km) and is characterized by both higher salinity (chloride 176–182 g/L) and higher temperature (93–106°C). A higher content of Pb should therefore be expected, as is indeed the case for the analyzed samples. However, the samples show relatively large variation in Pb content and are probably contaminated due to Pb-containing pipe dope in the pipe assemblies.

The concentration of Pb in formation water is controlled by the equilibrium with Pb-sulphide in geological deposits when there are reducing conditions. The concentration of Pb in the formation water is determined by the sulphide concentration, salinity, organic constituents, including organic acids, and reservoir temperature. Low sulphide content, high salinity and high temperature promote the conditions for high concentration of Pb. Leaching from nearby formations (organic-rich shales) may also significantly increase the Pb content.

The significantly higher Pb-content in the formation water from Bunter/Skagerrak Fm compared to Gassum Fm water is probably associated with the less reducing conditions in Bunter/Skagerrak Fm, which means lower sulphide content and thus a higher Pb-content in the water. In addition, the higher temperature (73°C) and higher salinity (chloride 137 g/L) of the water in Bunter/Skagerrak Fm cause the solubility of Pb-sulphide to increase, enabling a higher Pb-concentration in the water.

The subaerial conditions during the deposition of Bunter/Skagerrak Fm allow for the presence of other Pb-containing compounds, such as sulphate and carbonate in addition to various oxides. Burial of sediments causes a shift from oxic to a more reducing environment with the possibility of conversion of mentioned compounds. The detected occurrence of methane dissolved in the formation water must originate from degradation of organic matter. This means, in addition to methane formation, also reduction of sulphate in the formation water and thus formation of sulphide. Pb-sulphide is the most poorly soluble of Pb-minerals and probably the mineral that controls the Pb-concentration in the water.

Substantially fewest sulphides have precipitated in Bunter/Skagerrak Fm as compared with Gassum Fm, which is in accordance with the arid, terrestrial depositional environment for Bunter/Skagerrak Fm as opposed to the humid, fluvial-marine depositional environment for Gassum Fm. The relatively high content of pyrite in Gassum Fm, in which a content of Pb-sulphide is detected, thus confirms that the Pb-concentration in the formation water is controlled by the sulfide concentration.

5.3 Risk of NORM

Radioactivity analyses on wastewater from cleaning of the Margretheholm injection well demanded by the authorities (SIS), confirmed that wastewater from that operation was not a NORM issue. The wastewater analyses gave ^{210}Pb activity concentration in the range of 99–148 Bq/kg, which is significantly higher compared to that of the formation water itself of 2.46 Bq/kg (Table 3) probably due to presence of traces of solid lead from the cleaning operation. In spite of the relatively low content of ^{210}Pb in formation water, its concentration in lead deposits is sufficiently high for the contaminated solids to be recognized as TNORM (Table 6).

The significantly lower Pb-content that is found in the formation water in Gassum Fm in the Copenhagen area relative to the content measured in Bunter Fm reduces the risk of significant Pb precipitation and the associated problems such as clogging of the injection well with Pb. That deposition of Pb may occur on exposed places such as on sacrificial anode mounted over bag filters cannot be excluded, as shown from experiences of the Sønderborg plant (Table 6). The radioactivity measurements on the filters in Sønderborg showed that they were closely below the limit set by SIS to determine whether the object should be characterized as NORM waste. It should be noted though that the radioactivity of the Sønderborg filter is mainly due to radium and not lead-210, which only constitutes 11% (Table 6). Thus, it cannot be ruled out that this must be taken into account in the design of future facilities in Copenhagen in order to avoid handling NORM waste.

5.4 Evaluation of Gassum Fm in Copenhagen

Based on the new data combined with data from previous tests, the best estimate of the expected content of total Pb and radioactive Pb in formation water in Gassum Fm in Copenhagen is that it will be significantly lower than in the deeper Bunter Fm. The Pb-content in the formation water in Gassum Fm is probably a little higher in Copenhagen than in Thisted, Sønderborg and Stenlille due to the expected slightly higher salinity and higher temperature (about 54°C according to forecast) due to a slightly larger depth in Copenhagen.

These estimates are based on that the depositional conditions for Gassum Fm and the layers above and below are probably the same for the Copenhagen area as for Thisted, Sønderborg and Stenlille, from which we have reliable data regarding the Pb-concentration in the formation water. Particularly important is the organic content in Gassum Fm, which is important for the sulphide content of the formation water.

It must be emphasised that the material used for geothermal installations must be chosen carefully in order to inhibit scaling, so a conversion of the Margretheholm plant from production of Bunter Fm to Gassum Fm may not necessarily eliminate the Pb problems entirely since they also depend upon availability of corrodible material.

6. Conclusions

The contents of total lead and radioactive lead in the formation water from Gassum Formation in the Copenhagen area is expected to be significant lower than in formation water from Bunter Sandstone Formation. Furthermore, it has been shown that the source of the radionuclides is present within the formations. These conclusions are drawn from the more detailed observations and conclusions given below.

Specific comments on the results:

- Lead solids accumulate in pipes and filters at the geothermal facility at Margretheholm due to galvanic corrosion.
- Content of radioactive lead (^{210}Pb) in lead-contaminated objects exceeds the limit for NORM decided by the Danish authorities (SIS), which add to the cost of handling of such wastes.
- The content of ^{210}Pb and other radioactive isotopes in the geothermal water is far below the limit for NORM material, meaning that the NORM problem occurs only when lead accumulates.
- Whether lead deposits will form as a result of galvanic corrosion depends on the lead content in the geothermal water, together with the type of materials used in the installations.
- Initially, the lead content in the water depends upon reservoir temperature, organic constituents, salinity and sulphide concentration. The Bunter Formation is generally buried deeper than the Gassum Formation and therefore reach higher temperature and higher salinity.
- The Margretheholm plant exploits sandstones of the Bunter Formation that were deposited at oxic, arid terrestrial conditions resulting in a low sulphide concentration, whereas the geothermal plants in Thisted and Sønderborg exploit sandstones of the Gassum Formation, which were deposited in a marine, humid climate causing reducing conditions and accumulation of organic matter.
- The formation water in Bunter Formation has a higher lead content compared to that of the Gassum Formation, namely 0.4 versus 0.02 mg/L, respectively, which is in line with the abovementioned parameters. The relative lead-210 content is approximately the same for the three examined sites, constituting around 1 ppb of the total lead.
- Besides clogging of the injection well, the NORM implications of galvanic corrosion with lead accumulation should be considered when designing the production facilities for future geothermal plants that exploit these sandstones.
- The ^{210}Pb originates from uranium (^{238}U) within the reservoir, as evident from presence of the very short-lived ^{224}Ra in the formation water.
- Zircon is the only mineral in the formations that has both high uranium-content and occurs in amounts large enough to be a possible source of the radionuclides in the water.
- Zircon grains with very high uranium-content become degraded by the radioactivity so the decay products including ^{210}Pb can more easily escape to the water and such zircons are more abundant in Bunter Formation than Gassum Formation.

- This is consistent with the fact that the sand in Bunter Formation has been transported significantly shorter from source area to deposition than the sand in Gassum Formation, so it is likely that a higher number of fragile zircons with extra high uranium content have survived the transport and therefore accumulated in Bunter Formation.
- Gas-isotope analyses show that there has been no supply from a deeper and mature organic source, such as the uranium-rich Alum shale in the region.
- These insights are important for future development of geothermal energy in the Danish region in terms of plant design, economic considerations and safety precautions.

Acknowledgements

We would like to thank the people that performed the sampling and analyses or in another way assisted with the project, including Olga Nielsen, Mojagan Alaei, Ditte Kiel-Dühring, Carsten Guvad, Høgni Vesturklett, Charlotte Olsen, Annette Ryge, Sarah E. Kylborg, Julius C. Havsteen, Rasmus Madsen, Bjørn H. Christensen, Nynke Keulen, Dan Olsen, Marie-Louise Siggaard-Andersen and Per Roos.

References

Carpenter, A.B., Trout, M.L. & Pickett, E.E. 1974: Preliminary Report on the Origin and Chemical Evolution of Lead-and Zinc-Rich Oil Field Brines in Central Mississippi. Economic Geology 69, 1191–1206.

Clemmensen, L.B. 1985: Desert sand plain and sabkha deposits from the Bunter Sandstone Formation (L. Triassic) at the northern margin of the German Basin. Geologische Rundschau 74, 519–536.

Degering, D. & Köhler, M. 2016: Prognose und Monitoring natürlicher Radionuklide in Anlagen der tiefen Geothermi (ProRad). Abschlussbericht BMWi 035571, VKTA–Strahlenschutz, Dresden.

Degering, D., Krüger, F., Scheiber, J., Wolfgramm, M. & Köhler, M. 2015: Radionuclide Release in Geothermal Aquifers - the Role of Alpha Recoil. Proceedings World Geothermal Congress 2015, Melbourne.

Fisher, R.S. 1998: Geologic and geochemical controls on naturally radioactive materials (NORM) in produced water from oil, gas, and geothermal operations. Environmental Geosciences 5, 139–150.

Frei, D. & Gerdes, A. 2009: Precise and accurate in situ U-Pb dating of zircon with high sample throughput by automated LA-SF-ICP-MS. Chemical Geology 261, 261–270.

Gerling, P., Geluk, M.C., Kockel, F., Lokhorts, A., Lott, G.K. & Nicholson R.A. 1999: NW European Gas Atlas – new implications for the Carboniferous gas plays in western part of the Southern Permian Basin.

GEUS 2015: Blypartikler i posefiltre på GDA skyldes muligvis blyudfældninger i anlæg. GEUS datablad, 14. august 2015.

GEUS 2016: Koncentration af radionuklider i filtre fra geotermisk anlæg i Sønderborg. GEUS datablad, 22. februar 2016.

GEUS 2017a: Koncentration af radionuklider i belægninger og filtre fra Margretheholm geotermiske anlæg. GEUS datablad, 16. januar 2017.

GEUS 2017b: Koncentration af radionuklider i materiale fra posefiltre efter opstart og drift af Margretheholm geotermiske anlæg. GEUS datablad, 23. oktober 2017.

Hammond, D.E., Zukin, J.G. & Ku, T.L. 1988: The kinetics of radioisotope exchange between brine and rock in a geothermal system. J Geophys Res Solid Earth 93, 13175–13186.

Jackson, S.E., Pearson, N.J., Griffin, W.L. & Belousova, E.A. 2004: The application of laser ablation-inductively coupled plasma-mass spectrometry to in situ U–Pb zircon geochronology. Chemical Geology 211, 47–69.

Keulen, N., Frei, D., Bernstein, S., Hutchison, M.T., Knudsen, C. & Jensen, L. 2008: Fully automated analysis of grain chemistry, size and morphology by CCSEM: examples from cement production and diamond exploration, Geological Survey of Denmark and Greenland Bulletin 15, 93–96.

Keulen, N., Frei, D., Riisager, P. & Knudsen, C. 2012: Analysis of Heavy Minerals in Sediments by Computer--Controlled Scanning Electron Microscopy (CCSEM): Principles and Applications. Mineralogical Association of Canada Short Course 42, 167–184.

Kharaka, Y.K., Maest, A.S., Carothers, W.W., Law, L.M., Lamothe, P.J. & Fries, T.L. 1987: Geochemistry of metal-rich brines from central Mississippi Salt Dome basin, USA. Applied Geochemistry 2, 543–561.

Michelsen, O. & Clausen, O.R. 2002: Detailed stratigraphic subdivision and regional correlation of the southern Danish Triassic succession. Marine and Petroleum Geology 19, 563–587.

Michelsen, O., Nielsen, L.H., Johannessen, P.N., Andsbjerg, J. & Surlyk, F. 2003: Jurassic lithostratigraphy and stratigraphic development onshore and offshore Denmark. In: Ineson, J.R. & Surlyk, F. (Eds.): The Jurassic of Denmark and Greenland. Geological Survey of Denmark and Greenland Bulletin 1, 147–216.

Nelson, A.W., Eitrheim, E.S., Knight, A.W., May, D., Mehrhoff, M.A., Shannon, R., Litman, R., Burnett, W.C., Forbes, T.Z. & Schultz, M.K. 2015: Understanding the radioactive ingrowth and decay of naturally occurring radioactive materials in the environment: an analysis of produced fluids from the Marcellus Shale. Environ Health Perspect. 123, 689–696.

Nielsen, L.H. 2003: Late Triassic – Jurassic development of the Danish Basin and the Fennoscandian Border Zone, southern Scandinavia. In: Ineson, J.R. & Surlyk, F. (Eds.): The Jurassic of Denmark and Greenland. Geological Survey of Denmark and Greenland Bulletin 1, 459–526.

Norsk olje og gass 2012: Radioactive non-equilibrium in Produced Water. Zpire Report 03-12.

Paton, C., Hellstrom, J.C., Paul, P., Woodhead, J.D. & Hergt, J.M. 2011: Iolite: Freeware for the visualisation and processing of mass spectrometric data. Journal of Analytical Atomic Spectrometry 26, 2508–2518.

Petrus, J.A. & Kamber, B.S. 2012: VizualAge: A Novel Approach to Laser Ablation ICP-MS U-Pb Geochronology Data Reduction. Geostandards and Geoanalytical Research 36, 247–270.

Schmidt, A.P. 1998: Lead precipitates from natural gas production installations. J. Geochem. Explor. 62, 193–200.

Schmidt, A.P. 2000: Naturally Occurring Radioactive Materials in the gas and oil industry - Origin, transport and deposition of stable lead and 210Pb from Dutch gas reservoirs. Mededelingen van de Faculteit Aardwetenschappen Universiteit Utrecht, No. 195.

Schröder, H., Teschner, M. Köhler, M., Seibt, A., Krüger, M., Friedrich, H.-J. & Wolfgramm, M. 2007: Long term reliability of geothermal plants – Examples from Germany. Proceedings European Geothermal Congress 2007 Unterhaching, Germany, 137, 1–7.

Slama, J., Kosler, J., Condon, D.J., Crowley, J.L., Gerdes, A., Hanchar, J.M., Horstwood, M.S.A., Morris, G.A., Nasdala, L., Norberg, N., Schaltegger, U., Schoene, N., Tubrett, M.N. & Whitehouse, M.J. 2008: Plesovice zircon - a new natural reference material for U-Pb and Hf isotopic microanalysis. Chemical Geology 249, 1–2, 1–35.

Sohns, E., Gerling, P. & Faber, E. 1994: Improved stable nitrogen isotope measurements of natural gases. Analytical Chemistry 66, 2614–2620.

Thomsen, T.B., Heijboer, T. & Guarnieri, P. 2016: jAgeDisplay: software for evaluation of data distributions in U-Th-Pb geochronology. Geological Survey of Denmark and Greenland Bulletin 35, 103–106.

TNO 2014: Lead deposition in geothermal installations. Final report, No. 2014 R11416.

Vejbæk, O.V. 1997: Dybe strukturer i danske sedimentære bassiner. Geologisk Tidsskrift 4, 1–31.

Vosgerau, H., Mathiesen, A., Andersen, M.S., Boldreel, L.O., Hjuler, M.L., Kamla, E., Kristensen, L., Pedersen, C.B., Pjetursson, B. & Nielsen, L.H. 2016: A WebGIS portal for exploration of deep geothermal energy based on geological and geophysical data. Geological Survey of Denmark and Greenland Bulletin 35, 23–26.

Wiedenbeck, M., Allé, P., Corfu, F., Griffin, W.L., Meier, M., Oberli, F., von Quadt, A., Roddick, J.C. & Spiegel, W. 1995: Three natural zircon standards for U-Th-Pb, Lu-Hf, trace element and REE analyses. Geostandards Newsletter 19, 1–23

Wiedenbeck M, Hanchar JM, Peck WH, Sylvester P, Valley J, Whitehouse M, Kronz A, Morishita Y, Nasdala L, Fiebig J, Franchi I, Girard J-P, Greenwood RC, Hinton R, Kita N, Mason PRD, Norman M, Ogasawara M, Piccoli, PM , Rhede D, Satoh H, Schulz-Dobrick B, Skår Ø, Spicuzza MJ, Terada K, Tindle A, Togashi S, Vennemann T, Xie Q & Zheng Y-F 2004: Further characterisation of the 91500 zircon crystal. Geostandards and Geoanalytical Research 28, 9–39.

Worden, R.H., Manning, D.A.C. & Lythgoe, P.R., 2000: The origin and production chemistry of radioactive lead (210Pb) in NORM-contaminated formation waters. J. Geochem. Explor. 69–70, 695–699.

Zielinski, R., Otton, J. & Budahn J. 2001: Use of radium isotopes to determine the age and origin of radioactive Barite at oil-field production sites. Environ. Pollut. 113 (3), 299–309.

Appendixes

Appendix 1: Background of injectivity history at Margretheholm

The Margretheholm geothermal plant in operation since 2005 experienced decreasing injectivity due to partial clogging of the injection well after the first two years of production. Injectivity was partially restored by lowering the pH of the injected water under normal operation adding hydrochloric acid for a short period of time, the so-called soft acidizing procedure. However, injectivity continued to deteriorate over the following years while the ability of soft acidizing diminished as a remedy. Furthermore, the filters in the plant to tended to clog more frequently causing the pump to shut down automatically, particularly at start-up after periods of stand still.

Camera inspection of the injection well in September 2014 including bailer sampling gave no clear indication as to the cause of clogging. Several perforations were clearly blocked by indistinguishable solids while 20 m of reservoir sand had accumulated at the bottom of the well since the time of logging after completion and testing in 2002. Flow-logging performed after the camera inspection showed that loss of injectivity was mainly due to blocking of the lower perforations in the injection well.

In June 2015, filters clogged shortly after start of the pump, the reason being accumulation of mainly fine metallic lead as shown by XRD and chemical analysis (ICP-MS) (GEUS 2015). Two months later large quantities of metallic lead were observed in the flow line connecting the production well to the plant itself. The accumulation of lead was assumed to be due to galvanic corrosion whereby lead deposition from water is associated with iron dissolution from installations. Problems with deposition of lead have also occurred in Germany and The Netherlands (Schröder et al. 2007, TNO 2014). A closer examination of the lead deposits revealed low levels of radioactivity, so the Danish authorities (SIS) were called to inspect the objects at the Margretheholm site. A short account of the SIS' visit to the site was received by mail, while more fully instructions followed a month later when radionuclide analysis of the lead deposits had been performed. According to the result of radionuclide analyses the dose criteria for NORM waste - using the summation rule for mixtures of radionuclides – was exceeded by a factor of 600. Thus, specimen containing lead deposits had to be considered NORM waste (Naturally Occurring Radioactive Material) and be treated accordingly. Formation water produced during the following workover operation of the injection well was also analysed for its content of radionuclides and was found not to be NORM waste. After the completion of the workover of both of the Margretheholm wells in late 2015 the various types of waste were listed including their radionuclide contents, showing that all objects were to be considered NORM waste. The exemption limit for NORM wastes was exceeded by a factor 22 to 167 (GEUS 2017a). Resuming operation after the workover operation filters still had to be replaced regularly, though less frequently, which added to the amount of NORM wastes to be stored (GEUS 2017b). It may be added that in addition to the lead NORM issue, radium may also accumulate, e.g. traces in barium sulphate/ strontium sulphate deposits on heat exchanger plates causing a radiation issue.

Appendix 2: Radionuclide decay series

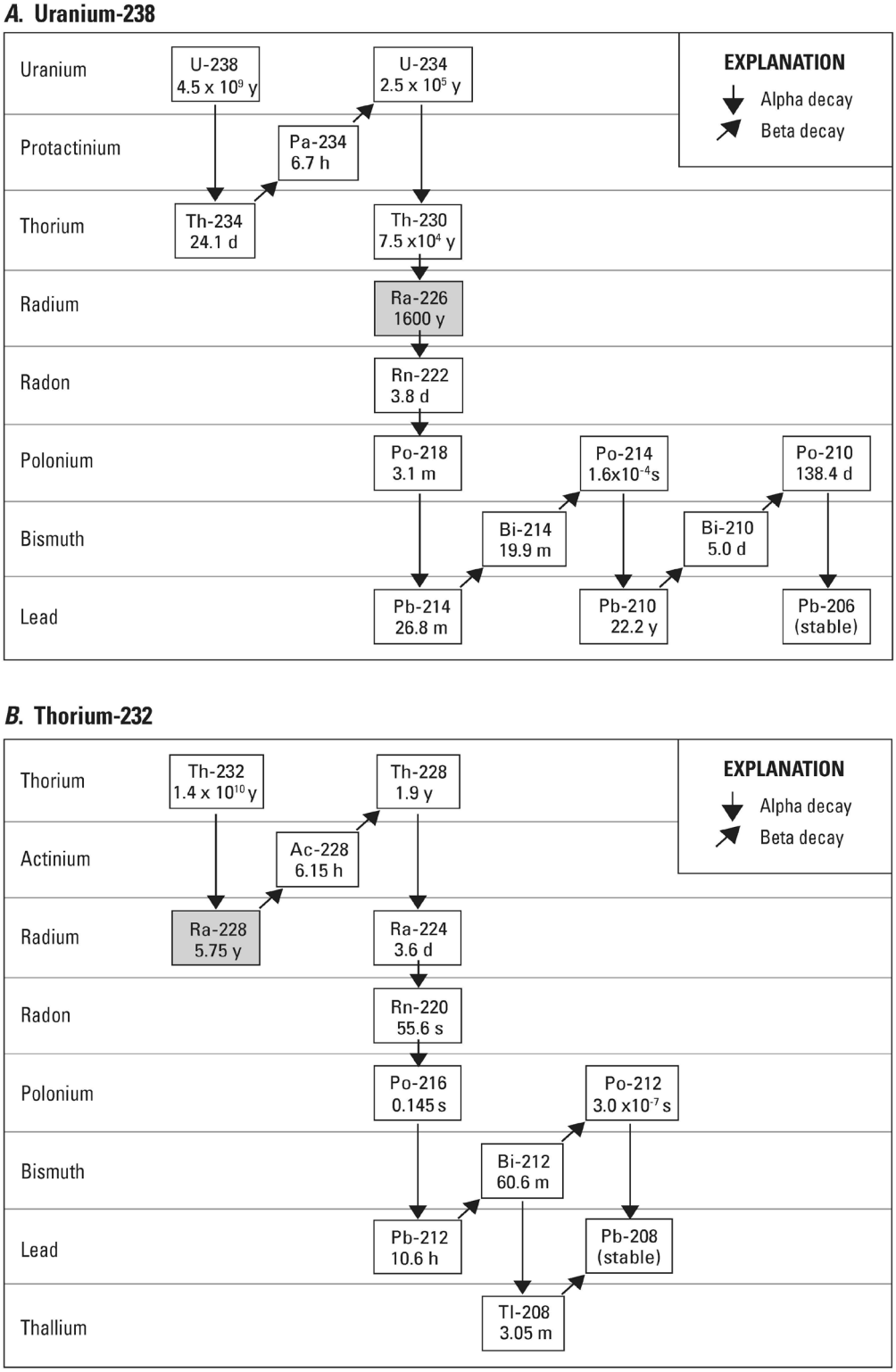

Figure 23: Radioactive decay chains for (A) U-238 and (B) Th-232. Times shown are half-lives: y, years; d, days; h, hours; m, minutes; s, seconds. Half-lives were obtained from the National Nuclear Data Center (www.nndc.bnl.gov/chart).

Appendix 3: Origin of lead in formation water

The Pb^{2+} ion is intermediate in size between K^{+} and Ca^{2+} and so it replaces these ions in K-feldspar, mica and, to a lesser extent, plagioclase and apatite. As a consequence, it is enriched in felsic igneous rocks relative to mafic rocks, and Pb is mobile in late-stage magmatic processes.

In sedimentary rocks, the distribution of Pb is controlled by the presence of primary detrital minerals, such as feldspar, mica and sulfides, clay and organic matter. Pure limestone (*c.* 5 mg/kg) and quartzitic sandstone (*c.*10 mg/kg) are typically depleted relative to shale and greywacke (*c.* 23 mg/kg). The sedimentary rocks with the highest concentrations are black shale, reflecting the affinity of Pb for organic matter.

Published data on Pb in formation water mainly focus on very high concentrations which may be important for the formation of lead sulfide e.g. the Mississippi Valley Type (MVT) deposits. The source of lead for the very high concentrations is probably black shales (Carpenter et al., 1974) which can promote levels up to 100 mg/L in certain strata. Decreasing Pb concentrations at higher strata was explained by the presence of hydrogen sulfide (Kharaka et al., 1987).

The mechanism by which Pb moves from rock matrix to formation water is usually not dealt with. One fortunate exception is the account given by Smith in 2000. The mechanism described by the author is probably relevant for the Bunter sandstone at Margretheholm too and will be described shortly in the following. The study comprised rocks of Rotliegend sandstones, conglomerates and mudstones from three gas fields in the northern Netherlands and southern North Sea area and from outcrops in northern Germany. The Pb concentrations in the rocks were comparable to average sandstones and shales.

Sequential extraction of Pb showed that feldspars are the main Pb-bearing mineral fraction in all types of sediment, containing up to 92% of total Pb. Fe-oxide grain coatings may account for up to 20% of total Pb, while carbonate cements may contain 10-40% of Pb in sandstones. Elevated Pb concentrations in bituminous sandstones from one of the gas fields are due to the presence of Pb-sulfide associated with the bitumens. Stable Pb isotope signatures of the reservoir sediments and signatures corrected for ingrowth of Pb from decay of U and Th since sediment deposition provide a Pb evolution curve of the sediments. Isotopic signatures of Pb minerals deposited from the reservoir brines plot on this Pb evolution curve, supporting large scale mobilization of Pb from Rotliegend sediments into Rotliegend brines between the time of deposition and the present. Reported Pb concentrations in Dutch gas reservoir brines of up to 150 mg/L can be explained by dissolution of feldspars and Fe-oxides from an average Rotliegend sediment. Mobilization of Pb from Rotliegend sediments was probably a single large scale event, controlled by diagenetic fluid fluxes.

Thus “high” Pb concentrations in formation water may be expected in reservoir rocks formed under arid conditions as is the case for the Bunter sandstone. However, in the event of mixing with sulfide as a result of fluid migration or diagenetic reactions involving sulfate reduction the Pb concentration in water will be lowered due to the formation of lead sulfide (Kharaka et al., 1987).

Low Pb concentration in formation waters is also to be expected when sulfide is present during burial under humid conditions as is the case for the Gassum Formation. Degradation of organic matter will lead to sulfate reduction via bacteria at moderate temperatures <70 °C producing hydrogen sulfide.

Appendix 4: Lead concentration in Gassum formation water

Assuming the concentration of lead in formation water is controlled by the solubility of lead sulfide present in the reservoir rock the actual Pb concentration will depend on the hydrogen sulfide content in the water. Unfortunately, hydrogen sulfide was below detection limit, 0.1 mg/L, in all of the formation waters analyzed and cannot be used as guide to predict Pb concentrations at other locations. Therefore, prediction of the Pb concentration in Gassum formation water from one locality to another has to rely on other parameters important for the solubility of lead sulfide. The solubility of lead sulfide depends on temperature and other constituents in the formation water particularly chloride. High chloride enhances PbS solubility by lowering the concentration of "free" Pb due to the formation of the PbCl42- in solution (Kharaka et al., 1987). The temperature dependence of PbS solubility is quite significant (Figure 24), compared to other salts or minerals such as BaSO4 which sometimes cause scaling problems.

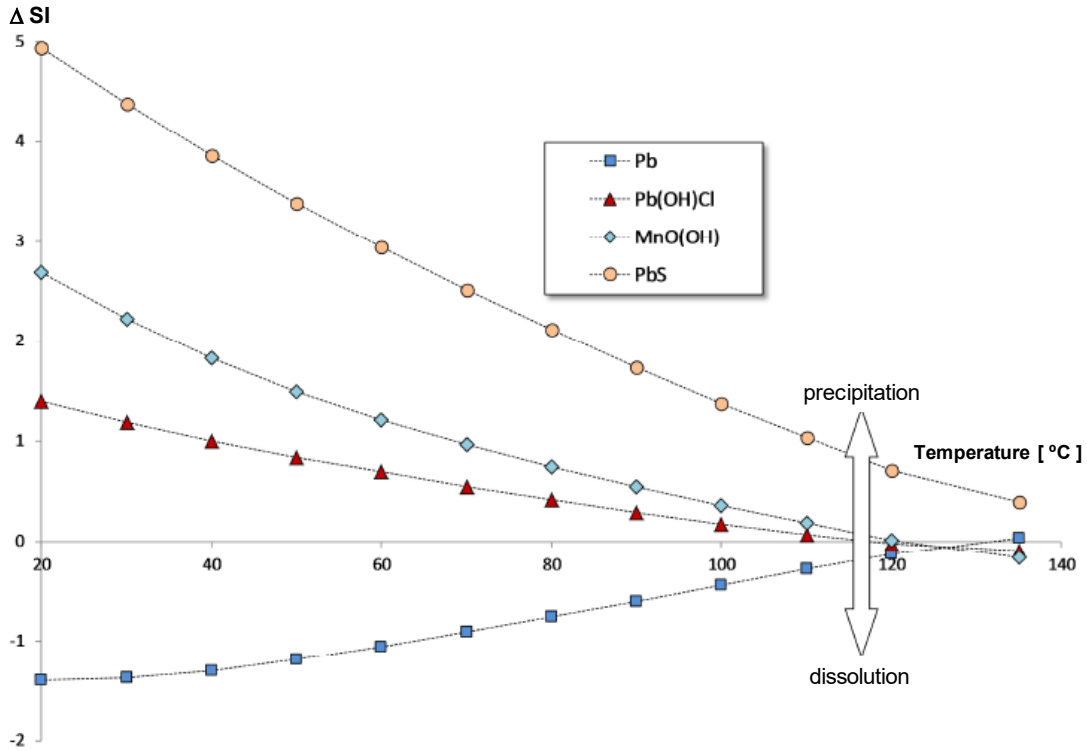

Figure 24: Change in saturation index ΔSI with temperature for high saline formation water (Wolfgramm pers. comm.). Note the ΔSI scale is logarithmic.

Reliable data on Pb concentration in Gassum formation water, 0.02 mg/L, are known from three sites, Thisted, Sønderborg and Stenlille which are almost identical with respect to reservoir depth, temperature and salinity. Deeper reservoirs at Aars and Farsø characterized by higher temperature and higher salinity show higher Pb concentrations, 0.7 – 8 mg/L, but the data are less reliable due to contaminants as illustrated by the scatter in Pb data during test pumping.

Since reliable data on Pb concentration in Gassum formation water only cover a narrow range with respect to reservoir depth, temperature and salinity the prediction of likely Pb

concentration at other sites must rely on the general trends known for lead sulfide solubility with respect to temperature and salinity. For sites within the Copenhagen area a slightly higher temperature, c. 54 °C compared to the ~50 °C for three sites mentioned above, should be expected. A slightly higher salinity may also be expected due to greater depth following the general salinity trend with depth in the Danish sub-basin for most reservoirs. Thus Pb concentration in Gassum formation water within the Copenhagen area may be expected to be a little higher than the 0.02 mg/L found for the three sites mentioned above.

Appendix 5: Lead content in formation water from Danish wells

This appendix summarizes the knowledge of Pb-content in formation water based on data from previous tests of Danish onshore wells.

Increasing pressure in the Margretheholm injection well caused by clogging due to lead deposition underlined the detrimental effect that the lead content in formation water may have even in sub-parts per million concentrations. In addition to the adverse effect on injectivity, lead has also added to the operating costs due to the special treatment needed for the NORM wastes caused by the presence of radioactive lead-210 in various lead contaminated objects, e.g. filters. The other geothermal plants in Denmark, Thisted and Sønderborg, do not suffer from problems caused by lead, which may be explained by the much lower lead content in the Gassum formation water, 0.02 mg/L that they exploit compared to the Bunter formation water used at Margretheholm, 0.4 mg/L.

In order to improve our understanding of where potential lead problems in future geothermal operations could occur, it was decided to compile all data available on lead contents in formation waters. Unfortunately, no information on lead was found among the few chemical analyses from tests of oil exploration wells onshore Denmark because of the little interest in analysing for trace elements in those operations.

However, precise knowledge on formation water chemistry was utterly important for prediction of the potential scaling problems exploiting deep formation waters for geothermal purpose. Therefore, a comprehensive analytical program, including adequate sampling, was applied for the three exploration wells drilled after the oil crisis in 1979, Aars-1a, Farsø-1 and Thisted-2.

Up to 21 samples were taken, usually once a day, during the production testing of different reservoirs showing a range of lead concentrations from 0,9 to 8,0 mg/L for the Skagerrak and 0,01 to 0,04 mg/L for the Gassum in the Thisted-2 well (Table 10). Lead concentration in formation water from other wells, including those drilled for natural gas underground storage at Stenlille and Tønder, is also shown in Table 10. The number of analyses for each reservoir including the range in lead concentrations is also shown in Table 10 together with the lead concentration considered the most plausible.

Table 10: Lead concentration in formation water from various geothermal well tests

Year	Well	Formation	Depth	Temp	Source	reported	Cl	SO4	Ba	Pb	min-max	No.	Remarks
			m	°C			g/l	g/l	mg/l	mg/l		analyses	
1979	Aars 1a	Gassum	3205-3385	106	airlift	DONG 1982	182	0.15	15	-	2-7	8	contaminated
1981	Aars 1a	Haldager	2460-2499	74	pump	DONG 1982	167	0.05	50	0.9	0,7-1,0	4	maybe OK
1982	Farsø 1	Gassum	2797-2939	94	pump	DGU 1982	172	0.13	20	-	0,7-8,8	21	contaminated
1980	Stenlille 1	Fjerritslev	1370	47	pump	DGU 1981	103	0.015	60	0.03		1	OK
1980	Stenlille 1	Gassum	1510	50	pump	DGU 1981	108	0.015	50	0.03		1	OK
1982	Thisted 2	Skagerrak	1850-2100	66	pump	DGU 1983	166	0.29	5	0.9	1,4-2,1	21	maybe OK
1983	Thisted 2	Gassum	1257	46	pump	DGU 1983	102	0.01	12	0.02	0,01-0,04	17	OK
1983	Tønder 5	L.Bunter SSt	1880	67	airlift	DONG test report	196	0.48	na	-	0.22	1	maybe OK
2001	Stenlille 19	Bunter	2475		airlift	GEUS 2002	197	0.14	8.1	-	4.6	1	contaminated
2001	Stenlille 19	Falster	2115		airlift	GEUS 2002	182	0.22	4.8	-	0.9	1	contaminated
2001	Stenlille 19	Gassum	1640		airlift	GEUS 2002	113	0	39	-	0.09	1	contaminated
2002	MAH-1	Bunter SST	2575		airlift	GEUS 2002	136	0.24	5.8	0.3		1	OK
2003	MAH-2	Bunter SST	2600	72	pump	GEUS 2003	135	0.284	5.5	0.4		2	OK
2010	Sønderborg-1	Gassum	1150	48	pump	GEUS 2010	99	0.82	0.9	0.02		2	OK

Barium (Ba) and sulphate (SO_4) which may influence the radium content in formation water is also included in Table 10.

A steady concentration of major constituents, e.g. chloride and sodium in produced water was usually observed after 1-3 well volumes. However, minor constituents, particularly lead, continued to vary, sometimes in an irregular manner. The fairly large range in lead concentrations during some tests was considered to be due to contamination from pipe dope which is known to contain lead (up to sixty percent) plus copper, zinc and graphite (1).

In order to explore how actual testing may affect the lead content in the produced water the daily test record was compared to changes in lead concentration, hoping to be able to trace the source of contamination and to be able to obtain a reliable number for the uncontaminated formation water.

Details for changes in lead concentration with actual test conditions will be presented for the Thisted-2 and the Farsø-1 wells in the chapter below. The succession of the different steps during testing was determined by the need to obtain as much information regarding reservoir hydraulic properties as possible and will not be explained further.

Thisted-2, Skagerrak Fm test

After having cleaned the Thisted-2 well with fresh water, the Skagerrak Formation was perforated in the interval 1849.0- 2114.5 m. A preliminary flow test was conducted after perforation of the first 6 m layer, 2108.0- 2114.5 m, whereby 24 m^3 of water was produced. Reservoir pressure was sufficient to maintain a flow 8 m^3/h for three hours. After a pressure build-up test, the rest of the interval was perforated followed by installation of the down-hole equipment for the well test (Figure 25). Running the pump for 10 hours at *c.* 11 m^3/h most fresh water in the well was replaced by formation water during clean-up. Test#1, lasting for 24 days (580 h), was commenced one day later producing a total of 6910 m^3 of formation water, the equivalent of 80 well volumes.

Frequent water sampling was conducted during clean-up and the first day of test#1 to be able to follow the change in salinity (Figure 26). Thereafter only one set of water samples were taken each day. The sample for trace metal analysis, including lead, was filtered (0.45 µm) and acidified immediately at the well site in order to exclude changes during storage.

The non-regular change in salinity during clean-up and at the beginning of test#1 seen in Figure 26 is most likely due to mixing of freshwater and formation water during the various well operations prior to test#1. Both lead and copper on the other head peak towards the end of the clean-up (8 and 10 mg/L) and shortly after the start of test#1 (5.6 and 1.6 mg/L). Comparing the changes in copper and lead with that of salinity (chloride) it becomes evident that the variation of the former is not just due to mixing, but that some contaminant most likely pipe dope contributes. After *c.* 1000 m^3 lead drops below 2 mg/L and copper below 1 mg/L, and both constituents continue to decrease, although not quite smoothly, towards the end of test (Figure 26). The final concentrations of lead and copper were 0.9 and 0.11 mg/L respectively.

It is hard to find a simple explanation for the change seen in lead and copper after the 1000 m^3 volume, which could be due to either a slow decrease in contribution from pipe dope, or a change in relative contribution from different layers in the 265 m perforated interval, as was mentioned in the Skagerrak summary test report (2).

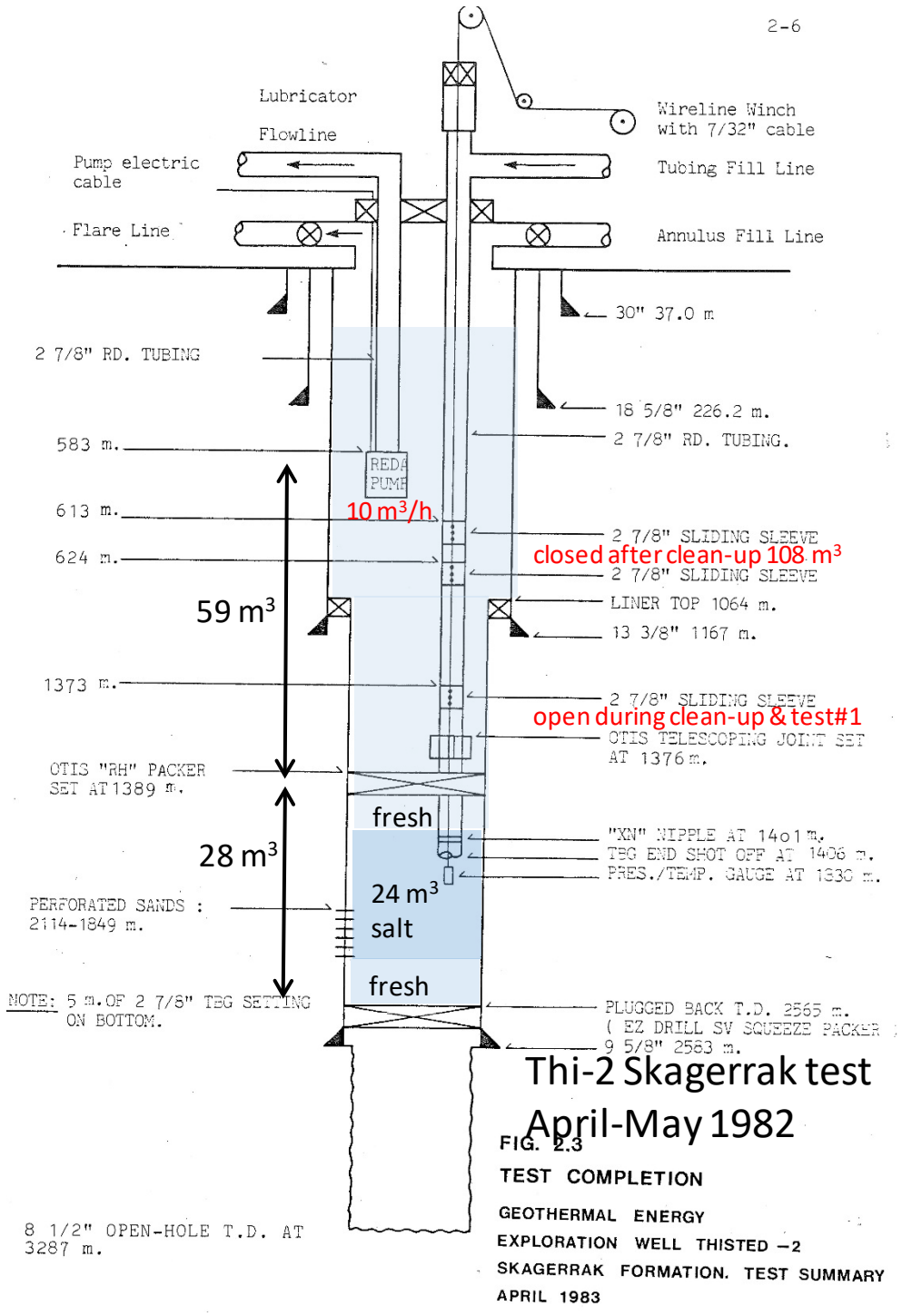

Figure 25: Down-hole set-up installed after a preliminary test of the deepest 6 m perforations of the 2114-1849 m interval. A volume of 24 m^3 of fresh water was produced by "free flow" during the test. Test#1 was performed after perforating the whole interval including a clean-up using the Reda pump, 10 m^3/h. Minimum volume estimated to obtain reservoir formation water was 87 m^3.

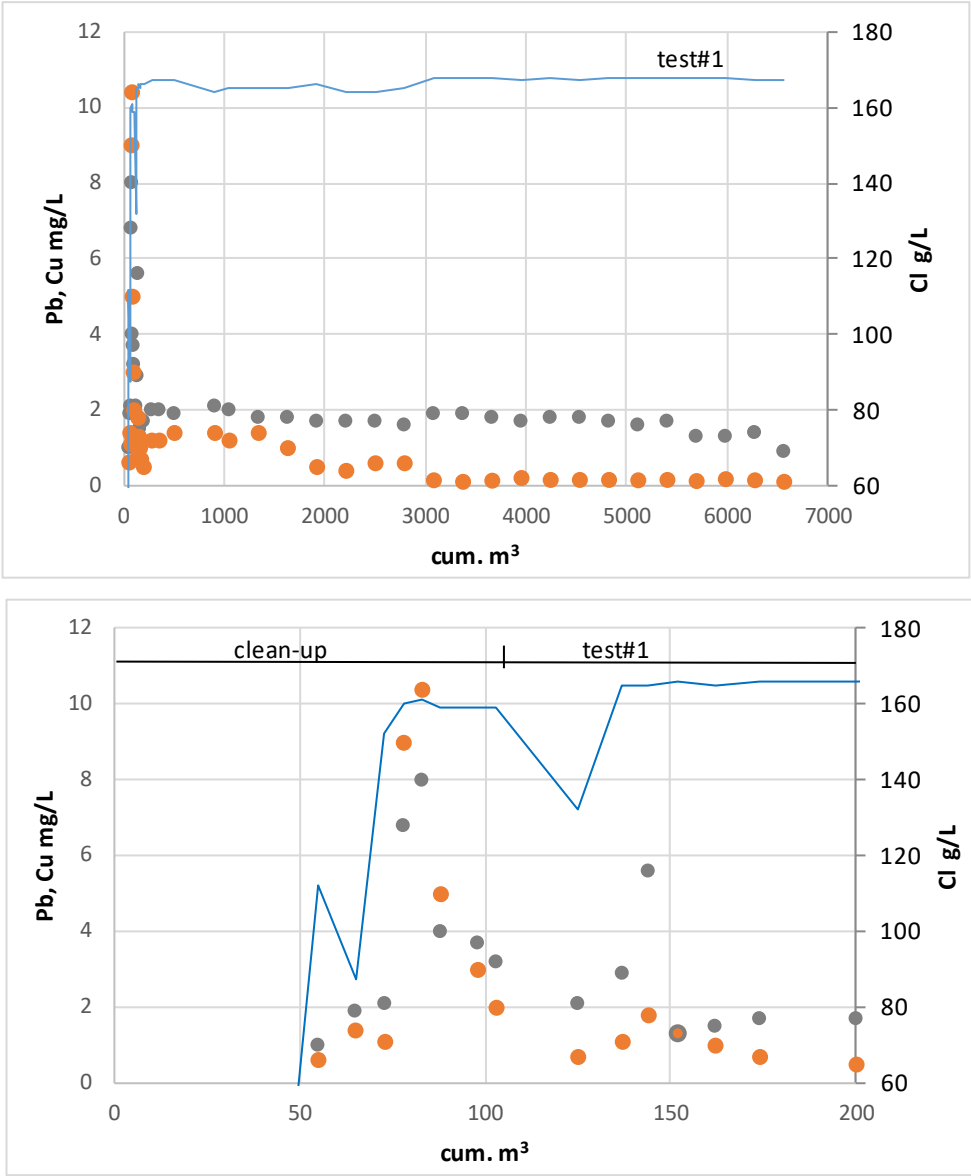

Figure 26: Chloride (blue line,) lead (grey) and copper (orange) in produced water during clean-up and test#1 of the Skagerrak F, Thisted-2. One day break in pumping after clean-up at 108 m^3.

One other possibility should be mentioned: The exchange reaction between iron pipe and formation water constituents such as copper and lead, which has higher redox potential compared to iron. This reaction which can take place when all traces of oxygen have been removed from the system will be more efficient for copper compared to lead. This may explain why copper concentration is reduced relative to lead (Figure 26). Given the uncertainties mentioned above we find that the most plausible concentration of lead in the Skagerrak formation water is that measured at the end of test#1 i.e. 0.9 mg/L (Table 10).

Loss of transmissivity possibly due to fines migration

Six more tests, three short term and tree long term, were performed on the Skagerrak interval during which transmissivity decreased from 70-77 mD to 20 mD, presumably due to near well bore blocking caused by fines migration. Therefore, analyses of the produced water were

focused on suspended solids rather than dissolved constituents. A total volume of 19,000 m^3 was produced during all of the seven tests on the Skagerrak Formation.

Thisted-2, Gassum Fm test

In order to examine the fines migration problem an interval of the Skagerrak (1842-1843.5 m) above the previous perforated zones was to be tested before proceeding to the Gassum testing. Unfortunately, due to misplacement of the perforations by five metres (1836.5-1838 m) and failure of the upper-most hydraulic packer (1212 m) (Figure 27), the test was not really performed. Facing these failures after 4 short term pumping tests, the sliding sleeves on the 2 7/8 inch tubing string was adjusted to allow flow from the perforated Gassum interval (1254.5-1259.5 m) from test#5 and onwards.

Frequent sampling during the initial testing showed a sharp decrease in chloride concentration from 167 to 109 mg/L (Figure 28), when approximately 50 m^3 of water had been produced, which is equivalent to the well volume between the pump and the packer below the Gassum perforations (Figure 27). After approximately 200 m^3 of pumping the chloride concentration remained constant around 101 mg/L. No analysis of lead was performed on the high chloride water sampled at the beginning of the test, but a gradually decrease in lead from 0.29 to 0.04 mg/L during pumping 55 to 640 m^3 suggests a higher lead concentration in the more salty water present before starting the pump. Assuming simple mixing between Skagerrak and Gassum water the ratio obtained from chloride in the intermediate samples indicates a lead concentration of 2 mg/L for the water present in the wellbore prior to testing. Given the few data plus the simple assumption the calculated lead concentration is not far off the value found for the Skagerrak formation water (Figure 26).

The lead concentration in the formation water produced during test#5 – test#7 was very low <0.01 – 0.02 mg/L, except for the sample taken just after the start of test#5 (Figure 28). The high lead concentration may in some way be associated with the high suspended solids contents at the beginning the test (Figure 29) although all samples for trace metal analysis were carefully filtered (0.45 µm) prior to storage. Copper and lead co-varies roughly speaking during the first four tests, but from test#5 and onwards copper increases from 0.06 mg/L to 0.4 mg/L. The reason for this increase is not known but may be related to different flow paths taken by the Gassum water before and after adjusting sliding sleeves on the 2 7/8 inch tubing string. During the first four tests water flowed in the well bore and pas the leaking hydraulic packer (1212 m) (Figure 27), whereas afterwards water was free to flow through the tubing. Unfortunately daily samples covering the 3900 to 6500 m3 pumping volume were lost, so no data could be obtained for late part of test#7. However, water samples taken during the short term pumping after an acid job show much lower copper concentration 0.03 mg/L, except for the very low pH sample directly affected by the acid treatment (Figure 28).

The low concentration of lead in the Gassum formation water (0.02 mg/L) observed during the well tests in 1983, was also found in 2015 when the Thisted geothermal plant had been operation for more than thirty years.

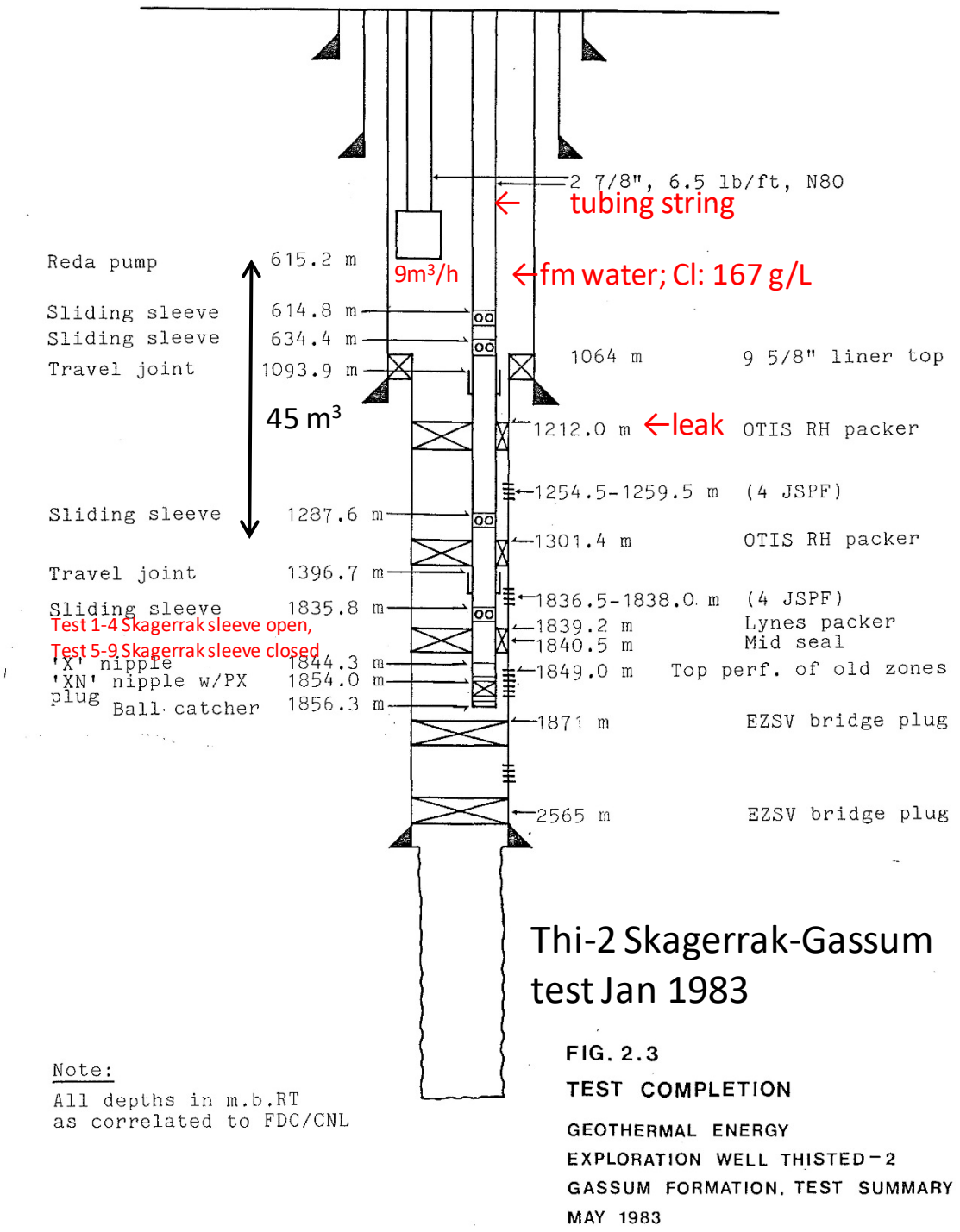

Figure 27: Down-hole set-up for the planned consecutive tests of upper Skagerrak Fm interval (1836.5-1838.0 m) and Gassum Fm (1254-1259). Initial Skagerrak tests were unsuccessful due to leak at 1212 m packer and misplacement of perforations by 5 m. Skagerrak sleeve closed while Gassum sleeve (1287m) was opened during test#5-#9. Minimum volumes to be displaced for tests via the tubing string were c. 7 m^3 for both Skagerrak and Gassum.

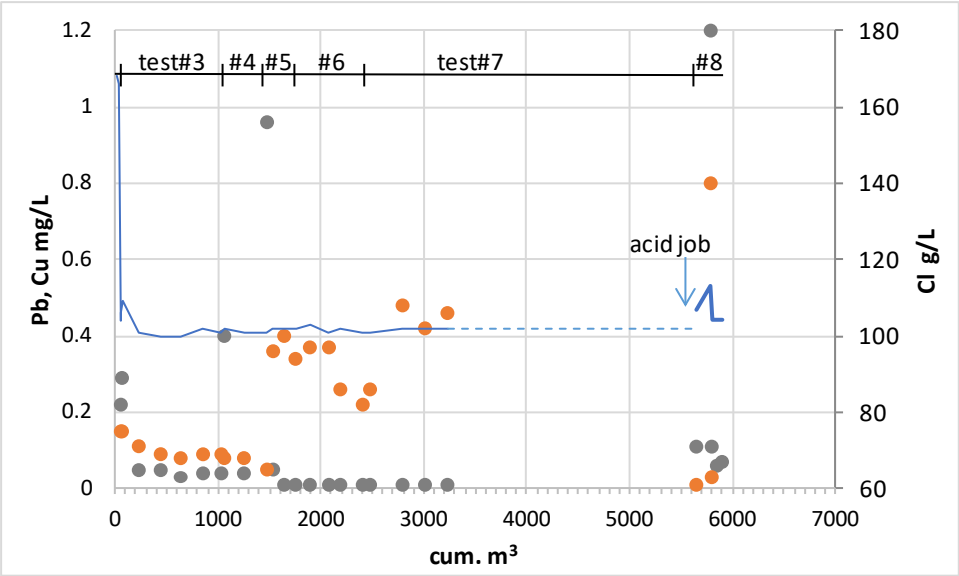

Figure 28: Chloride (blue line), lead (grey) and copper (orange) in produced water during test#1-#7 of the Gassum Fm, Thisted-2. Each pumping test was followed by a build-up test. Test# 8 was performed after an acid job. Daily samples from 3900 to 6500 m³ were lost, therefore no analyses for this interval.

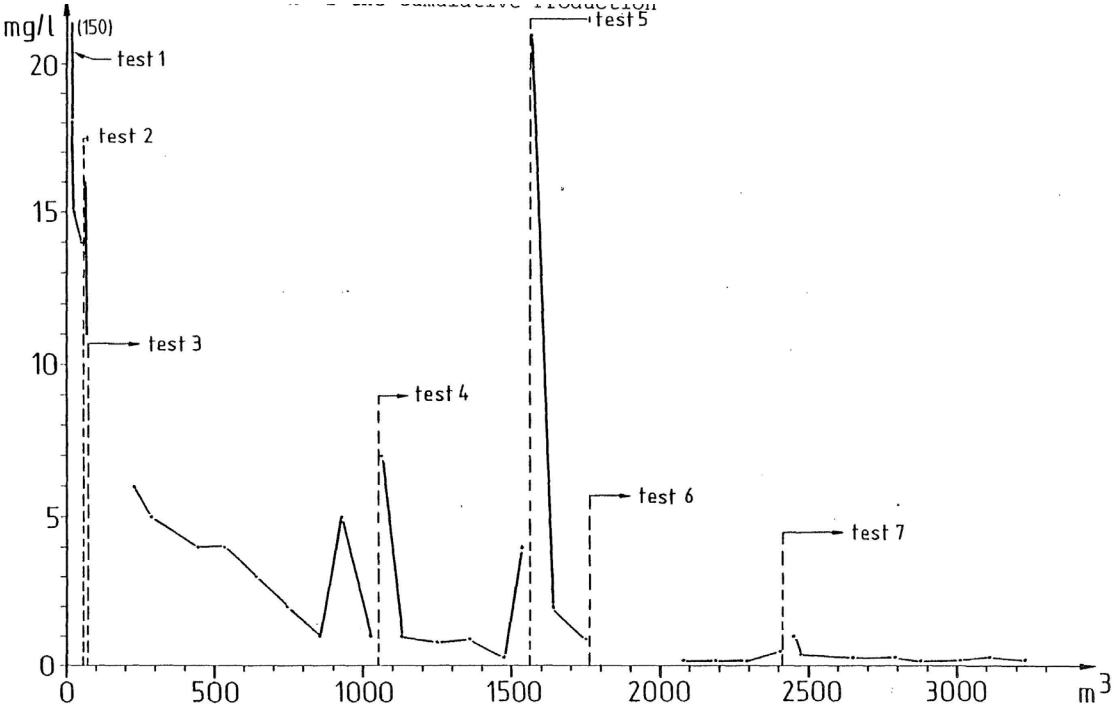

Figure 29: Particle concentration in water produced during Gassum Fm testing of Thisted-2.

Farsø-1, Gassum Fm test

Testing was planned using an open hole completion for the Gassum Formation, however due to various hole problems a 4½ inch liner was set. Having cleaned the hole using a 3 %

KCl completion fluid the liner was perforated to test the G3 member of the Gassum Formation. Following the perforation job the well flowed with approximately 25 m^3, after which the down-hole equipment including the pump was installed (Table 11).

Table 11: Operational sequence of the Farsø-1 test.

Date, 1982	Action	Brine prod. m^3	Samples
13/2	Perforated 2833.7 - 2840.3 m	approx. 25	
14/2 - 20/2	Set up surface & downhole eq.		
17/2 - 18/2	Clean up wellbore	approx. 90	21
20/2 - 26/2	Drawdown test Q = 4.6 m^3/h	740	14
26/2 - 7/3	Build up test		
7/3 - 10/3	Drawdown test Q = 10 m^3/h	540	3
10/3 - 13/3	Build up test		
13/3	Velocity survey	35	
19/3 - 20/3	Clean up wellbore for fill	180	4
20/3	Perforated 2933.0 - 2939.3 m		
	2869.6 - 2882.3 m	290	2
	2792.0 - 2797.3 m		
21/3 - 24/3	Build up after perf.		
25/3 - 3/4	Drawdown test Q = 8-6 m^3/h	1705	9
2/4	Flowlog and Fluid Density log		
3/4 - 14/4	Buildup test		
14/4 - 20/4	Rig down		
	Total production approx.	3600 m^3	

Onsite chloride analysis on 21 samples collected during the clean-up pumping whereby 90 m^3 was produced helped to establish the shift from completion fluid *c.* 32 mg/L to formation water 172 mg/L (Figure 30). A full chemical analysis on the last sample collected during the wellbore clean-up showed a lead content equal to 0.38 mg/L.

Lead and copper contents in the produced formation water during the subsequent three draw down tests (Table 11) are shown in Figure 30. During the first test the lead content deceased from 1.3 to 0.7 mg/L whereas the second test gave 2.4 to 1.9 mg/L, indicating that the produced water was not yet free of contaminants. The clean-out of bottom fills by a forceful hydro jet prior to a second perforation job and the third test apparently lead to an enhanced contamination of the produced fluid as evidenced by marked increase in lead content up to 8.8 mg/L (Figure 30). The flow log indicated only insignificant contribution from the last perforated zones, which rules out a particular high lead content from these zones as the reason for high lead observed during test#3.

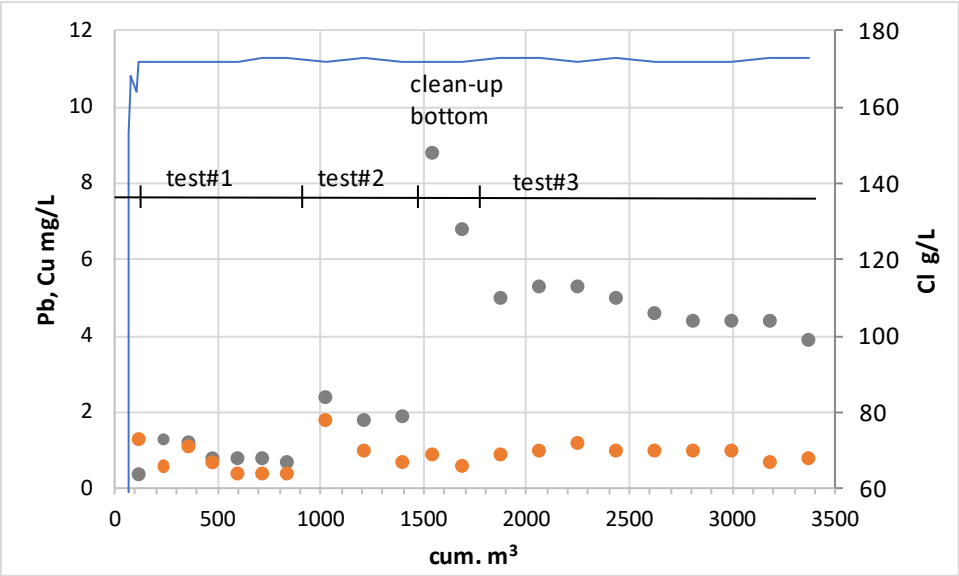

Figure 30: Chloride (blue line), lead (grey) and copper (orange) in produced water during test#1-#3 of the Gassum Fm (c. 2800 m) of Farsø-1 well. Each pumping test was followed by a build-up test. Test#3 was performed after bottom clean-up job. Minimum volume to be replaced to obtain reservoir formation water was 90 m^3.

Aars-1a, Gassum Fm test

Water samples obtained on surface during the three airlift tests and down-hole samples using the "formation tester" were all contaminated by residues of mud filtrate and completion fluid to various extents. The reason for this was the rather low volumes produced due the low permeability caused by extensive cementation of the sandstone layers, 3205-3385 m. The lead content of the eight samples, 2-7 mg/L, is therefore expected to be affected by contaminants as well. Thus, no reliable lead data exist for the deep Gassum Formation.

Aars-1a, Haldager Fm test

The Haldager sand member in Aars-1a was pump tested in May – June 1981 to evaluate the reservoir characteristics for geothermal energy production. The interval 2465 - 2499 meters of the Haldager sand was divided into three zones by packers, individually acid treated, and short term pump tested. The down-hole equipment was much the same as that used for Thisted (Figure 27). A long term pumping test of the combined zones lasting for 14 days followed by a 14 days buildup was then performed. Multiple samples were taken during each pumping test showing identical chemical composition for the three different zones. However, trace metal analysis (Pb, Cu, Cd) was only performed on the sample taken at the end of each of the four tests. The lead content in formation water obtained after c. 3,200 m^3 of the combined test of all three zones was 1 mg/L, which is close to the values found for the individual zones, 0.7-1 mg/L. Given the large volume produced during the 14 days test one might expect the produced water to be free of contaminants although we cannot be certain.

Stenlille-1, Gassum Fm & Fjerritslev Fm tests

The Stenlille-1 well was the first well in Denmark to be drilled to investigate the feasibility of storing natural gas in an aquifer. The geological objective for the aquifer storage was primarily the Upper Gassum sandstone found from 1507 m to T.D. After conventional and sidewall

cores of the well upon completion, the Gassum reservoir from 1507.0-1512.5 m (zone 1) and one zone in the Fjerritslev Formation, 1369.5-1376.0 m (zone 2) was selected for investigation. In order to ensure that the tested zone was isolated from underlying aquifers during the test an annulus cement circulation repair was carried out for both zones before testing.

The lead content in formation water from both zones was 0.03 mg/L. Only one sample from each test was analyzed. The samples were collected at the end the tests when approximately 1300 and 1800 m^3 had been produced.

Tønder-5, Bunter Fm test

Formation water samples for chemical analysis were only available from the short term airlift test, since the long term test had to be done by fresh water injection due to the extreme salinity of the formation water. The lead content in formation water from 1880 m depth was equal to 0.22 mg/L. Only the sample taken at the end of the test was analyzed with respect to lead, so it is not possible to decide to what extent the sample may have been contaminated.

Stenlille-19

A twelve hour airlift test was performed for each of these formations: Bunter, Falster and Gassum. Multiple samples were collected during each test indicating clean formation water, at least with respect to major constituents for the last samples taken. The lead content for the three different formation waters were: 4.6; 0.9 and 0.09 mg/L. However, the higher lead content for Gassum formation water in Stenlille-19 compared to that of Stenlille-1 (Table 10) indicate a certain degree of contamination for the former. The lead content found in the Bunter and the Falster formation waters may be affected by contaminants as well in view of the experience gained from previous well tests mentioned above.

Margretheholm, Bunter Fm tests

Formation water obtained from airlift and pump tests of the two wells showed the same level of lead content, 0.3-0.4 mg/L. The same lead content was obtained when the geothermal plant had been in operation for 10 years.

Series of lead measurements performed at various sampling points indicated a minor loss of lead (0.02 mg/L) from the water on passage through the plant, caused by galvanic corrosion.

Sønderborg, Gassum Fm test

The formation water lead content was 0.02 mg/L for both wells at the time of the pump tests. Furthermore the same content was found when the plant had been in operation for a few years. Given the low content no difference in lead was found between the inlet and outlet of the plant.

Appendix 6: Compilation of mineralscan results

This appendix contains the results of mineralscans made by SEM of a core sample from Thisted-3 and a total of four cuttings samples from Margretheholm-1 and Sønderborg-1.

Mineral	Area %	Weight %	Grain Size (µm)
Al-(hydr)oxid (gibbsite, diaspore)	0,00	0,00	10,00
Albite	12,47	14,60	42,53
Albite exsolution laminae in K-feldspar	1,37	1,60	14,18
Anatase	0,45	0,80	19,67
Ankerit	0,00	0,00	13,33
Apatite	0,14	0,20	38,86
Biotite	3,51	4,71	16,90
Calcite	0,01	0,01	11,76
Chlorite	0,00	0,00	10,00
Dolomite	0,00	0,00	38,68
Epoxy	12,95	5,79	36,19
Fe-oxide	0,00	0,00	11,43
Garnet	0,01	0,02	13,03
Illite	0,00	0,00	10,00
Ilmenite	0,13	0,27	21,90
Kaolinite	2,71	3,15	15,36
Kaolinitized mica	0,73	0,88	12,71
Kaolinized chlorite	0,25	0,32	11,17
Muscovite	0,55	0,68	11,75
Olivine	0,00	0,00	10,00
Orthoclase/microcline	10,83	12,39	50,81
Plagioclase	1,37	1,59	26,49
Pyrite	0,02	0,05	11,80
Quartz	44,06	52,20	88,79
Rutile	0,22	0,44	19,20
Smectite	0,01	0,01	10,00
Tourmaline	0,00	0,00	10,00
Zircon	0,12	0,26	34,75
Unclassified	8,09		19,95

Thisted-3
Gassum Fm
1222.80 m

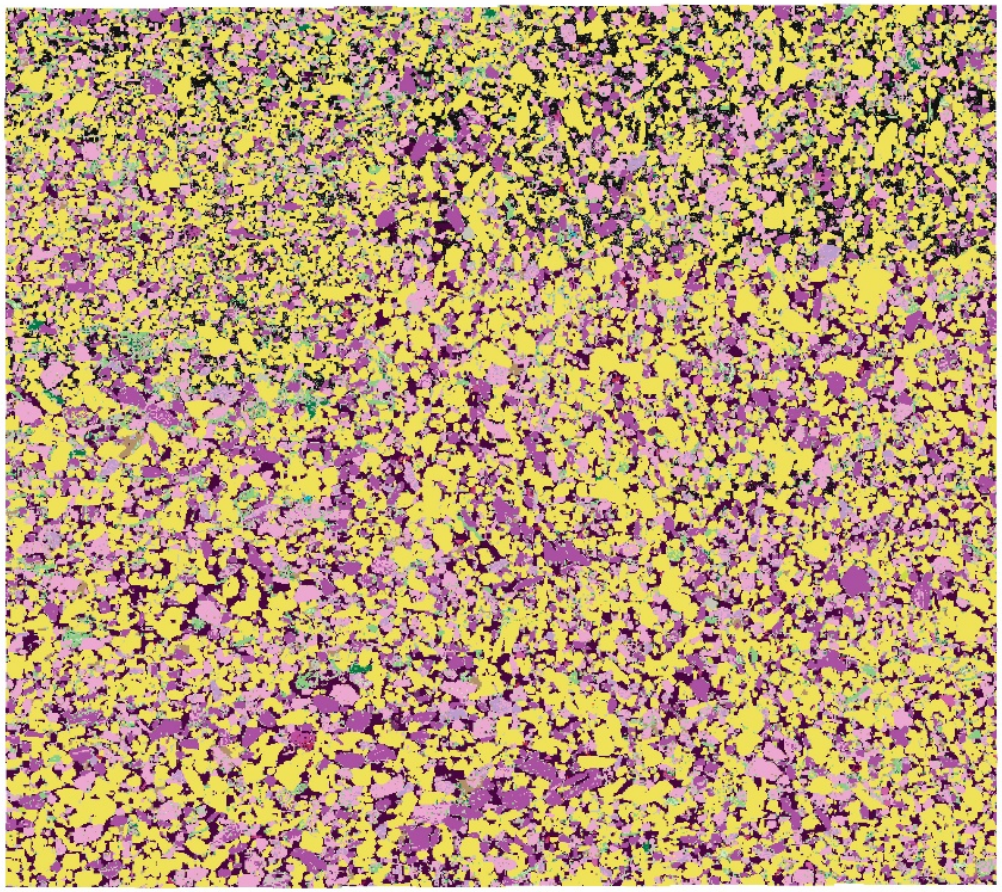

Mineral	Area %	Weight %	Grain Size (µm)	
Al-(hydr)oxid (gibbsite, diaspore)	0,00	0,00	14,79	
Albite	0,28	0,47	19,86	
Albite exsolution laminae in K-feldspar	0,05	0,09	15,42	
Alumohydrocalcite	0,01	0,01	14,79	
Anatase	0,05	0,14	15,82	
Anhydrite/gypsum	0,00	0,00	18,76	
Ankerit	0,00	0,00	14,79	
Apatite	0,00	0,01	15,93	
Ba-Feldspar (Hyalophane)	0,00	0,00	14,79	
Biotite	12,70	24,89	39,67	
Calcite	1,80	3,20	23,19	
Dolomite	0,00	0,01	15,89	
Epoxy	56,40	36,84	89,05	
Fe-oxide	0,01	0,05	15,22	
Garnet	0,10	0,22	16,11	
Illite	0,01	0,01	15,15	
Ilmenite	0,00	0,01	15,85	
Kaolinite	0,37	0,62	15,88	
Kaolinitized mica	4,36	7,69	24,42	
Kaolinized chlorite	1,34	2,44	18,76	
Mn-oxides	0,00	0,00	14,79	
Monazite	0,00	0,00	14,79	
Muscovite	0,35	0,65	15,87	
Olivine	0,00	0,00	14,79	
Orthoclase/microcline	0,78	1,30	23,29	
Plagioclase	0,02	0,03	15,57	
Pyrite	0,03	0,09	29,09	
Quartz	12,08	20,91	37,09	
Rutile	0,02	0,06	16,60	
Siderite (Ca)	0,02	0,06	16,85	
Smectite	0,14	0,16	15,39	
Tourmaline	0,00	0,00	14,79	
Zircon	0,01	0,04	17,87	
Unclassified	9,05		36,70	

Sønderborg-1
Gassum Fm
1190.00 m

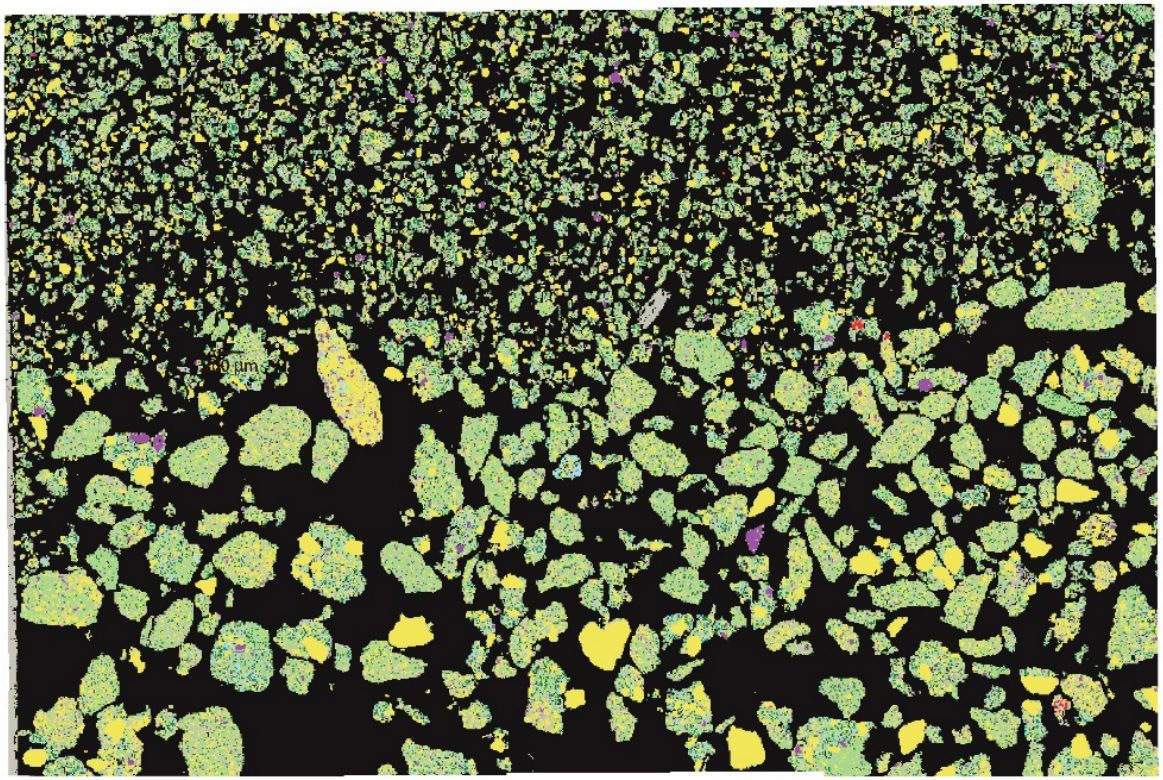

Mineral	Area %	Weight %	Grain Size (µm)	
Al-(hydr)oxid (gibbsite, diaspore)	0,01	0,01	10,50	
Albite	0,22	0,25	27,45	
Albite exsolution laminae in K-feldspar	0,05	0,06	11,90	
Alumohydrocalcite	0,00	0,00	10,00	
Anatase	0,06	0,11	16,06	
Ankerit	0,02	0,03	23,66	
Apatite	0,00	0,01	10,00	
Biotite	4,26	5,62	18,55	
Calcite	0,05	0,06	10,15	
Dolomite	0,00	0,00	10,00	
Epoxy	16,29	7,16	31,90	
Fe-oxide	0,00	0,01	11,18	
Garnet	0,01	0,01	10,00	
Illite	0,01	0,01	10,00	
Ilmenite	0,00	0,01	22,82	
Kaolinite	3,22	3,67	20,84	
Kaolinitized mica	0,55	0,66	12,48	
Kaolinized chlorite	0,16	0,20	10,55	
Mn-oxides	0,00	0,00	10,00	
Monazite	0,00	0,00	10,00	
Muscovite	0,36	0,44	12,30	
Olivine	0,00	0,00	11,43	
Orthoclase/microcline	2,46	2,76	50,70	
Plagioclase	0,00	0,00	10,00	
Pyrite	0,00	0,01	12,85	
Quartz	67,54	78,64	102,81	
Rutile	0,07	0,14	25,42	
Siderite (Ca)	0,01	0,01	10,45	
Smectite	0,01	0,01	10,55	
Tourmaline	0,00	0,00	20,48	
Zircon	0,05	0,10	46,53	
Unclassified	4,56		20,94	

Margretheholm-1
Gassum Fm
1861.25 m

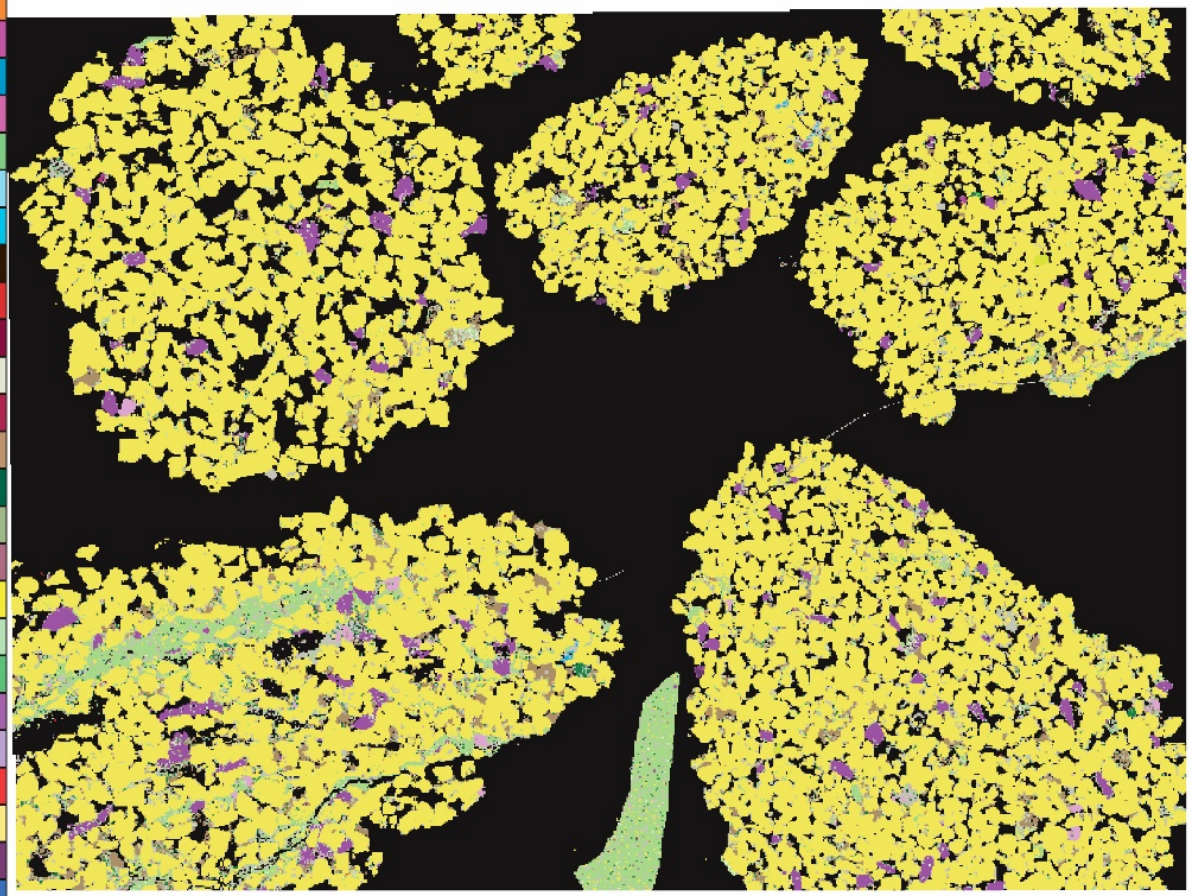

200 µm

Mineral	Area %	Weight %	Grain Size (µm)
Albite	2,49	2,62	25,16
Albite exsolution laminae in K-feldspar	0,74	0,78	17,93
Anatase	0,05	0,07	16,63
Ankerit	0,00	0,01	24,99
Apatite	0,01	0,01	18,60
Ba-Feldspar (Hyalophane)	0,00	0,00	14,79
Biotite	27,78	33,45	53,77
Calcite	0,57	0,62	25,86
Dolomite	0,21	0,24	27,13
Epoxy	3,59	1,44	25,34
Fe-oxide	0,04	0,09	17,27
Garnet	0,01	0,01	14,79
Illite	0,05	0,06	15,32
Ilmenite	0,02	0,03	17,25
Kaolinite	0,09	0,10	15,37
Kaolinitized mica	0,26	0,28	17,65
Kaolinized chlorite	0,03	0,04	15,54
Muscovite	0,46	0,52	15,71
Olivine	0,00	0,00	14,79
Orthoclase/microcline	11,41	11,72	33,84
Plagioclase	0,01	0,02	15,27
Pyrite	0,00	0,00	14,79
Quartz	44,93	47,79	51,28
Rutile	0,02	0,04	17,59
Siderite (Ca)	0,00	0,01	15,85
Siderite (Mg)	0,00	0,00	14,79
Smectite	0,06	0,04	16,58
Tourmaline	0,00	0,00	14,79
Zircon	0,01	0,02	25,72
Unclassified	7,13		29,58

Margretheholm-1
Bunter Fm
2502.50 m

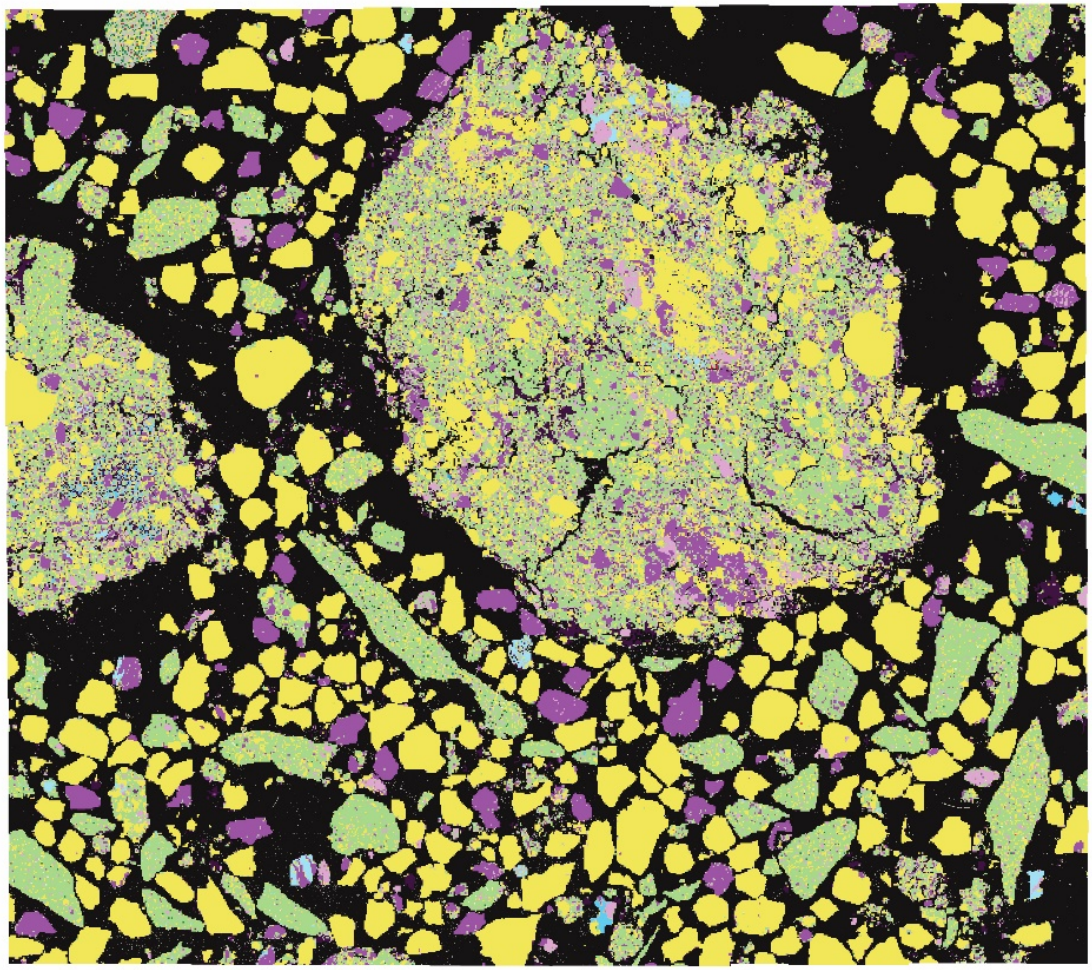

Mineral	Area %	Weight %	Grain Size (µm)	
Albite	3,22	4,23	38,99	
Albite exsolution laminae in K-feldspar	0,79	1,05	20,74	
Anatase	0,02	0,05	18,74	
Anhydrite/gypsum	0,00	0,00	14,79	
Ankerit	0,14	0,21	47,30	
Apatite	0,01	0,01	24,07	
Biotite	3,97	5,97	29,29	
Calcite	2,28	3,10	46,02	
Chlorite	0,01	0,01	19,25	
Dolomite	1,69	2,41	52,95	
Epoxy	25,44	12,77	60,78	
Fe-oxide	0,02	0,05	27,80	
Garnet	0,01	0,02	25,14	
Illite	0,02	0,02	15,98	
Ilmenite	0,00	0,01	19,89	
Kaolinite	0,08	0,10	15,72	
Kaolinitized mica	0,23	0,32	24,93	
Kaolinized chlorite	0,04	0,06	16,33	
Mn-oxides	0,00	0,00	14,79	
Muscovite	0,21	0,30	15,91	
Olivine	0,01	0,01	14,79	
Orthoclase/microcline	15,54	19,98	66,36	
Plagioclase	0,04	0,05	17,22	
Quartz	36,97	49,19	84,67	
Rutile	0,01	0,02	19,86	
Siderite (Ca)	0,00	0,01	27,14	
Siderite (Mg)	0,00	0,00	14,79	
Smectite	0,03	0,03	18,48	
Zircon	0,01	0,03	32,42	
Unclassified	9,21		30,78	

Margretheholm-1
Bunter Fm
2557.50 m

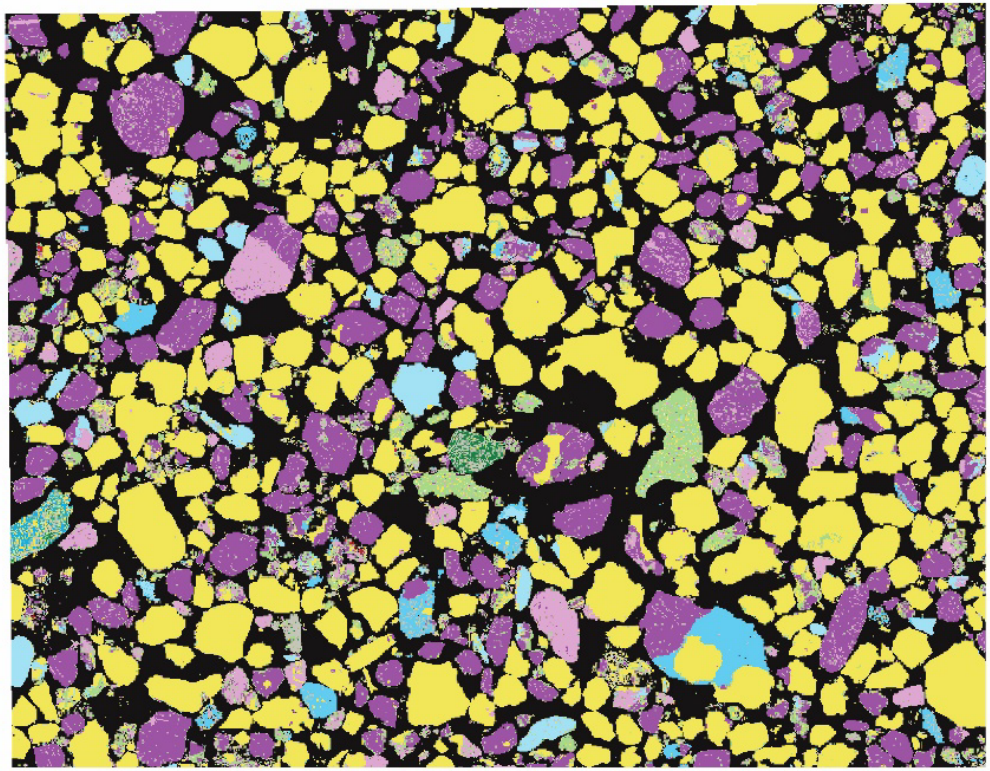

200 µm